THESIS

# NEW INSIGHTS INTO PLEISTOCENE HOMININ BUTCHERY AND TOOL CHOICE FROM A 0.9 MA FOSSIL ASSEMBLAGE FROM THE HEB SITE, OLDUVAI GORGE, TANZANIA.

Submitted by

Ipyana F. Mwakyoma

Department of Anthropology

In partial fulfillment of the requirements

For the Degree of Master of Arts

Colorado State University

Fort Collins, Colorado

Spring 2021

Master's Committee:

Advisor: Michael C. Pante

Michelle M. Glantz
John McKay

ABSTRACT

NEW INSIGHTS INTO PLEISTOCENE HOMININ BUTCHERY AND TOOL CHOICE FROM A 0.9 MA FOSSIL ASSEMBLAGE FROM THE HEB SITE, OLDUVAI GORGE, TANZANIA.

Cut marks on animal bones have the potential to inform on hominin diet and tool use. Although these important traces of behavior appear as early as 3.4 Million years ago, they normally are rare in fossil assemblages in part due to the exceptional preservation of bone surfaces required to study them. Olduvai Gorge is unique in having many fossil assemblages with well-preserved cortical surfaces that allow identification and study of bone surface modifications. Most of these assemblages are from Beds I and II as fossil preservation is generally poor in the younger Beds.

The present study analyzes the well-preserved fossil assemblage recovered from renewed excavations of the HEB site by the Olduvai Gorge Coring Project (OGCP). The HEB site is stratigraphically positioned in lower Bed IV, just above Tuff IVA, dating to ~0.9 Ma and was first excavated by Mary Leakey's team in 1962. These fossils exhibit a large number of cut marks and are in direct association with Acheulean tools; making this site important for inferring the feeding and tool use behavior of *Homo erectus.*

Optical profilometry protocols developed by Pante et al (2017) were used to obtain 3D quantifiable micromorphological measurements of 256 experimentally created cutmarks, and 20 archaeological cutmarks from HEB site Olduvai Gorge. Focusing on the micromorphological measurements, this study used quadratic discriminant analyses models to classify the archaeological cutmarks from HEB site based on technology and raw materials types of the stone tools used to create those marks. The discriminant models on raw material types only, tool types only and both raw material and tool types had 64.8%, 77.3% and 68.4% classification accuracies respectively. Results from the models indicate that cut marks at HEB were made by using both flakes and biface tools, made from lava and quartzite raw materials. These results are consistent with Leakey (1994) excavations, which showed a significant prevalence of flakes and bifaces made from volcanic lava and quartzite raw materials. When interpreted in conjunction with butchery experiments, this study can help us understand hominin tool use and choices at HEB site, Olduvai Gorge - around 0.9 million years ago.

# ACKNOWLEDGEMENTS

I am especially grateful to my advisor, Dr. Michael Pante, for his guidance throughout this degree, for offering opportunities to study and learn from him at Colorado state university and during Olduvai Gorge Field schools. Am also grateful to my other committee members - Dr. Mica Glantz and Dr. John McKay; for their tireless work on editing and advising this study in the midst of a very tight schedule and Covid-19 pandemic unpleasantries. I am grateful to Colorado State University for funding my master's degree studies. And I would also like to thank Dr. Andrew Du, Dr. Kathleen Galvin, and Dr. Heidi Hausermann, for their help in improving my academic writing skills and for their guidance.

I am also grateful to the Leakey Foundation for funding my master's degree and research travel expenses. I would also like to thank OGCP (Olduvai Gorge Coring Project) and the Stone Age Institute – Bloomington, Indiana, for allowing me to use their lab and field equipment at Olduvai Gorge, and for providing me with the fossil bone specimens for this study. I am grateful to the Tanzanian institutions that permitted and cooperated with OGCP's research, including the Tanzanian Commission for Science and Technology (COSTECH), the Tanzanian Department of Antiquities, Ngorongoro Conservation Area Authority (NCAA).

This thesis would not have been possible without the support of my family and friends. My mom Grace and sister Atumpoki, have always been supportive and a huge source of strength. I thank my friends; April, Cameron, Kush, Jeremy and Vatsal for their moral and intellectual support, which was fundamental in completing this thesis, and in my acculturation within the US. And lastly but not least, I would like to thank Dr. Fidelis Masao, Dr. Jackson Njau and Trevor Keevil, for their inputs and help on this study and throughout my Master's degree.

TABLE OF CONTENTS

LIST OF TABLES

LIST OF FIGURES

# CHAPTER 1 INTRODUCTION

## 1.1 Background and Research problem

Cutmarks on fossilized bone surfaces have been used to establish hominin processing of animal tissue using stone tools during the Pleistocene in Africa (Bunn et al, 1986; Fisher, 1995; Potts & Shipman, 1981). Association of Early Stone Age (ESA) tools with cut marks at many Pleistocene sites, further solidified the butchery utility of these tools (Potts & Shipman, 1981; Semaw et al. 2003). Discovery of early *Homo* remains (Leakey et al. 1964) and further research at these ESA sites has characterized early *Homo* as the actor responsible for butchering animals using ESA tools that they produced (Bunn, 1981; 2001; Bunn et al, 1986; Roche et al. 2006).

Nonetheless, despite the assertion that hominins were using ESA lithic tools for butchery purposes; variability and succession of the ESA technologies from Oldowan (characterized by flake and core tools) to Acheulian (characterized by biface handaxes) raised questions over similarity in function across these lithic industries (technologies) (de la Torre & Mora, 2014; de la Torre, 2016; Galan & Dominguez-Rodrigo, 2014; Toth, 1985). Broader questions on the evolutionary significance of lithic technological variability (flakes and bifaces) during the ESA are being addressed by ongoing research and efforts to understand the transition from the Oldowan to Acheulian (de la Torre et al. 2012; de la Tore et al, 2018).

In addition to the questions on hominin butchery behavior raised from observed technological variability of the ESA, recent lithic and taphonomic studies have also shown that, different representation of raw material type within and across lithic assemblages can be useful in understanding hominin butchery behavior (Blumenschine et al. 2008; Braun et al. 2009; Goldman-

Neuman & Hovers, 2012; Stout et al. 2005). Major hypotheses on raw material-type use and preferences revolve around questions on whether hominins used certain raw materials based on their suitability for knapping (size, shape and material properties), edge functionality (durability, retouch frequency), production efficiency and expediency, cultural differences or their relative accessibility or availability for hominins (distance from butchery sites) (Braun et al. 2009; Key et al. 2020).

Recent taphonomic advances in quantitative classification of cut mark micromorphology (Gonzalez et al. 2015; Keevil, 2018; Keevil et al. 2018; Pante et al. 2017) have presented novel ways of addressing some of these questions. By quantitatively studying variations between micromorphological measurements (width, length, volume, surface area, depth etc.) of cut marks made by varying technologies; researchers now have a means to study the functions of ESA technologies in butchery (Keevil, 2018; Keevil et al. 2018; Machin et al, 2007; Merrit & Peters, 2019). These quantitative methods have also been applied to classify cut marks based on raw material types (Keevil, 2018; Keevil et al. 2018) further offering insights into hominin tool use and choice during butchery, which is significant in understanding hominin behavioral ecology during the Pleistocene (Blumenschine et al. 1994).

The renowned paleoanthropological site Olduvai Gorge, Tanzania, is particularly suited for studies that address hominin butchery behavior from bone surface modifications such as cut marks (Bunn et al. 1986; Shipman, 1986; Potts & Shipman, 1981). Attempts to use cut mark micromorphological measurements to infer hominin tool use during butchery need the availability of large fossil bone assemblages with well-preserved cortical surfaces and these are abundant at Olduvai Gorge (Bunn et al. 1986). Researchers have recorded many potential Pleistocene sites at Olduvai Gorge that have fossil bone assemblages with cut mark traces, and are associated with

ESA artifacts as well as hominin remains (Bunn et al. 1986; Leakey, 1971; Leakey & Roe, 1995; Shipman, 1986; Pante & de la Torre, 2018; Potts & Shipman, 1981). Additional advantages such as reliable radiometric dates, well established stratigraphy, paleoenvironmental markers, and proximity to analogy sources like contemporary hunter gatherer groups (such as the Hadzabe), makes Olduvai Gorge sites suited for zooarchaeological studies of hominin butchery during the Pleistocene (Bunn et al. 1986; Key et al 2020; Shipman, 1986; Uno et al. 2018).

Among important Olduvai Gorge sites, is the HEB site, which was named after Professor Herberer by Lois Leakey. The HEB site is stratigraphically positioned in lower Bed IV, just above Tuff IVA, dating to ~0.9 Ma and was first excavated by Mary Leakey’s team in 1962 (Leakey & Roe, 1994). Recently, the site has yielded a well-preserved fossil assemblage recovered from renewed excavations by the Olduvai Gorge Coring Project (OGCP). From the project, 60 fossil bones were diagnosed with 110 cutmarks that are in direct association with Acheulean stone tools, making this site important for inferring the feeding and tool use behavior of *Homo erectus*. Pioneering research at Olduvai Gorge, involving the use of cut marks to infer hominin feeding behavior was largely based on Frida Leakey Korongo (FLK) *Zinjanthropus* site assemblage (Blumenschine, 1995; Blumenschine et al, 2007; Dominguez-Rodrigo & Barba, 2005; Dominguez-Rodrigo & Piquares, 2005; Dominguez-Rodrigo et al, 2010; Dominguez-Rodrigo et al, 2014; Egeland et al, 2004; Pante, 2010; Pante, 2012; Pante et al, 2012, 2013; Pickering & Dominguez-Rodrigo, 2006), and has greatly progressed from simple identification of patterning in the butchering techniques (which is done by analyzing the location and frequency of cut marks on different skeletal parts in conjunction with knowledge of animal anatomy) (Bunn et al. 1986), to inferences on hominin timing and access to carcasses (whether hominins or carnivores had the first or earliest access to a carcass) which implies hunting or scavenging modes of subsistence

(Blumenschine et al. 2007; Dominguez-Rodrigo et al. 2015; Pante et al. 2012; Pante et al. 2015; Parkinson, 2013; 2018).

The analysis of hominin timing and access to carcasses is done by analyzing the overall percentage of cut marks in an assemblage and their positions relative to carnivore tooth marks (Blumenschine, 1995). Resulting frequencies will suggest either passive scavenging (late access to carcasses by hominins – mostly exploiting non-meat products like marrow), aggressive scavenging (late access to carcasses by hominins – accessing both meat and marrow) or hunting (hominins having had primary access to carcasses and the majority of the meat) (Dominguez-Rodrigo & Barba, 2007; Blumenschine et al. 2007; Pante et al, 2012, 2013, 2015). This means that such models relied heavily on accurate identification of mark traces on bone surfaces made by different actors (hominin cut marks versus carnivore tooth marks), a feat that has advanced as researchers have abandoned qualitative descriptions of bone surface modifications (Blumenschine et al. 1988; Blumenschine et al. 1996; Fisher, 1995; Shipman & Rose, 1983), in favor of more quantifiable, replicable and standardized micro-morphometric methods for diagnosing marks made by human actors (cut marks) (Bello & Soligo, 2008; Bello et al. 2009; Boschin & Crezzini, 2012; Courtney et al. 2019; Dominguez-Rodrigo et al, 2009; Otárola-Castillo et al. 2018; Pante et al. 2017)

The use of quantifiable micro-morphometric methods for diagnosing cut marks has proven successful and researchers have further developed these methods to distinctively infer cut marks made by specific tool types (flakes versus hammerstones or simple versus retouched flakes/tools) and even, specific raw materials of the tools used to create such cutmarks (De Juana et al. 2010; Greenfield, 2006; Keevil et al. 2018; Maté-González et al. 2018). These advancements then provided novel ways of investigating dynamic human behaviors, such as using cutmark measurements to infer hominin choice and use of ESA technology and raw material types during butchery (Keevil, 2018).

Keevil (2018) used high-resolution 3-D laser scanning (optical profilometry) protocols developed by Pante et al (2017), and statistical models (quadratic discriminant analyses) to characterize cut mark micromorphology into classes that distinguish different ESA technologies (flakes or bifaces) and raw material types. Furthermore, Keevil (2018) demonstrated that it was possible to identify such relationships between cut mark morphology and properties of stone tools that created the mark in the fossil record with similar accuracy.

This thesis, therefore, applies Keevil's (2018) model to the analysis of the recently discovered cut marks from the 0.9 Ma HEB site – fossil assemblage. The study uses variations in the micro-morphometric measurements of cutmarks obtained using 3D optical profilometry, to classify cutmark traces into specific technology and raw materials used to create those cutmarks. Experimental cutmark data from Keevil (2018) are used as training dataset to the discriminant statistical models classifying the technology and raw material types of the unknown archaeological cutmarks from HEB site. Results coupled with frequency and distribution of artifacts at the site and actualistic butchery studies, can indicate patterns in which ESA tools were used for butchery based on their technology and raw material types.

## 1.2 Goal of the study

The main goal of the study is therefore, to investigate *Homo erectus* butchery behavior at HEB site, with specific interests in the tool use and choice of the species. Understanding how and why *H. erectus* used and preferred certain ESA tool characteristics for butchery purposes is significant in understanding their strategies for mitigating costs of acquiring and processing meat resources (butchery) (Blumenschine & Pobiner, 2007; Shipman &Walker, 1989). Major evolutionary milestones during the Pleistocene (such as evolution of *H. erectus'* bigger brain) were tied to their ability to obtain high caloric food resources (such as meat) with minimum energetics costs (Bunn, 2006; Isler & Van Schaik, 2014; Pante, 2010; Pante, 2013; Ungar, 2006). The excess caloric return from carnivory provided the energetics budget required to evolve and maintain a bigger brain (Isler & Van Schaik, 2014). Therefore, in order to investigate *H. erectus* tool use and preference during butchery, this study has the following objectives.

### 1.3 Objectives of the study

The first objective of this study is to apply the discriminant models from Keevil's (2018) experimental study, to the 0.9 Ma cut marked fossil bones from HEB site, Olduvai Gorge, in order to identify stone tool technology (biface or flake) used by *H. erectus* for butchery at that site. This is accomplished by applying Keevil's (2018) quadratic discriminant analyses (QDA) models on the archaeological cut mark data from HEB. Keevil's (2018) QDA classification, uses variations in micromorphological measurements (such as volume, weight, length, width etc.) of the cut marks to discriminate technology of the tools used to create the cut marks. Since HEB is a known Acheulian and *H. erectus* site, results from the study will help us diagnose proportion of usage (from frequencies) between the two prominent Acheulian technologies (flake or biface) at HEB site, around 0.9Ma.

The second objective is to apply the discriminant models from Keevil's (2018) experimental study to the 0.9Ma cut marked fossil bones from HEB site, Olduvai Gorge, in order to identify the raw material types used by *H. erectus* to make stone tools that were used for butchery at that site. Like with the first objective, this is also done by applying Keevil (2018) quadratic discriminant analyses (QDA) models on the archaeological cut mark data from HEB. Capitalizing on the connection between stone tool properties (raw materials) and resulting cut mark morphology; Keevil's (2018) QDA models use variations in micro-measurements of those cut mark (such as volume of the cut mark, cut mark weight, length, cut mark width etc.) to diagnose raw material types used to create the cut marks.

Butchery studies using contemporary analogies (Jones, 1980; 1981) have demonstrated that technology and raw material properties of stone tools affect their efficiency as animal butchery tools. This efficiency is reflected through the influence of both technology and raw material on the tool's edge durability and sharpness (among others) during a butchery event (Jones, 1981; Key et al. 2020). Therefore, results from this study can illuminate what technology and raw materials were preferred and used by *H. erectus* in making butchery tools at HEB site, and underlying factors for such choices.

### 1.4 Research Questions

To achieve these objectives, the study seeks to answer the following questions:

First, what ESA technology type (flake or biface) was mostly used by *H. erectus* for butchery at HEB site? Second, what raw material type was mostly used by *H. erectus* for making butchery tools at HEB site? The first two questions can be investigated by looking at the frequencies and proportions of the ESA tools diagnosed from 3D metrological study of the HEB cuts in conjunction with the ESA artifacts found at the site (Leakey & Roe, 1994). This leads to the third question with seeks to determine if the tool frequencies and proportion diagnosed from 3D optical metrology will be reflective of the technology and raw material distribution at HEB site?

### 1.5 Research Hypothesis

Based on the posed research questions, the study therefore hypothesizes ($H_1$) that, 3D optical profilometric study of butchery marks at HEB indicate hominin tool use and choice, and that the tool frequencies diagnosed from the 3D optical profilometric study, are reflective of the technology and raw material distribution at HEB site. This means that, in order for this hypothesis ($H_1$) to be validated, this study has to refute an alternate hypothesis ($H_0$) that, the 3D optical profilometric study of butchery marks at HEB do not indicate hominin tool use and choice, and that the tool frequencies diagnosed from the 3D optical profilometric study, are not reflective of the technology and raw material distribution at HEB site.

# CHAPTER 2 LITERATURE REVIEW

## 2.0 Theoretical background

This study aims to understand the butchery practices of *Homo erectus* at HEB site by studying the relationship or link between the micromorphology of cut marks found on surfaces of HEB bone assemblage, and ESA tools properties (technology and raw material types). To accomplish this task, the study primarily uses uniformitarianism and middle range theoretical approaches.

One of the necessary assumptions this study makes follows the principle of uniformitarianism proponed by Charles Lyell in 1830s, which states that, the rate of geological change, as well as geologic and natural laws behave and remain constant throughout time and space (Gould,1965). From this principle, Gould (1965) identifies dual concepts of uniformitarianism, which are; substantive and methodological uniformitarianism. Substantive uniformitarianism is based on the idea that, we can extrapolate present-day observed rates or conditions to past times because they remain constant throughout time. However, recent scientific research has proven that this assumption is no longer valid or true (Cameron, 1993; Gould, 1965). On the other hand, methodological uniformitarianism is based on the idea that the natural and geological laws behave and remain constant throughout time and space – a statement that withstood the test of time and proved to be valid (Cameron, 1993; Gould, 1965).

Therefore, this study employs methodological uniformitarianism which assumes that only the geological and natural laws remain constant through time and space, and therefore allowing natural and observable processes in the present to be considered analogous to similar processes in the past (Cameron, 1993; Gould, 1965). Since this study, uses a model created through actualistic study by

Keevil (2018), it therefore assumes that the processes used to create Keevil's (2018) experimental cutmarks – are similar to processes used by hominins to create cutmarks at HEB site around 0.9 million years ago.

Another theoretical framework employed in this study is the middle-range theory. Middle range theory relies on empirical observations of the processes and principles responsible for the formation of the archaeological record, in order to interpret the past (Binford, 1981; Reitz et al. 1999). Middle range theoretical approach involves the use of empirical and observable analogies in the present to infer dynamic behaviors in the past (Binford, 1981). This can be done through actualistic experimentation aimed at identifying direct cause and effect relationships between a dynamic behavior and the resulting trace. The approach therefore uses, inferences from present day dynamic behaviors, to interpret the static traces recovered from the archaeological record (Binford, 1981; Gifford-Gonzalez, 1991).

Gifford-Gonzalez (1991) developed a nested hierarchical system of relational analogies to link six taphonomic contextual categories together. The system uses empirical and experimentally tested causal relationships, to hierarchically connect a static trace: first to its causal agent, then effector, actor and finally to its broader behavioral and ecological contexts (Gifford-Gonzalez, 1991). As such, both this study, and the Keevil (2018) actualistic research applied in this study; investigates hominin butchery behavior in the archeological record by identifying the causal relationships between cutmark micromorphology (a static trace) and the structural characteristics of stone tools (an effector).

## 2.1 Bone surface modification (BSM) studies

The core method of this study involves inferring characteristics (technology and raw material types) of ESA tools, from the static cutmark traces left on bone surfaces. The general term, 'bone surface modification' (BSM) is used to refer to traces found on bone surfaces, which can either be natural or humanmade. Natural BSMs includes; trampling marks (Courtney et al. 2019; 2020; Fisher, 1995), bioerosion marks (Blumenschine et al. 2007; Dominguez- Rodrigo & Barba, 2006; Prassack & Pante, 2007) and carnivore tooth marks (Blumenschine, 1988; Blumenschine, 1995; Blumenschine et al. 1996; Selvaggio, 1994; Selvaggio & Wilder, 2001). Humanmade BSMs includes; cut marks (Blumenschine, 1995; Blumenschine et al. 1996; Potts & Shipman, 1981) and percussion marks (Blumenschine & Selvaggio, 1988; Blumenschine, 1995; Blumenschine et al. 1996; Capaldo & Blumenschine, 1994).

Taphonomic study of BSMs in zooarchaeology has been evolving in the last four decades. The use of bone surface modifications (BSMs) on fossil assemblages to study and infer early hominin behavior became popular in zooarchaeology during second half of the 20$^{th}$ century (Binford, 1981; Blumenschine & Selvaggio, 1988; Blumenschine et al. 1996; Bunn et al. 1986; Gonzalez, 1991; Fisher, 1995; Potts & Shipman, 1981; Shipman, 1986; Shipman & Rose, 1983). The Majority of these pioneering studies were done at Olduvai Gorge (Bunn et al. 1986; Blumenschine & Selvaggio, 1988; Fisher, 1995; Potts & Shipman, 1981; Shipman & Rose, 1983) partly due to the abundance of well-preserved BSMs on the large fossil assemblages that were being recovered at FLK Zinj site (Bunn et al. 1986). Since then, tremendous improvements have been made in taphonomic studies of bone surface modifications (BSM). These advancements have been growing from simple qualitative diagnosis of actors creating varying traces on fossil bones (such as diagnosing cut marks, tooth marks and other BSMs) (Binford, 1981; Blumenschine, 1995;

Capaldo, 1998; Domínguez-Rodrigo, 1999; Domínguez-Rodrigo and Pickering, 2003; Pante et al., 2012; Selvaggio, 1998; Shipman, 1986) to more quantitative methods (Gumrukcu et al. 2017; Keevil et al. 2018; Maté-González et al. 2015; Muttart et al. 2018; Pante et al. 2017; Yravedra et al. 2017). This study contributes to this body of knowledge by applying quantitative methods developed by Pante et al. (2017) and Keevil's (2018) statistical models for diagnosing ESA technology and raw materials from cut mark traces found on fossil bone assemblages from the HEB site, Olduvai Gorge, Tanzania.

### 2.2 Cut marks

The primary BSMs investigated in this study are cutmarks. Cut marks on bone surfaces can indicate defleshing, skinning, or disarticulation which implies that cut marks serve as undisputed evidence of carcass access or processing by humans (Blumenschine, 1995; Blumenschine et al. 1996; Fisher, 1995; Potts & Shipman, 1981). What cut marks can tell us about hominins' access or processing of carcasses (hominin butchery behavior) has also been advancing. The early utility of cut marks on interpreting hominin butchery behavior was identification of patterning in the butchering techniques (which is done by analyzing the location and frequency of cut marks on different skeletal parts in conjunction with knowledge of animal anatomy) (Bunn, 1986; Bunn et al. 1986; Bunn & Ezzo, 1993; Marshall, 1986; Shipman & Rose, 1983a; 1983b). These studies are very useful, because location and frequency of cut marks on different skeletal parts can be used to make inferences on hominin timing and access to carcasses (Blumenschine, 1995). This is done by analyzing the overall percentage of cut marks in an assemblage and their positions relative to carnivore tooth marks. Higher cutmark frequency relative to toothmarks on a bone indicates that hominins had first or early access to that carcass followed by carnivores and vice versa. Therefore, cutmark patterning and frequency on fossil bone assemblages can infer different hominin dietary strategies such as: passive scavenging (late access to carcasses by hominins – mostly exploiting non-meat products like marrow), aggressive scavenging (late access to carcasses by hominins – accessing both meat and marrow) or hunting (hominins have primary access to carcasses, accessing majority of the meat) (Blumenschine, 1995; Blumenschine et al, 2007; Dominguez-Rodrigo & Barba, 2005; Dominguez-Rodrigo & Piquares, 2005; Dominguez-Rodrigo et al, 2010; Dominguez-Rodrigo et al, 2014; Egeland et al, 2004; Pante, 2010; Pante, 2012; Pante et al, 2012; Pickering & Dominguez-Rodrigo, 2006; Pobiner, 2007).

### 2.3 Different methods of modelling mark morphology

Correct diagnosis of BSM is very crucial considering the implications attached. Previously, equipment like handheld lenses, or low power optical stereomicroscope (Blumenschine et al. 1996; Bunn, 1981) with natural light were used to identify different BSMs (Blumenschine, 1995; Blumenschine et al. 1996; Fisher, 1995; Potts & Shipman, 1981; Selvaggio, 1994; Shipman, 1986; Shipman & Rose, 1983). This method involved looking for qualitative traits (For example, the cross section of a carnivore tooth mark under a microscope appeared to be 'U-shaped' while that of a cut mark was considered more 'V-shaped') that could broadly discriminate different agencies/actors (carnivores for tooth marks and hominins for cut marks) (Fisher, 1995). Recent diagnoses of BSMs have progressed towards classifications made from multiple qualitative and quantitative micromorphological and morphometric traits of the BSMs. The micromorphological data is obtained using high-resolution modelling techniques such as scanning electron microscope (SEM), micro- photogrammetry, and 3D optical profilometry/metrology (Fisher, 1995; Pante et al. 2017).

2.3.1 *Scanning electron microscope (SEM)*

Pioneering use of scanning electron microscope (SEM) in archaeology started in 1980's, with observation of surface topography of archaeological materials (such as metals, glass, faience, pottery, stone, soil particles, pigments, bone, teeth, fingernails, skin, hair, eggshell, mollusks, insects and parasites, plant remains, wood, pollen, fibers etc.) being the primary objective (Fisher, 1995; Freestone & Middleton, 1987; Olson, 1988; Potts & Shipman, 1981). In terms of studying cut mark traces and other bone surface modifications, Fisher (1995) identified various strengths of SEM such as; continuous magnification over a much greater range, high resolution, increased depth of field, and the capability to make high quality microphotographs. These descriptions were based on comparisons with other microscopes at that time and may no longer be viable or sound if weighed against modern microscopy technologies. However, SEM remains the earliest method for producing high quality images of surface topography and was superior to the hand lens or other optical magnifying instruments (such as low power optical stereomicroscopes) when it came to producing models of cut mark micromorphology (Fisher, 1995). SEM has some disadvantages, including; high operating costs (expensive to buy the instruments), time-consuming, and challenges related to preparation and examination of specimens (Fisher, 1995; Fram, 2014).

2.3.2 *Micro- photogrammetry*

Micro-photogrammetry showed promise as a slightly cost-accessible, and analytically less expensive alternative to SEM (Maté-González et al. 2015). The technique incorporates treatment of high-resolution images with macro-photogrammetry and computer visualization for tri-dimensional reconstruction of cut marks on bones. These micromorphological data are later analyzed (classified) quantitatively using statistical methods (Maté-González et al. 2015). The method was developed using experimental datasets, where variations in microscopic geomorphometric measurements of cut marks modeled with macro-photogrammetry (such as width along the cut mark, opening angle, and cut mark depth) were used to discriminate cut marks from other types of trace marks (BSMs) using statistical models (Maté-González et al. 2015). Yravedra et al (2017) applied this method on archaeological data sets from BK (Bell's Korongo) site, Olduvai Gorge, and went further by demonstrating that the method could be used to diagnose different stone tool raw material types from the cut marks.

However, this method faces multiple replicability, inter-observer objectivity, and testability challenges (Keevil, 2018). For example, measurements of the deepest part of the profile can significantly vary from measurements of the central profiles of the same mark. This shows that multiple cross-sections of a single mark, can vary in profile measurements, depending on the position in the mark where that profile was taken from (Keevil et al. 2018; Maté-González et al. 2015; Pante et al. 2017). Furthermore, the average time used to analyze one cut mark is considered too long (50 minutes) compared to other modern alternatives.

2.3.3 *3-D optical profilometry/metrology*

Advent of high-resolution 3D scanning methods in BSM studies steered scientists to develop discipline-wide, objective and replicable protocols for diagnosing effector (tools) from cut mark micromorphology (trace). Among such efforts, were Bello & Soligo (2008) who presented a scanning method that allowed 3D reconstruction of cut mark micromorphology and quantification of profile parameters. Their technique used quantitative measurements of cut mark cross-sectional shape, shoulder heights, sharpness as well as inclination and depth of a cut; to characterize cut marks based on tool effectors (Bello & Soligo, 2008). When developed the method was used to discriminate between experimentally created cut marks made by metal knife from unretouched flints (Bello & Soligo, 2008). The method was then expanded and applied to archaeological butchery marks made by handaxes (Bello et al. 2009), and to slicing marks found on human teeth (Bello, 2011). Boschin & Crezzini (2012) also conducted a 3D microscopic analyses of bone surfaces in order to identify origin of different kinds of marks on bones. They used a HIROX Digital Microscope KH-7700 to obtain morphometric measurements of cut marks (such as depth, breadth, angles etc.), which were then used as objective criteria for identifying origin of cut marks (effector tools) through statistical analyses. However, one of the greatest critiques for these pioneering 3D microscopic methods of studying BSMs, is lack of inter- analysts' reproducibility (Keevil, 2018; Pante et al. 2017). This limits the methods' ability to identify meaningful or informative trends in the micromorphological characteristics of cut marks (Keevil, 2018, p.22)

Recently, Pante et al. (2017) overcame the problems of replicability and testability in 3-D scanning methodologies, by creating a standardized and quantitative protocol for diagnosing cut marks, using 3D reconstruction and measurement of the micromorphological features (such as surface area, volume, depth, length etc.) of the cut mark. The replicability of this methodology has been tested using an inter-observer approach with promising results, which showed that this methodology is both replicable and accurate (Keevil et al. 2018; Pante et al. 2017). This protocol has been expanded and developed over the years to include models that distinguish cut marks from tooth marks with 97.5% accuracy (Pante et al. 2017), classification of different tooth marks based by actors or carnivore taxa (Muttart et al. 2017), assessing effects of fluvial action on cut mark micromorphology (Gumrukcu et al. 2018; Gumrukcu & Pante, 2018), and classifying cut marks made by specific raw material and technology types (Keevil, 2018; Keevil et al. 2018). Many of these studies were applied to archaeological samples with promising results. This study uses the same protocol in trying to predict raw material and technology type from HEB cut mark micromorphology.

## 2.4 Early Stone Age (ESA) Technology

The Early Stone Age marks a very crucial time in human history, as hominins, through tool making and use, were able to expand their niche for efficient access to animal carcass products. The ESA (Early Stone Age) is dominated by two well-known stone tool industries. The Oldest – Oldowan industry (from 2.8 to 1.6 million years ago), was as the name suggests, first discovered at Olduvai Gorge by Louis Leakey in 1930's (Leakey, 1936). The term "Oldowan" was first used by Louis Leakey in 1936 to describe materials at Olduvai Gorge predating Acheulian handaxes and cleaver industries, which at that time were already known to archaeologists (Leakey, 1936; Schick & Toth, 2006). Technology of the Oldowan industry is relatively simple and involves flexible breakage of cobbles in order to obtain sharp edges. The Oldowan toolkit is made up of several tool types such as flakes, choppers, hammer stones, scrappers, anvils, polyhedrons, discoids, occasional subspheroids and burins (Leakey, 1971; Schick & Toth, 2006).

Around 1.7Ma, the Oldowan industry was replaced by the Acheulian industry or techno-complex (de la Torre, 2016). The Acheulian industry is the second and the longest lasting in prehistory, lasting from 1.7 Ma to 0.1 Ma (de la Torre, 2016). Technology of the Acheulian industry is made up of: biface handaxes (usually ranging between 13 and 25 cm in length and shaping covers less than 50% of the surface), cutting tools (LCTs), cleavers, flakes, picks, and bifaces made on flakes and cobbles (de la Torre, 2016).

Research on emergence of the Acheulian technology or transition from Oldowan to Acheulian technology is still ongoing (Arroyo & de la Torre, 2018; Bibi et al. 2018; de la Torre et al. 2012; de la Torre & Mora, 2014; de la Torre, 2016; de la Torre et al. 2018; McHenry & Stanistreet, 2018; McHenry & de la Torre, 2018; Prassack et al. 2018; Uno et al. 2018). However, one of the central questions is whether these emerging bifacial tools (in the Acheulian industry) were used for the same butchery purposes as the Oldowan flake tools or served a different function, for example sexual selection (because of aesthetic properties presumed to be in the tear-dropped shaped of the Acheulian tools) (Kohn & Mithen, 1999; Mithen, 2003).

This study, and other research (Keevil, 2018; Maté-González et al. 2018; Yravedra et al. 2017) on cutmark micro-morphology can inform us on how different tool types (Oldowan flakes vs Acheulian bifaces) were used in an archaeological butchery event. Taphonomic studies on cut mark micro-morphometrics can identify specific ESA tool types used by hominins during butchery, and thus provide better understanding on butchery functions of different stone tool technologies of the ESA industries (Keevil, 2018; Maté-González et al. 2018; Yravedra et al. 2017).

2.4.1 *ESAs technology at HEB site, Olduvai Gorge*

Even with improved methods for studying cut mark micromorphology, there aren't many ESA sites that can offer well preserved cut marks that are in association with ESA artifacts (Bunn et al. 1986). Olduvai gorge is suitable for BSM studies, because it contains sites like HEB, that have well dated artifacts that are in association with cut marked fossils bones (Bunn, 1986; Bunn et al. 1986; Leakey & Roe, 1995). The HEB site is 0.9 million years old, and stratigraphically located in Lower Bed IV (geological beds at olduvai, identified by their sedimentological composition, color, and sometimes artifact composition). Based on artifacts assemblages (more than 40% handaxes) and temporal contexts, the HEB site is considered to be an Acheulian site, and is associated with the species *Homo erectus* (Leakey & Roe, 1994; Njau et al. 2020).

In terms of raw material distribution at the site, HEB site is dominated by quartzite and lava. Earliest well detailed accounts of raw materials found at the HEB site came from M.D Leakey's excavations during 1960's (Leakey & Roe, 1994) where she documented the raw material composition at HEB to be primarily quartzite (63.5%) and lava (a composite name used in this study to include phonolite, basalt and/or any volcanic rock) which made up 31.9%. In level 4, Leakey & Roe (1994), found that quartzite made up 81.4% of the total assemblage (n=1110), followed by basalt (lava), which made up 14.2% of the assemblage (see table 2.1).

Table 2. 1: Re-make of a table from Leakey & Roe (1994), showing ESA raw material distribution at HEB site (level 3 & 4).

| Stratigraphic Level | Quartzite* | Lava (Phonolite & Basalt) * | Chert |
|---|---|---|---|
| Level 3 | 588 | 315 | 0 |
| Level 4 | 903 | 203 | 0 |

**Quartzite (includes fine-grained quartzite), Lava (includes phonolite, basalt, trachyte, and other volcanic rocks). Unlike in Leakey & Roe (1995), this re-make of raw material distribution table should be interpreted independent of stone tool technology.*

Technology-wise, HEB has an abundance of flake tools and bifaces. Mary Leakey reported that out of 303 lithic materials recovered from HEB site (level 3), a significantly large portion (n=201) of the assemblage was made up of flakes (66.3%), while bifaces made up about 33% of the assemblage (n=100), and cores made up about 0.6% (n=2) of the assemblage. In level 4, she found that flakes made up about 72.5 % (eq. 158 specimens) of the total assemblage (n=218), followed by bifaces – which made up about 27.5% (60 specimens) of the assemblage. At level 4, Mary Leakey did not record any core tools (see Table 2.2).

Table 2. 2: Produced from table from Leakey & Roe (1994), showing ESA technology distribution at HEB site (level 3 & 4).

| Stratigraphic Level | Flake* | Biface | Cores |
|---|---|---|---|
| Level 3 | 201 | 100 | 2 |
| Level 4 | 158 | 60 | 0 |

Recently the HEB site was re-excavated by OGCP (Olduvai Gorge Coring Project) where they recovered several thousand ESA tools and fossil bones from multiple levels of their two trenches (T4 & T5) (Njau et al. 2020). While studies on the ESA artifacts (n = 3500) recovered by OGCP has not yet been published, preliminary findings indicating abundance of ESA artifacts associated with cut marked fossil fauna has been reported in Njau et al (2020). This study will be applying Keevil (2018) classification models on some of the cut marks found on these fossil bones recovered by OGCP at HEB T4 & T5.

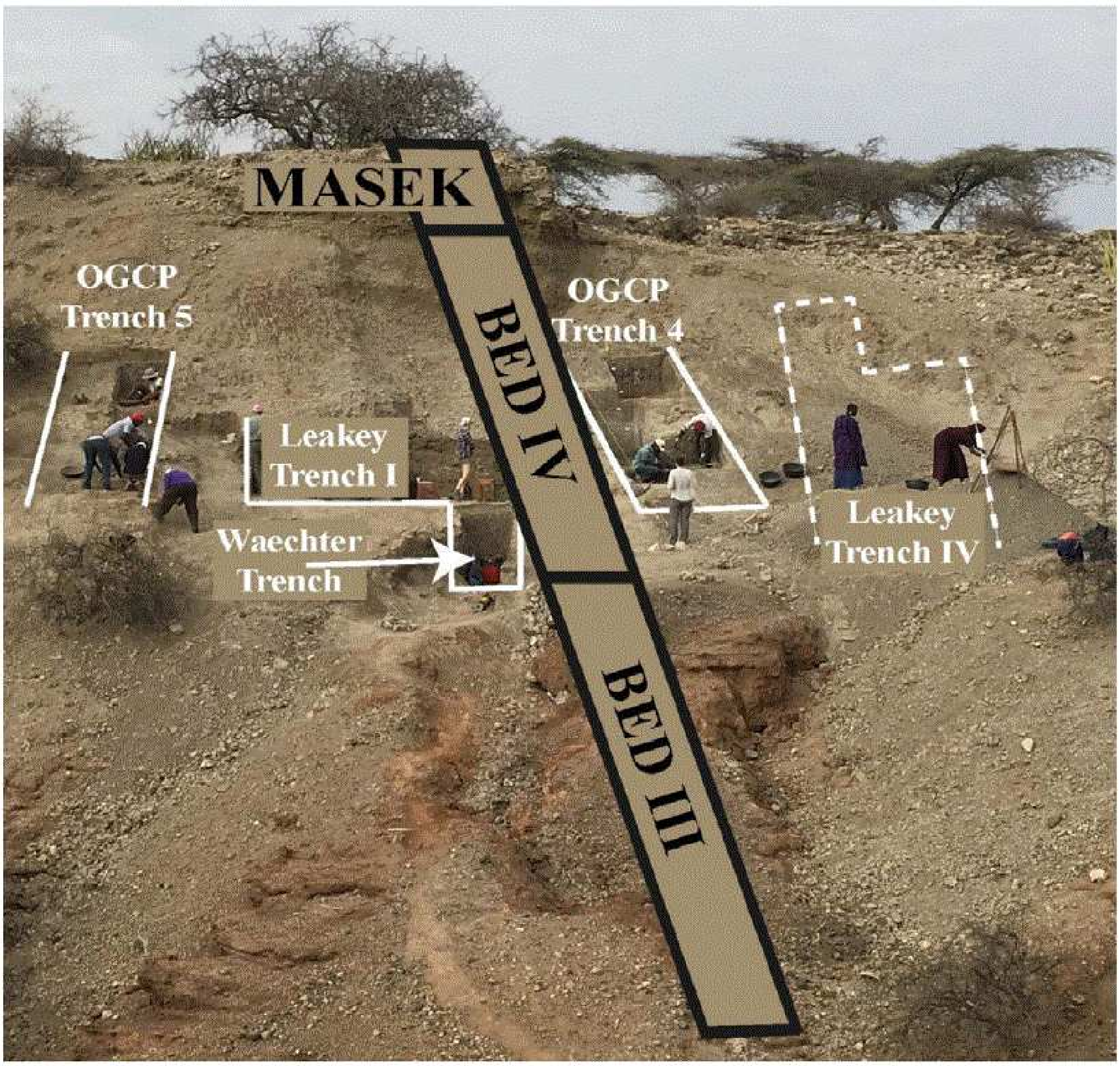


Figure 2. 1: Image showing the ongoing OGCP excavations at HEB site (OGCP Trench 4 & 5) and adjacent trenches that were excavated by Mary Leakey in 1960's. (source: Njau et al. 2020).

## 2.5 Cut mark utility on interpreting Homo erectus butchery behavior

Generally, the recovered cut mark traces from HEB site, offer significant taphonomic insights into how the assemblage was formed, and ecological behaviors of the actors (*H. erectus*). Presence of cut marks from butchery practices (defleshing, cutting, scraping and disarticulation of animal carcasses), are undisputed evidence for meat access by hominins. Higher frequency of cutmarks on a carcass, has been used infer early (first) access to those carcasses by hominins or access to significant quantities of meat resources by hominins, which implies hunting or aggressive scavenging mode of subsistence (Blumenschine, 1995; Blumenschine et al, 2007; Dominguez-Rodrigo & Barba, 2005; Dominguez-Rodrigo & Piquares, 2005; Dominguez-Rodrigo et al, 2010; Dominguez-Rodrigo et al, 2014; Egeland et al, 2004; Pante, 2010; Pante, 2012; Pante et al, 2012; Pickering & Dominguez-Rodrigo, 2006; Pobiner, 2007). Recent methods (Keevil, 2018; and this study) allows identification of the technology and raw material types that were used to create such cut mark traces – offering more insights into high order inferences of hominin behavioral ecology attributes such as: land use patterns (from relations such as original raw material sources and tool frequencies at a site), tool manufacture, tool use (such as differences in utility between tool made by different technologies – flakes and handaxes or between tools made of different raw materials, budgeting and resource allocation behaviors of hominins and many more.

# CHAPTER 3 MATERIALS AND METHODOLOGY

This study uses the 3D optical metrology protocols designed by Pante et al (2017) for collection and processing of cut mark micro-morphometrical data, and applies them to compare an actualistic database of cut mark measurements created by Keevil (2018) to interpret cut marks found on fossils in the HEB assemblage.

## 3.1 Experimental Sample

This study uses Keevil's (2018) experimental data to train, the multivariate Quadratic discriminant analysis models that use variations in cut mark micromorphology to diagnose (classify) specific raw materials and technology types (flakes and bifaces). The Keevil (2018) experimental data came from bones that were collected with an emphasis on keeping bone surface and materials as consistent as possible (Keevil, 2018). Keevil (2018) bone collection involved sectioned bovid femur and tibia midshafts that were obtained from Beaver's Market, a local butcher in Fort Collins, Colorado (Keevil, 2018). Those bones were sectioned transversely across the bone shaft using a mechanized bone saw. Then Keevil (2018) only used hind limb long bone midshafts in his study, in order to keep cortical bone density consistent throughout all cutting trials - allowing for better cut mark comparability and experimental control (p. 26).

All bones analyzed in Keevil (2018), were from size four bovid (in this case a cow), which includes all animals that weigh between 750 and 2000 pounds (based on animal size class definitions established by Bunn (1982) (Keevil, 2018). Keevil, then removed any remaining flesh from the surface of each bone using plastic knives and wooden skewers as to not alter the bone surface, leaving only the periosteum intact and preventing unintentional bone surface markings.

All bone surfaces were thoroughly inspected before proceeding with the study to identify pre-experimental bone surface marks. The location of these marks was noted to ensure that any pre-study bone surface modifications were not confused with experimentally created cut marks. The Keevil (2018), randomly assigned tibia and femur bones to each tool class during the cutting trial portion (Table 3.1). A total of 256 cut marks were made in this experiment and will be used in this study as the training dataset.

Table 3. 1:Number and type of hind limb bones used in Keevil (2018) for each cut mark group.

| **Cut mark group** | **ID** | **Bone** | **Cut mark group** | **ID** | **Bone** |
|---|---|---|---|---|---|
| Quartzite Biface | 1 | Tibia | Chert Biface | 1 | Tibia |
| | 2 | Femur | | 2 | Tibia |
| | 3 | Tibia | | 3 | Tibia |
| Quartzite Flake | 1 | Tibia | Chert Flake | 1 | Tibia |
| | 2 | Tibia | | 2 | Tibia |
| | 3 | Femur | | 3 | Femur |
| | 4 | Femur | | | |
| Basalt Biface | 1 | Femur | Phonolite Biface | 1 | Tibia |
| | 2 | Tibia | | 2 | Tibia |
| | 3 | Tibia | | | |
| Basalt Flake | 1 | Tibia | Phonolite Flake | 1 | Tibia |
| | 2 | Femur | | 2 | Femur |
| | 3 | Femur | | 3 | Tibia |

### 3.2 Archaeological Sample

The archaeological sample of fossil trace marks used in the study were collected from fossils recovered from the HEB site, by the OGCP (Olduvai Gorge Coring Project) research team. This site is dated to about 0.9 million years ago. This particular period is preferable for this study because it is contemporaneous with *Homo erectus* and Acheulian techno complex (Njau et al. 2020). Mary Leakey's excavation and analyses information regarding raw material and technological distribution for HEB site (Leakey & Roe, 1994), is also used here to inform interpretations in this study.

### 3.3 Diagnosing Cut Marks using 3D optical metrology

Cut marks traces on the fossilized bone surfaces were initially qualitatively identified by Dr. Michael Pante using natural light and a hand lens – in accordance to standard protocols described by Blumenschine et al (1996). Then a total of 110 cut marks from 66 fossil bones were scanned following Pante et al's (2017) protocol for BSM diagnosis. The scanning process was done on site, in one of OGCP's field laboratories at Olduvai Gorge – using SENSOFAR® S Neox non-contact 3D optical profilometer; which generated 3-dimentiaonal models of cut mark micromorphology that were viewed using Sensoview® software.

### 3.4 Processing 3D data using SensoMap Standard Version 7.4

All measurements and analysis of the 3D cut mark models were done in the 3-D imaging and analysis laboratory at Colorado State University (CSU), Fort Collins, Colorado. The 3D cut mark models were exported from the Sensoview® software to another software called Senso Map® (standard version 7.4) for metrological measurements. Out of the scanned 66 3D cutmarks, a sample of (*n*= 20) was non-randomly selected for measurements (Table 3.2), based on analytical criteria – mainly related to quality of the scan (3D model). Furthermore, cut marks that crossed on top of each other and cut marks that were superimposed on other types of marks (such as trampling, weathering etc.) were not selected for measurement.

Table 3. 2: Fossilized trace marks from HEB analyzed in this study.

| **ID** | **Skeletal Element** | **Body Size** | **Number of Marks** |
|---|---|---|---|
| HEBT4_L7_195-1 | Rib | Shaft | 1 |
| HEBT4_L7_232-1 | Tibia | Epiphysis | 1 |
| HEBT4_L8_147-1 | Lumbar | Spine | 1 |
| HEBT4_L8_188-1 | Femur | Midshaft | 1 |
| HEBT4_L8_223-1 | Femur | Midshaft | 1 |
| HEBT4_L8_232-1 | Femur | Midshaft | 1 |
| HEBT4_L8_294-2 | Radius/Ulna | Epiphysis | 1 |
| HEBT4_L8_351-1 | Long bone | Midshaft | 2 |
| HEBT4_L8_359-1a | Tibia | Near Epiphysis | 2 |
| HEBT4_L8_372-1 | Radius | Midshaft | 5 |
| HEBT4_L8_359-2 | Tibia | Near Epiphysis | 2 |
| HEBT4_L8_373-2 | Radius | Midshaft | 1 |
| HEBT4_L8_391-1 | Long bone | Midshaft | 1 |
| HEBT4_L8_468-2 | Tibia | Midshaft | 1 |

Using the SensoMap® software, the 3D cut mark models were processed, starting with an 'operators' studiable called "Extract layers" found in the software. This strips away visualization noise on the model to create a "topographic layer" as shown in the figures below.

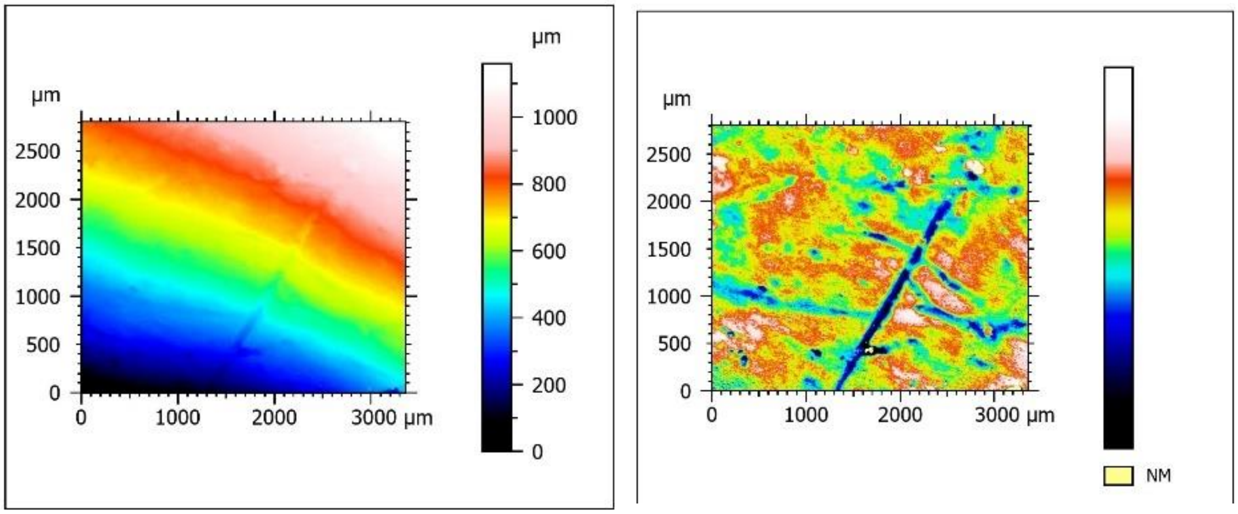


Figure 3. 1: Left image shows the original 3D cut mark model after importing it from Senso view®. Right image shows the same 3D model after removing the “3D layer” (also called Topographic layer). Color scales (on far right of both images) indicate depth, from (white = shallow) to Black = deep)

For marks that are slanted (this depends on how the bone or mark was positioned relative to the optical pen or objective during the scanning processes), it is good practice to rotate them into a straight vertical line and Pante et al (2017) has demonstrated that slanted marks can reduce accuracy of other measurements on the marks (measurements that require tracing of the mark to assign points).

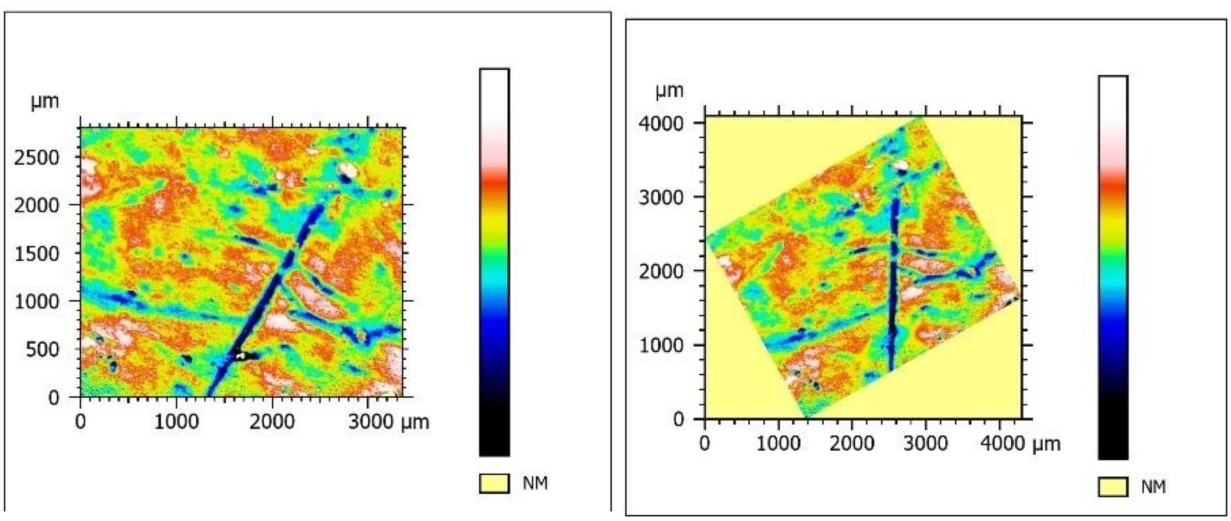


Figure 3. 2: left image shows a side-ways slanted 3D model of the mark. Right image shows the same 3D model after being rotated towards left one time – to make it vertically straight.

Then, an ‘operator’ studiable named “fill in NM” (fill in missing/non-measured points) was applied to the 3D models. This algorithm fills any missing points that were not captured during the scanning process. Then, influence of the shape of the bone on the actual shape of the cut marks was removed by the software’s algorithm, through an ‘operator’ studiable named “remove form” set at a polynomial degree of 2. Then, after applying the operator studiables - “threshold” (that defines extent of the mark’s profile) and “fill in NM” (for the second time); the area of the mark (by closely tracing the cut mark on the 3D model) was extracted using an operator studiable named “extract area”.

### 3.5 Measurements of 3D cut mark models

Similar to processing the 3D cut mark models above, the measurement process followed Pante et al (2017) protocol. Initial measurements included Maximum length (μm) and width measurements (μm), which were recorded using the “distance” tool provided by the SensoMap Standard Version 7.4® software. Length was taken as the maximum distance from one end of a cut mark to the other and could be measured in multiple increments if the cut mark was not straight. Width was recorded perpendicular to this length measurement and was taken along the widest part of the entire cut mark. Then, volume ($\mu m^3$), surface area ($\mu m^2$), maximum depth (3-D) (μm), and mean depth (μm) measurements were recorded using the “volume of a hole” function provided by the software.

During volume of a hole measurements, the software allows users to manually outline the boundary of a mark using a series of interconnected points and records the measurements from within this defined area (Figure 3.5 below). This tool uses a least squares plane parameter to create a covering overtop of the cut mark, which represents an estimation of the pre-cut mark bone surface and allows 3-dimensional volume measurements to be recorded from within this enclosure (Pante et al. 2017).

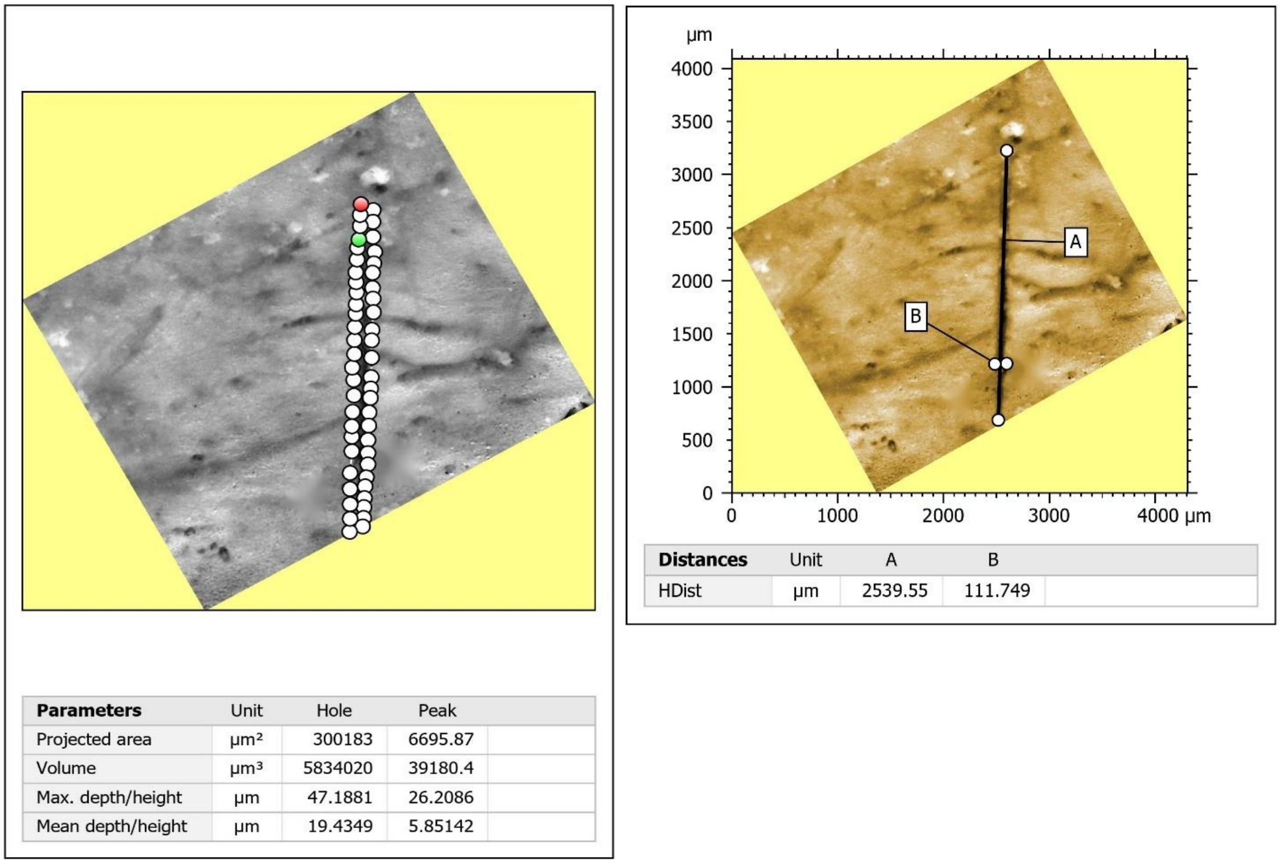


| Parameters | Unit | Hole | Peak |
|---|---|---|---|
| Projected area | µm² | 300183 | 6695.87 |
| Volume | µm³ | 5834020 | 39180.4 |
| Max. depth/height | µm | 47.1881 | 26.2086 |
| Mean depth/height | µm | 19.4349 | 5.85142 |

| Distances | Unit | A | B |
|---|---|---|---|
| HDist | µm | 2539.55 | 111.749 |

Figure 3. 3: volume of a hole measurement from a 3D model of the mark (left). This studiable yields multiple cut mark measurements such as surface area, volume, maximum and minimum depths or heights. Right image shows distance measurements of the mark (Length × Width) from a 3D model of the cut mark

### 3.6 Measurements of cut mark profiles

A profile was then extracted from the 3D cut mark model (through the lowest point in the mark). Following Pante et al (2017) protocol, variables measured from the extracted profile include depth, area, width, roughness (Ra), opening angle and floor radius. The "area of a hole" function was used to measure depth and area of mark profiles. The "under the waterline" option was used because it most accurately identified the edge of marks. The function works by filling in the mark to the lower of the two edges, effectively eliminating mark shoulders from influencing depth and area measurements. The use of the "under the waterline" option is important to enhance comparisons between cut marks on modern and fossilized bones where shoulders can be lost due to exfoliation or abrasion (Pante et al. 2017, p. 5).


| Parameters | Value | Unit |
|---|---|---|
| Maximum depth | 35.8637 | µm |
| Area of the hole | 2528.92 | µm² |

Figure 3. 4: image (above) showing profile measurements for area of a hole (under the waterline)

The maximum width, roughness, angle and floor radius measurements are based on the portion of each profile that reflects the actual mark. The x-coordinates for both edges of the mark were taken from the "area of a hole" studiable and the portion of the profile in between these coordinates was isolated using the "extract area" function. The length of the new profile was recorded as the maximum width of the mark. Roughness (Ra) was measured from the modified profile using the "parameters table" function of the program and is defined as the arithmetic mean deviation from the roughness profile, which is the mean line recorded in the evaluation length.

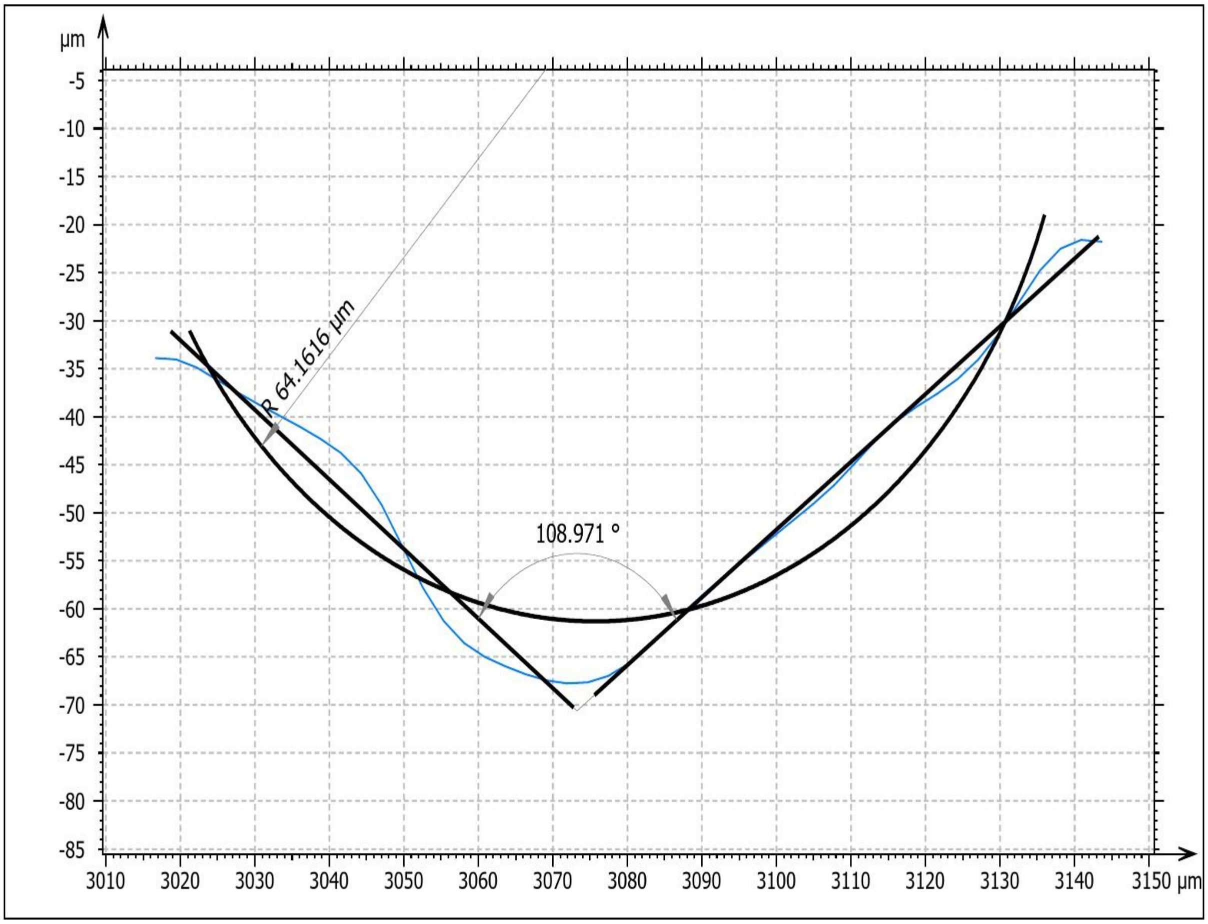


Figure 3. 5: image (above) showing cut marks profile measurements of the opening angle and floor radius

The "contour analysis" function was used to find the opening angle and floor radius of each mark (Figure 3.7). Opening angle was measured by first drawing two segments and then calculating the angle between them. One segment was drawn from the first measured point to the deepest point and another from the deepest point to the last measured point. The segments represent a best fit for all of the points between the two that are selected. The floor radius was found by drawing an arc between the first and last point of the profile. The arc represents a best fit for all of the points in the profile (Pante et al. 2017, p. 5)

## 3.7 Statistical analysis

Statistical analyses were performed using Microsoft Excel, PAST-Paleontological Statistics Software Package 4.03 and JMP® Pro 15.0.0 (SAS Institute Inc, 2019). Since the goal is to use Keevil (2018) experimental data and statistical model, this study followed all of Keevil's analytical procedures so as not to affect replicability of results.

### 3.7.1 *Data exploration*

Following Keevil et al (2018), cut mark data used in the analysis was grouped into eight categories based on the technological form and raw material of the tool that created each mark. Then, Shapiro-Wilks tests were used to identify whether each recorded measurement was normally distributed for all cut mark groups. These tests were conducted using the statistical PAST 4.03 software, and following Keevil (2018), measurements indicating the presence of at least one non-normally distributed group were corrected using Box-Cox transformations. Optimal lambda values (Table 4.1) for the Box-Cox transformations were calculated using the PAST software as well.

The final multivariate data exploration analysis done was predictor screening analysis, which examined contributions or influence of individual cut mark measurement to the models. In a much simpler version, the predictor Screening test on JMP software was useful in showing which cut mark measurements are more influenced by technological variations and less influenced by raw material variations, versus those that are more influenced by raw materials and less influenced by technological variations. This information is useful, even for future research in deciding best measurements (variables) to use as predictors for raw materials and or technology.

### 3.7.2 *Multivariate analysis: Quadratic discriminant analysis (QDA)*

Quadratic discriminant analyses (QDA), as a standard approach to supervised classification problems where within-group covariance matrices are not assumed equal - was used for this study. This was preferred because Keevil (2018) had already identified the lack of homogenous variance-covariance matrices across groups from the Box's M tests he had conducted in R (Keevil, 2018).

Quadratic discriminant analysis, models the likelihood of each class as a Gaussian or normal distribution, then uses the posterior distributions to estimate the class for a given test point (Srivastava et al. 2007). The Gaussian parameters for each class can be estimated from training points using maximum likelihood (ML) estimation. This Gaussian model assumption is best suited when there isn't much information to characterize a class. For example, if there are too few training samples to infer much about the class distributions (Srivastava et al. 2007). The QDA analyses done in this study, were performed using the "QDA" function found under the multivariate analysis in JMP® Pro 15.0.0.

A total of seven (7) quadratic discriminant models (QDA) were created using JMP® Pro 15.0.0. Three 'raw material' models, three (3) 'technology' models (using 3D measurements only, using profile measurements only, and using both 3D and Profile measurements) and finally, a comprehensive QDA model predicting both raw material and technology at once using all the 12 variables.

Before running the raw material model, a 'shrink covariances' option was checked (this was only done for the raw material model). This JMP algorism shrinks off the diagonal elements of covariances to improve stability and hence reduce variance of prediction. In all QDA models, a 90% (training): 10% (testing) split of the dataset was set on JMP for cross validation of the model's accuracy.

CHAPTER 4 RESULTS

## 4.1 Data exploration results

### 4.1.1 *Normalization: Box-Cox transformations*

Shapiro-Wilk tests for normality that was conducted individually on all measurements for each cut mark group (Appendix A and B), indicated a non-normal distribution for multiple cut mark groups. Therefore, a Box-Cox transformation was applied individually to all twelve variables (measurements) used in the study for both the experimental dataset (from Keevil, 2018) and the archaeological sample. Like Keevil (2018), the lambda values used in the transformation (Table 3.3) were automatically generated by the Paleontological Statistics Software (PAST).

Table 4. 1: Optimal lambda values applied for each Box-Cox measurement transformation.

| **Categories** | **Measurement (Variable)** | **Optimal Lambda values** |
|---|---|---|
| 3D Measurements | Surface Area (SA) | -0.103619 |
| | Volume (VOL) | -0.131457 |
| | Maximum Depth (MD) | -0.596197 |
| | Mean Depth (MEAN) | -0.2694409 |
| | Maximum Length (ML) | -0.210894 |
| | Maximum Width (MW) | -0.43252 |
| Profile Measurements | Maximum Depth (MDP) | -0.406873 |
| | Area (A) | -0.212219 |
| | Width (W) | -0.180908 |
| | Roughness (RA) | -0.102344 |
| | Angle (ANG) | 2.18259 |
| | Radius (RAD) | -0.194121 |

### 4.1.2 *Univariate detection for outliers*

The univariate distribution of the dataset analyzed in JMP made sure that categorical columns were coded correctly (checking for data recording errors, typos, or difference in coding after combining archaeological and experimental datasets), as well as checking for univariate outliers for individual measurements groups (Figure 4.1). Comprehensive results (distribution, quantile and summary statistics) of the univariate distributions for each measurement, are attached at the end of this study (Appendix B), and they depict box plot distribution of each measurement (row) as well as outliers found on those measurements.

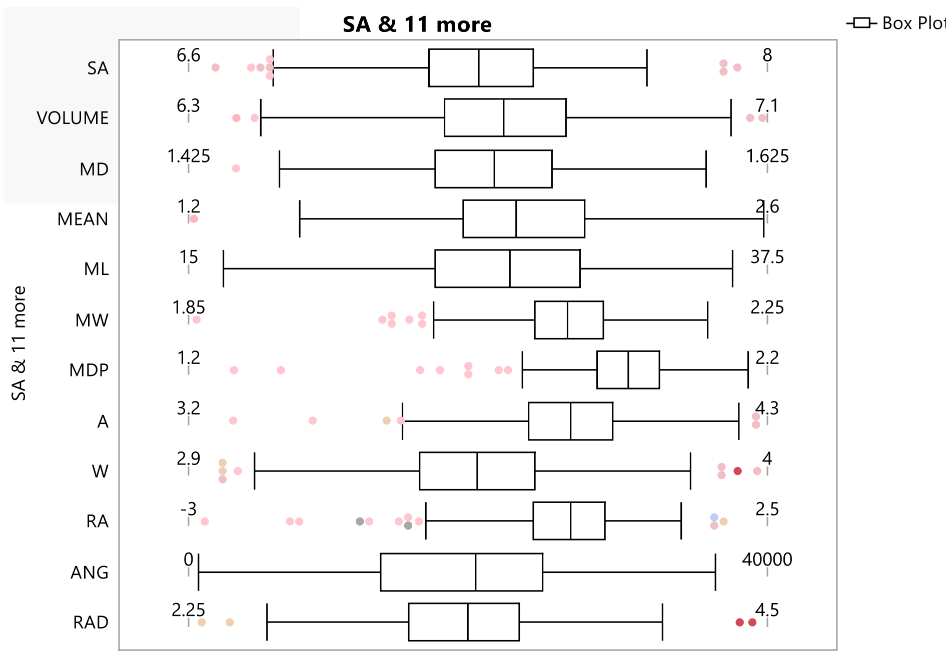


Figure 4. 1: Univariate Box Plot distribution showing rows that have outliers for each of the 12 numeric variables (columns) in the combined dataset/table (experimental + archaeological tables)

4.1.2 *Predictor Screening analyses*

The final multivariate data exploration analyses examined contributions or influence of individual cut mark measurement to the models. In a much simpler version, the predictor Screening test on JMP software was useful in showing which cut mark measurements are more influenced by technological variations and less influenced by raw material variations, versus those that are more influenced by raw materials and less influenced by technological variations. This information is useful, even for future research in deciding best measurements (variables) to use as predictors for raw materials and or technology.

Table 4. 2: Experimental dataset- Predictor Screening for "TECHNOLOGY" Model

| Predictor | Contribution | Portion | Rank |
|---|---|---|---|
| SA | 6.1751 | 0.0816 | 5 |
| VOLUME | 6.6891 | 0.0884 | 4 |
| MD | 2.7311 | 0.0361 | 12 |
| MEAN | 4.5520 | 0.0602 | 8 |
| ML | 10.9488 | 0.1447 | 2 |
| MW | 15.2384 | 0.2014 | 1 |
| MDP | 3.2044 | 0.0424 | 10 |
| A | 7.8706 | 0.1040 | 3 |
| W | 5.9571 | 0.0787 | 6 |
| RA | 2.8818 | 0.0381 | 11 |
| ANG | 4.3934 | 0.0581 | 9 |
| RAD | 5.0213 | 0.0664 | 7 |

****Top 3 best contributors (in green) and top 3 least contributors (in red)*

Table 4. 3: Experimental dataset – Predictor Screening for "RAW MATERIAL" Model

| Predictor | Contribution | Portion | Rank |
|---|---|---|---|
| SA | 4.6540 | 0.0615 | 6 |
| VOLUME | 10.3851 | 0.1372 | 2 |
| MD | 7.6646 | 0.1012 | 4 |
| MEAN | 15.3330 | 0.2025 | 1 |
| ML | 4.4398 | 0.0586 | 7 |
| MW | 4.2835 | 0.0566 | 9 |
| MDP | 6.2085 | 0.0820 | 5 |
| A | 7.7643 | 0.1026 | 3 |
| W | 4.2417 | 0.0560 | 10 |
| RA | 4.0581 | 0.0536 | 11 |
| ANG | 4.2886 | 0.0566 | 8 |
| RAD | 2.3829 | 0.0315 | 12 |

****Top 3 best contributors (in green) and top 3 least contributors (in red)*

## 4.2 Multivariate analyses results: Quadratic discriminant analyses (QDA)

A total of seven (7) quadratic discriminant models (QDA) were created using JMP® Pro 15.0.0. Three 'raw material' models, three (3) 'technology' models (using 3D measurements only, using profile measurements only, and using both 3D and Profile measurements) and finally, a comprehensive QDA model predicting both raw material and technology at once using all the 12 variables. Only results for the three models (Raw material only, technology only, and ALL) will be shown in this chapter, along with the 20 discriminant scores from predicting the unknown (archaeological/testing) datasets. A more comprehensive table that also includes all 256 training discriminant scores (from the labeled experimental dataset) is attached at the end of this study (Appendix B & C).

### *4.2.1 QDA Raw material Model*

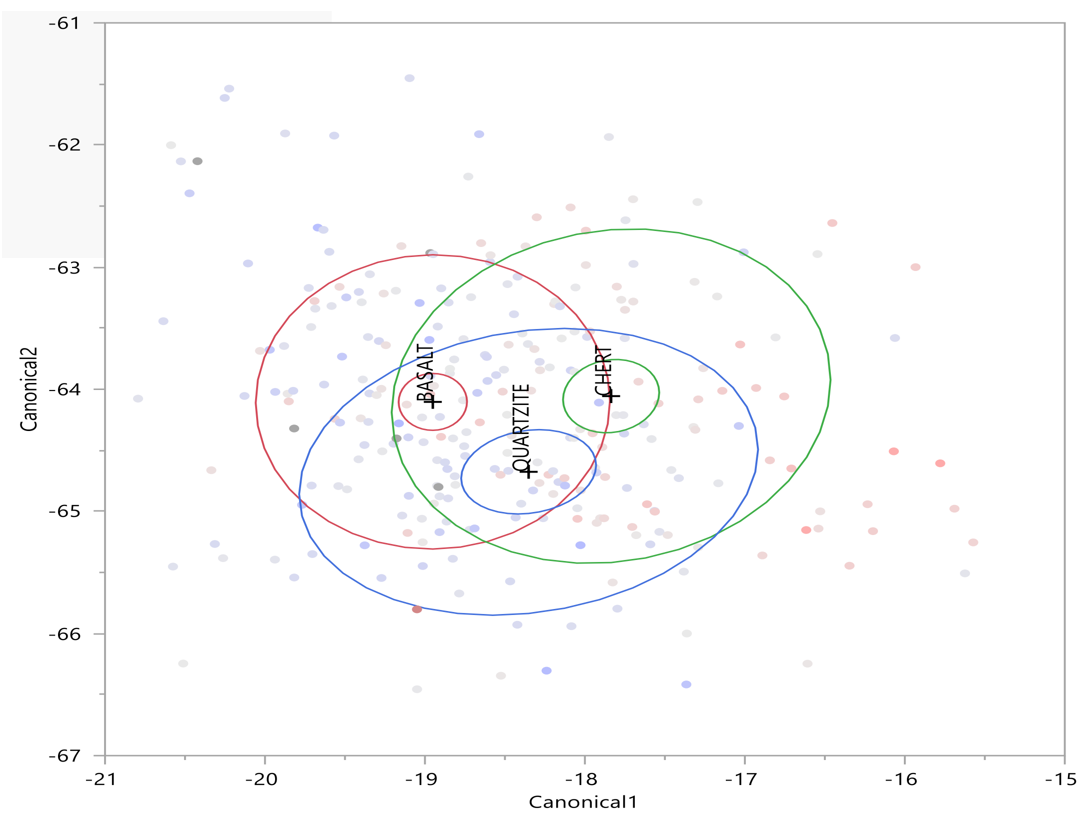


Figure 4. 2: QDA Canonical plot showing classification of raw materials

Table 4. 4: Shrinkage Details

| Overall Shrinkage | Overall Lambda |
|---|---|
| 0.97809 | 0.02191 |

| RAW MATERIALS | Shrinkage | Lambda |
|---|---|---|
| BASALT | 0.94355 | 0.05645 |
| CHERT | 0.95823 | 0.04177 |
| QUARTZITE | 0.84463 | 0.15537 |

Table 4. 5: Score Summaries (experimental or training dataset) – Raw material model

| Source | Count | Number Misclassified | Percent Misclassified | Entropy Rsquare | -2LogLikelihood |
|---|---|---|---|---|---|
| Training | 256 | 90 | 35.1563 | 0.31783 | 365.047 |

Table 4. 6: Confusion matrix – Raw material model

| Actual | Predicted Count | | |
|---|---|---|---|
| RAW MATERIALS | BASALT | CHERT | QUARTZITE |
| LAVA | 98 | 7 | 11 |
| CHERT | 34 | 51 | 5 |
| QUARTZITE | 23 | 10 | 17 |

| RAW MATERIALS | Count |
|---|---|
| LAVA | 116 |
| CHERT | 90 |
| QUARTZITE | 50 |

Table 4. 7: Discriminant Scores (Archaeological or Testing dataset) – Raw material model

| Row | Actual | Predicted | Prob (Pred) | Others |
|---|---|---|---|---|
| 1 | HEBT4_L7_232-1 | LAVA | 0.8915 | QUARTZITE 0.11 |
| 2 | HEBT4_L8_147-1 | QUARTZITE | 0.5114 | LAVA 0.49 |
| 3 | HEBT4_L8_223-1 | QUARTZITE | 0.7246 | LAVA 0.16 CHERT 0.12 |
| 4 | HEBT4_L8_294-2 | LAVA | 0.7848 | QUARTZITE 0.21 |
| 5 | HEBT4_L8_359-2 | QUARTZITE | 0.9020 | LAVA 0.25 QUARTZITE 0.22 |
| 6 | HEBT4_L8_359-2b | QUARTZITE | 0.5274 | LAVA 0.23 CHERT 0.24 |
| 7 | HEBT4_L8_372-3a | QUARTZITE | 0.5209 | LAVA 0.39 |
| 8 | HEBT4_L8_372-3b | QUARTZITE | 0.4306 | LAVA 0.40 CHERT 0.17 |
| 9 | HEBT4_L8_373-2 | CHERT | 0.9272 | LAVA 0.23 QUARTZITE 0.38 |
| 10 | HEBT4_L7_195-1 | LAVA | 0.6092 | QUARTZITE 0.37 |
| 11 | HEBT4_L8_351-2 | CHERT | 0.9933 | |
| 12 | HEBT4_L8_372-4 | QUARTZITE | 0.5055 | LAVA 0.34 CHERT 0.16 |
| 13 | HEBT4_L8_391-1 | LAVA | 0.9155 | CHERT 0.12 |
| 14 | HEBT4_L8_359-1a | LAVA | 0.9219 | |
| 15 | HEBT4_L8_188-1 | LAVA | 0.9714 | |
| 16 | HEBT4_L8_232-1 | LAVA | 0.9558 | |
| 17 | HEBT4_L8_351-1 | LAVA | 1.0000 | |
| 18 | HEBT4_L8_372-1 | LAVA | 0.9839 | |
| 19 | HEBT4_L8_468-2 | LAVA | 0.9652 | |
| 20 | HEBT4_L8_359-1b | LAVA | 1.0000 | |

The QDA raw material model classifying cut marks made by tools of different raw materials (Basalt, Chert and Quartzite) had about 65% accuracy (Table 4.4). Out of the 20 archaeological samples, 55% (11 samples) were classified as Lava (Basalt & Phonolite), with a mean posterior probability of 90%. 35% (7 archaeological samples) were classified as quartzite with a mean posterior probability of 60%, and 10% (2 archaeological samples) were classified as chert, with a mean posterior probability of about 96% (see Table 4.6).

*4.2.2 QDA Technology Model*

| | |
|---|---|
| Discriminant Method: | Quadratic |
| Classification: | TECHNOLOGY |

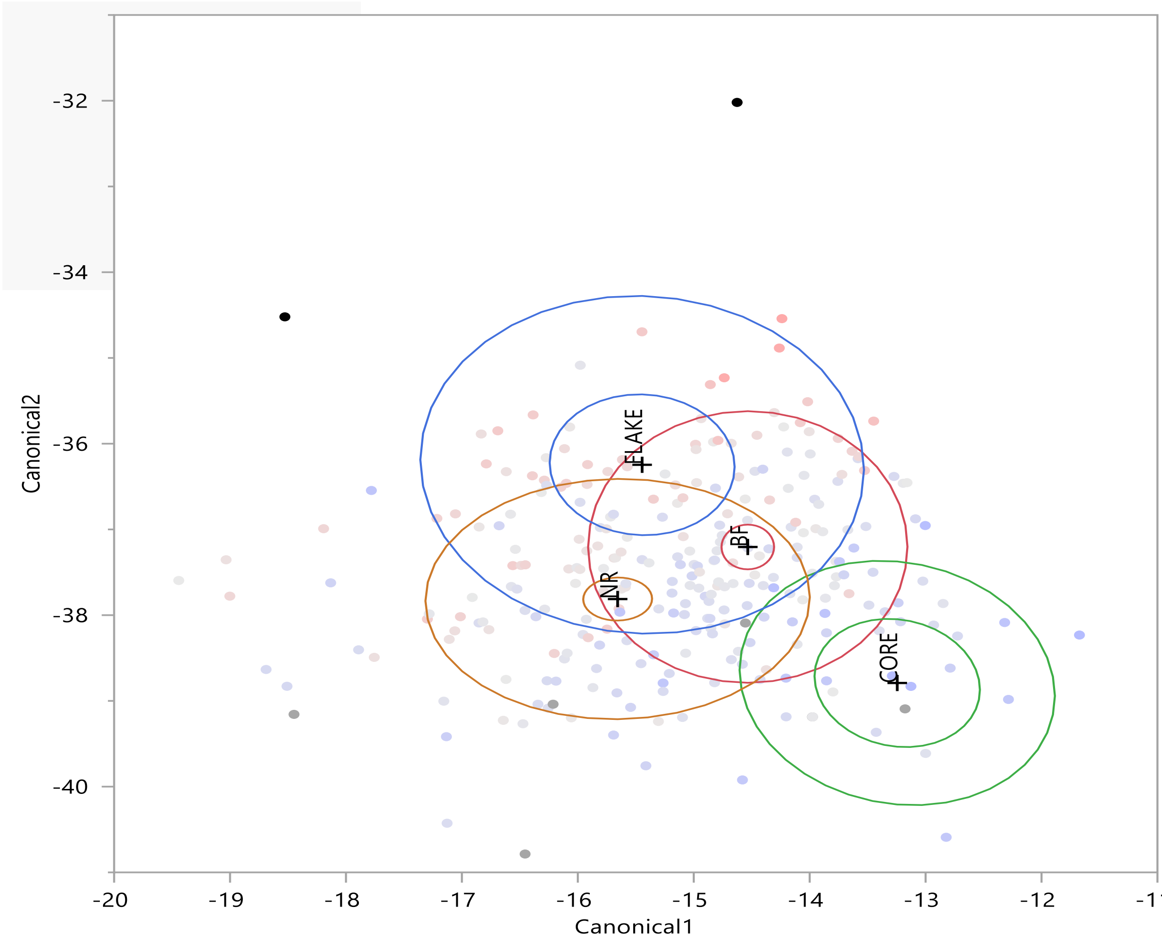


Figure 4. 3: QDA Canonical plot showing classification of technology

Table 4. 8: Score Summaries – Technology model

| Source | Count | Number Misclassified | Percent Misclassified | Entropy RSquare | -2LogLikelihood |
|---|---|---|---|---|---|
| Training | 256 | 58 | 22.6563 | 0.49763 | 271.617 |

Table 4. 9: Confusion matrix – Technology model

| Actual | Predicted Count | | | |
|---|---|---|---|---|
| TECHNOLOGY | BF | CORE | FLAKE | NR |
| BF (Biface) | 89 | 3 | 3 | 27 |
| CORE | 2 | 10 | 0 | 0 |
| FLAKE | 1 | 0 | 18 | 0 |
| NR (No retouch flake) | 20 | 1 | 1 | 81 |

**Groups**

| TECHNOLOGY | Count |
|---|---|
| BF (Biface) | 122 |
| CORE | 12 |
| FLAKE | 19 |
| NR (No retouch flake) | 103 |

Table 4. 10: Discriminant Scores (Archaeological or Testing dataset) – Technology model

| Row | Actual | Predicted | Prob (Pred) | Others |
|---|---|---|---|---|
| 1 | HEBT4_L7_232-1 | NR | 0.9992 | |
| 2 | HEBT4_L8_147-1 | NR | 0.9998 | |
| 3 | HEBT4_L8_223-1 | BF | 0.9524 | |
| 4 | HEBT4_L8_294-2 | NR | 0.6533 | BF 0.35 |
| 5 | HEBT4_L8_359-2 | NR | 0.9311 | |
| 6 | HEBT4_L8_359-2b | BF | 0.8437 | NR 0.16 |
| 7 | HEBT4_L8_372-3a | NR | 0.8639 | BF 0.14 |
| 8 | HEBT4_L8_372-3b | NR | 0.9952 | |
| 9 | HEBT4_L8_373-2 | BF | 0.9001 | |
| 10 | HEBT4_L7_195-1 | NR | 0.8556 | BF 0.14 |
| 11 | HEBT4_L8_351-2 | NR | 1.0000 | |
| 12 | HEBT4_L8_372-4 | NR | 0.9999 | |
| 13 | HEBT4_L8_391-1 | NR | 0.9892 | |
| 14 | HEBT4_L8_359-1a | NR | 0.9997 | |
| 15 | HEBT4_L8_188-1 | NR | 0.9960 | |
| 16 | HEBT4_L8_232-1 | BF | 0.6835 | NR 0.32 |
| 17 | HEBT4_L8_351-1 | NR | 0.9978 | |
| 18 | HEBT4_L8_372-1 | NR | 0.9538 | |
| 19 | HEBT4_L8_468-2 | NR | 0.9952 | |
| 20 | HEBT4_L8_359-1b | NR | 1.0000 | |

The QDA technology model classifying cut marks made by tools of different technologies (BF, CORE, FLAKE, and NR) had about 77% accuracy (Table 4.7). Out of the 20 archaeological samples, 80% (16 samples) were classified as NR (No retouch flake), with a mean posterior probability of 96%. On the other hand, 20% (4 archaeological samples) were classified as BF (biface) with a mean posterior probability of about 85% (see Table 4.9).

*<u>4.2.3 QDA Technology + Raw material (ALL) Model</u>*

Discriminant Method: Quadratic
Classification: ALL (Raw material + Technology)

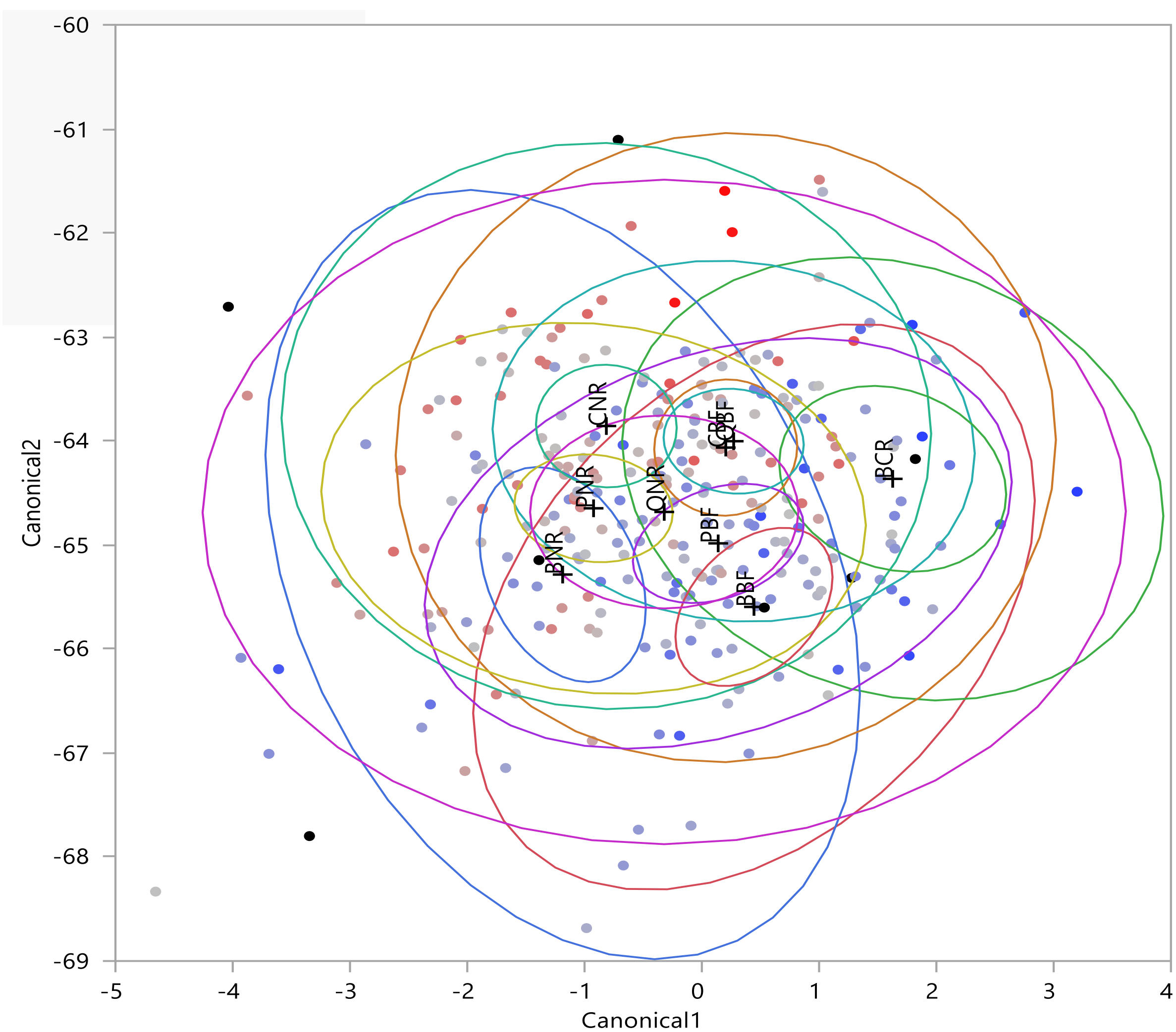


Figure 4. 4: QDA Canonical plot showing classification for both technology and raw material groups combined

Table 4. 11: Score Summaries – ALL model (raw material + technology)

| Source | Count | Number Misclassified | Percent Misclassified | Entropy RSquare | -2LogLikelihood |
|---|---|---|---|---|---|
| Training | 256 | 81 | 31.6406 | 0.58268 | 456.79 |

Table 4. 12: Confusion matrix – ALL model (raw material + technology)

| Actual | Predicted Count | | | | | | | | |
|---|---|---|---|---|---|---|---|---|---|
| ALL | BBF | BCR | BNR | CBF | CNR | PBF | PNR | QBF | QNR |
| BBF | 20 | 0 | 1 | 0 | 1 | 3 | 1 | 0 | 1 |
| BCR | 0 | 11 | 0 | 0 | 0 | 0 | 0 | 0 | 1 |
| BNR | 0 | 0 | 18 | 0 | 2 | 0 | 0 | 0 | 7 |
| CBF | 1 | 1 | 2 | 22 | 9 | 1 | 3 | 1 | 5 |
| CNR | 1 | 0 | 1 | 0 | 31 | 1 | 1 | 0 | 10 |
| PBF | 0 | 0 | 1 | 0 | 2 | 17 | 1 | 1 | 3 |
| PNR | 0 | 0 | 0 | 0 | 2 | 0 | 21 | 1 | 1 |
| QBF | 0 | 2 | 0 | 0 | 3 | 0 | 0 | 14 | 6 |
| QNR | 1 | 0 | 0 | 0 | 1 | 1 | 1 | 0 | 21 |

Table 4. 13: Discriminant Scores - ALL model (raw material + technology).

| Row | Actual | Predicted | Prob (Pred) | Others |
|---|---|---|---|---|
| 1 | HEBT4_L7_232-1 | LBF | 0.5491 | BNR 0.45 |
| 2 | HEBT4_L8_147-1 | LBF | 1.0000 | |
| 3 | HEBT4_L8_223-1 | CNR | 0.8601 | QBF 0.14 |
| 4 | HEBT4_L8_294-2 | LBF | 0.9989 | |
| 5 | HEBT4_L8_359-2 | LBF | 0.9996 | |
| 6 | HEBT4_L8_359-2b | CNR | 0.7972 | BBF 0.19 |
| 7 | HEBT4_L8_372-3a | LNR | 0.3982 | CBF 0.10 CNR 0.11 PNR 0.38 |
| 8 | HEBT4_L8_372-3b | LNR | 0.9998 | |
| 9 | HEBT4_L8_373-2 | CBF | 0.8068 | CNR 0.11 |
| 10 | HEBT4_L7_195-1 | CNR | 0.9686 | |
| 11 | HEBT4_L8_351-2 | LNR | 0.9139 | |
| 12 | HEBT4_L8_372-4 | LNR | 0.5397 | CBF 0.46 |
| 13 | HEBT4_L8_391-1 | LNR | 0.9817 | |
| 14 | HEBT4_L8_359-1a | LBF | 0.6717 | BNR 0.33 |
| 15 | HEBT4_L8_188-1 | LBF | 1.0000 | |
| 16 | HEBT4_L8_232-1 | LBF | 1.0000 | |
| 17 | HEBT4_L8_351-1 | LBF | 1.0000 | |
| 18 | HEBT4_L8_372-1 | LBF | 1.0000 | |
| 19 | HEBT4_L8_468-2 | LNR | 0.6894 | BBF 0.31 |
| 20 | HEBT4_L8_359-1b | LBF | 1.0000 | |

The final QDA model 'ALL' (combining raw materials + technology) classified cut marks made by tools of different technologies and raw materials classes/types; LBF (Lava Biface), LNR (Lava No retouch flake), CBF (Chert Biface), CNR (Chert No retouch flake), with 68.4% accuracy (Table 4.10). Out of the 20 archaeological samples, 50% (10 samples) were classified as LBF, with mean posterior probability of 92%. 15% (3 archaeological samples) were classified as CNR with mean probability of 88%. 30% (6 archaeological samples) were classified as LNR with a mean posterior probability of 80%. And finally, 5% (1 archaeological sample) was classified as CBF with mean posterior probability of about 81% (see Table 4.12).

### *4.2.3 Conflicts between models and arbitration*

The three QDA models had different classification accuracies, with the combined model (technology + raw material) having the lowest classification accuracy. Following Keevil (2018), the tool raw material and technology classifications of each archaeological cut mark were recorded and compared between the tool technology only QDA model, the raw material only QDA model and technology + raw material (ALL) QDA models. Eleven of the 20 fossil marks analyzed in this thesis had agreeing raw material classifications in both the raw material only and the combined (raw material + technology) discriminant models (Table 4.13). Fossil mark technology classifications were assessed by comparing the tool classifications in the technology only model and the combinative discriminant model as well. Only nine of the 20 fossil cut marks had agreeing raw material classifications in both the raw material only and combinative discriminant models (Table 4.13). The first and second posterior probabilities of the 11 cut marks that recorded conflicting tool characteristic classifications were recorded to visualize the classification confidences of each model (Table 4.13; Table 4. 14 and Table 4. 15).

Table 4. 14: HEB Fossil trace mark classifications based on the Tool Technology Only, Raw Material Only, and Tool Technology and Raw Material (ALL) discriminant models. Bolded ID numbers indicate fossils that had differing tool technology classifications between models. Starred ID numbers indicate fossils that had differing raw material classifications between models.

| ID | Skeletal Element | Cut Mark location | Raw Material only | Technology only | Raw material + Technology |
|---|---|---|---|---|---|
| **HEBT4_L7_232-1** | Tibia | Epiphysis | Lava | Flake | Lava Biface |
| **HEBT4_L8_147-1*** | Lumbar | Spine | Quartzite | Flake | Lava Biface |
| **HEBT4_L8_223-1*** | Femur | Midshaft | Quartzite | Biface | Chert Flake |
| **HEBT4_L8_294-2** | Radius/Ulna | Epiphysis | Lava | Flake | Lava Biface |
| **HEBT4_L8_359-2*** | Tibia | Near Epiphysis | Quartzite | Flake | Lava Biface |
| **HEBT4_L8_359-2b*** | Tibia | Near Epiphysis | Quartzite | Biface | Chert Flake |
| HEBT4_L8_372-3a* | Radius | Midshaft | Quartzite | Flake | Lava Flake |
| HEBT4_L8_372-3b* | Radius | Midshaft | Quartzite | Flake | Lava Flake |
| HEBT4_L8_373-2 | Radius | Midshaft | Chert | Biface | Chert Biface |
| HEBT4_L7_195-1* | Rib | Shaft | Lava | Flake | Chert Flake |
| HEBT4_L8_351-2* | Long bone | Midshaft | Chert | Flake | Lava Flake |
| HEBT4_L8_372-4* | Radius | Midshaft | Quartzite | Flake | Lava Flake |
| HEBT4_L8_391-1 | Long bone | Midshaft | Lava | Flake | Lava Flake |
| **HEBT4_L8_359-1a** | Tibia | Near Epiphysis | Lava | Flake | Lava Biface |
| **HEBT4_L8_188-1** | Femur | Midshaft | Lava | Flake | Lava Biface |
| HEBT4_L8_232-1 | Femur | Midshaft | Lava | Biface | Lava Biface |
| **HEBT4_L8_351-1** | Long bone | Midshaft | Lava | Flake | Lava Biface |
| **HEBT4_L8_372-1** | Radius | Midshaft | Lava | Flake | Lava Biface |
| HEBT4_L8_468-2 | Tibia | Midshaft | Lava | Flake | Lava Flake |
| **HEBT4_L8_359-1b** | Tibia | Near Epiphysis | Lava | Flake | Lava Biface |

Table 4. 15: First posterior probabilities for the HEB cut marks that had disagreeing classifications in the technology only QDA model. Second posterior probabilities are only shown in the raw material and tool technology model when the first posterior probability is less than 95%.

| | **Technology Model** | | **Raw Material + Technology (ALL) Model** | | |
|---|---|---|---|---|---|
| **ID** | *Classification* | *1st Posterior Probability* | *Classification* | *1st Posterior Probability* | *2nd Posterior Probability* |
| HEBT4_L7_232-1 | Flake (NR) | 99% | Lava Biface (LBF) | 54% | 45% Lava Flake (LNR) |
| HEBT4_L8_147-1 | Flake (NR) | 99% | Lava Biface (LBF) | 100% | |
| HEBT4_L8_223-1 | Biface (BF) | 95% | Chert Flake (CNR) | 86% | 14% Quartzite Biface |
| HEBT4_L8_294-2 | Flake (NR) | 65% | Lava Biface (LBF) | 99% | |
| HEBT4_L8_359-2 | Flake (NR) | 93% | Lava Biface (LBF) | 99% | |
| HEBT4_L8_359-2b | Biface (BF) | 84% | Chert Flake (CNR) | 80% | 20% Lava Biface |

| | | | | | |
|---|---|---|---|---|---|
| HEBT4_L8_359-1a | Flake (NR) | 99% | Lava Biface (LBF) | 67% | 33% Lava Flake (LNR) |
| HEBT4_L8_188-1 | Flake (NR) | 99% | Lava Biface (LBF) | 100% | |
| HEBT4_L8_351-1 | Flake (NR) | 99% | Lava Biface (LBF) | 100% | |
| HEBT4_L8_372-1 | Flake (NR) | 95% | Lava Biface (LBF) | 100% | |
| HEBT4_L8_359-1b | Flake (NR) | 100% | Lava Biface (LBF) | 100% | |

Table 4. 16: First posterior probabilities for the HEB cut marks that had disagreeing classifications in the raw material only QDA model. Second posterior probabilities are only shown in the raw material and tool technology model when the first posterior probability is less than 95%.

| ID | **Raw Material Model** | | **Raw Material + Technology (ALL) Model** | | |
|---|---|---|---|---|---|
| | Classification | 1st Posterior Probability | Classification | 1st Posterior Probability | 2nd Posterior Probability |
| HEBT4_L8_147-1 | Quartzite | 51% | Lava Biface (LBF) | 100% | |
| HEBT4_L8_223-1 | Quartzite | 72% | Chert Flake (CNR) | 86% | 14% Quartzite Biface |
| HEBT4_L8_359-2 | Quartzite | 90% | Lava Biface (LBF) | 99% | |
| HEBT4_L8_359-2b | Quartzite | 52% | Chert Flake (CNR) | 80% | 20% Lava Biface |
| HEBT4_L8_372-3a | Quartzite | 52% | Lava Flake (LNR) | 79% | 10% Chert Biface<br>11% Chert Flake |
| HEBT4_L8_372-3b | Quartzite | 43% | Lava Flake (LNR) | 99% | |
| HEBT4_L7_195-1 | Basalt | 60% | Chert Flake (CNR) | 96% | |
| HEBT4_L8_351-2 | Chert | 99% | Lava Flake (CNR) | 91% | |
| HEBT4_L8_372-4 | Quartzite | 50% | Lava Flake (LNR) | 54% | 46% Chert Biface |

Following Keevil's (2018) strategy to solve the classification conflicts across models, when the HEB cut marks reported conflicting tool characteristic classifications, between either the technology only and the combined (technology and raw material) models, or between the raw material only and the combined (technology and raw material) models; further assessment was conducted by investigating the posterior probabilities of each model. When one discriminant model reported a significantly larger first posterior probability than the other discriminant model, the tool characteristic classification with the larger first posterior probability was deemed more accurate (Keevil, 2018, p.85). Based on this strategy, this study was able to assign the most accurate classification for all HEB cut marks (Table 4.16)

Table 4. 17: Final ESA Tool classifications (Technology + Raw material) for the 20 HEB cut marks analyzed. Cut mark classifications are based on the posterior probability data of each cut mark reported in the technology only QDA model, raw material only QDA model, and tool technology/raw material QDA model.

| HEB Cut Mark | ESA Tool Classification |
|---|---|
| HEBT4_L7_232-1 | Lava Flake |
| HEBT4_L8_147-1 | Lava Biface |
| HEBT4_L8_223-1 | Quartzite Biface |
| HEBT4_L8_294-2 | Lava Biface |
| HEBT4_L8_359-2 | Lava Biface |
| HEBT4_L8_359-2b | Quartzite Biface |
| HEBT4_L8_372-3a | Lava Flake |
| HEBT4_L8_372-3b | Lava Flake |
| HEBT4_L8_373-2 | Biface tool (unknown raw material) |
| HEBT4_L7_195-1 | Flake tool (unknown raw material) |
| HEBT4_L8_351-2 | Lava Flake |
| HEBT4_L8_372-4 | Lava Flake |
| HEBT4_L8_391-1 | Lava Flake |
| HEBT4_L8_359-1a | Lava Flake |
| HEBT4_L8_188-1 | Lava Biface |
| HEBT4_L8_232-1 | Lava Flake |
| HEBT4_L8_351-1 | Lava Biface |
| HEBT4_L8_372-1 | Lava Biface |
| HEBT4_L8_468-2 | Lava Flake |
| HEBT4_L8_359-1b | Lava tool (Unknown technology) |

However, there were instances where archaeological cut marks reported disagreeing raw material classifications in the raw material only model and the tool technology and raw material model with similar or identical posterior probabilities in each model. For example, cut mark ID: HEBT4-L8_359-1b (Table 4.16) was classified as a flake in the technology only model, and as a biface in the combined (technology + raw material) model, with both models having 100%

posterior probabilities. Therefore, this archaeological cut mark was classified as being created by a lava tool of unknown technology type. Other misclassifications that were impossible to identify, was when archaeological cut marks were classified as being made by chert raw material types in both the raw material only model and the combined (technology + raw material) model. Since there is no evidence supporting use or presence of any chert artifact or chert raw material sources at the HEB T4 & T5 (Leakey & Roe, 1994) all cut marks classified as chert were considered to be of “unknown raw material types” despite their posterior probabilities in the models. .

# CHAPTER 5 DISCUSSION

## 5.1 Using cut mark micromorphology to predict stone tool technology and raw material types

The importance of understanding what technology or raw material was used by hominins during butchery cannot be underestimated. The study has implications to broader aspects of hominin behavioral ecology (Blumenschine et al. 1994; Blumenschine & Pobiner, 2007) as it contributes to our understanding of strategies employed by *H. erectus* during butchery as they attempted to minimize costs of extracting the high-caloric meat resources that could fund the metabolic demands of evolving and maintaining bigger brains (Bunn, 2006; Isler & Van Schaik, 2014; Pante, 2010; Pante, 2013; Ungar, 2006). This study used optical profilometry to obtain quantitative data (cut mark measurements) that could diagnose technology and raw material types used by hominins for butchery, through statistical analyses.

### *5.1.1 Identifying ESA industries at HEB site from cut marks micromorphology*

Classification (diagnosis) results from QDA analyses done in this study, reinforces the plausibility of Pante et al (2017) optical profilometry protocols and Keevil (2018) QDA statistical models as promising contenders for objective and replicable methods of studying BSMs. There were, however, some variations in classification accuracy levels between Keevil (2018) and this study. When identifying the archaeological cut marks (cut marks from recovered from archaeological fossils), Keevil (2018) models achieved; 71.22% accuracy in identifying raw material types (raw material only model), 78.54% accuracy in identifying technology types (technology only model), and 80.97% accuracy in identifying both raw materials and technology (combined raw material and technology model). On the other hand, this study achieved; 64.84%

accuracy when identifying raw material types (raw material only model), 77.34% accuracy when identifying technology types (technology only model), and 68.36% accuracy when identifying both raw materials and technology (combined raw material and technology model).

The variations in classification accuracy levels between the two studies is caused in part by the methodological differences when applying the statistical models. For example, unlike in Keevil (2018), this study combined Basalt and Phonolite into one classification group and shrunk the covariance matrices on JMP when classifying raw materials for better accuracy. Furthermore, cross validation protocols for this study were different from Keevil's. The study defined a 90% (training) to 10% (testing) split of the dataset for randomized cross validation on JMP. While this procedure is not explained in Keevil (2018), it's most likely that his cross-validation protocols were different from this study resulting in differences in accuracy levels of the models.

However, not every methodological difference between this study and Keevil (2018) was the cause of varying classification accuracies between the two studies. For example, the varying types of statistical softwares used to compute QDA models by both Keevil (used R statistical software) and this study (used JMP) have small or negligible influence on the results. In order to negate such suspicions, mock QDA analyses were done on both R and JMP to test if the differences in algorismic designs for computing the QDA discriminant models (e.g. definition and inclusion of floating-point numbers, criteria for defining model accuracy levels etc.) had any influence on the results. The mock models showed a 1-3% difference in accuracy levels between the two softwares. This means that, if everything else is constant, software packages (R and JMP), should yield relatively similar results.

Furthermore, since the scanning process (measuring cut mark micromorphology) in both Keevil (2018) and this study followed Pante et al (2017) protocols, using different 3D scanners (optical profilometers) did not affect replicability of Keevil's methods. Preliminary studies have shown that both NANOVEA ST400 (used on Keevil, 2018) and S NEOX scanners (used in this study) produced the same measurements of cut marks, with differences being on the amount of time used in the scanning process. While Nanovea ST400 scanner can take up to 1 hour to scan one cut mark (Pante et al. 2017), the new S Neox scanner only requires a few seconds or minutes to scan a cut mark. These technical differences are reflected on their prices.

Figure 5. 1**:** Left image is the Nanovea ST400 white light non-contact confocal profilometer used in Pante et al (2017). Right image is the S Neox non-contact 3D optical profilometer used in this study

<u>A: Diagnosing technology types of ESA butchery tools at HEB site around 0.9Ma.</u>

The study used Keevil's (2018) statistical discriminant models to identify and classify the relationship between cut mark micromorphology and stone tool form. The 'technology only' quadratic discriminant analysis model used in the study; classified cut mark measurements based on the technological form of the tool used to create those cut marks with 77.34% accuracy. 80% (16 samples) were classified as NR (No retouch flake), and 20% (4 archaeological samples) were classified as BF (biface). These results are consistent with what Mary D. Leakey found during her excavations at HEB site where flake instances surpassed all other technology types (Leakey & Roe, 1994). Mary Leakey reported that, out of 303 lithic materials recovered from HEB site (level 3), a significantly large portion (n=201) of the assemblage was made up of flakes (66.3%). Bifaces made up about 33% of the assemblage (n=100), and cores made up about 0.6% (n=2) of the assemblage. In level 4, she found out that flakes made up about 72.5 % (eq. 158 specimens) of the total assemblage (n=218), followed by Bifaces – which made up about 27.5% (60 specimens) of the assemblage. At level 4, Mary Leakey did not record any core tools (see Table 5.1).

ESA technology types diagnosed from the 3D measurements of cut mark micromorphology indicates how much a certain technology type was used during butchery (to create cut marks). Results from 3D analyses done in this study, therefore, ignores all unused tools at the HEB site (regardless of their technology types), and would only count tools used for butchery (to create butchery marks). Frequency of ESA technology types discovered at HEB site (Leakey & Roe, 1995) provides a general count of tools manufactured by hominins at HEB site (whether used during butchery or not). Therefore, consistency in greater proportions of flake frequencies in both the 3D diagnoses and artifacts studies at the site, indicate that hominins at HEB made and used flakes more than other tool types.

Reasons for flakes preference over bifaces at HEB can be inferred from actualistic butchery experiments, which have been instrumental in demonstrating technological efficacy of different ESA tools (Jones, 1980;1981; Key & Lycett, 2017; Key et al. 2020). The most obvious advantage of flake tools is that it takes a significantly shorter time and less complicated process to make them in comparison to the biface handaxes. This is very advantageous in a highly competitive environment where meat extraction from carcasses must be done faster. Furthermore, studies have demonstrated flake tools to be significantly more efficient than handaxes when undertaking relatively small, precise cutting tasks (Key & Lycett, 2017). Based on this, scientists have argued that bifaces were probably used on special cases as a requirement to undertake specific type of tasks (when cutting relatively large and resistant portions of carcasses), rather than them being inherently superior to flakes in all cutting tasks (Key & Lycett, 2017).

<u>B: Diagnosing raw material types of ESA butchery tools at HEB site around 0.9Ma.</u>

The QDA raw material model classifying cut marks made by tools of different raw materials (Basalt, Chert and Quartzite), classified 55% of the tested archaeological sample from HEB site as Basalt, 35% were identified as quartzite, and 10% as chert. Unlike results from technology model discussed above, the frequency and proportion of the raw material types diagnosed from the 3D studies of cut mark micromorphology are not consistent with the artifact distribution at the HEB site. Mary D. Leakey's excavation at HEB site (Leakey & Roe, 1994) recorded that, out of the 905 lithic materials recovered from HEB site (level 3), significantly large portions of the assemblage were made up of quartzite (63.5%) and Lava (31.9%). Also, in level 4, she found out that Quartzite made up 81.4% (eq. 903 specimens) of the total assemblage (n=1110), followed by Lava (Basalt & Phonolite) – which made up 14.2% (158 specimens) of the assemblage. This pattern suggests that, at HEB hominins used more lava-made tools during butchery (as diagnosed from 3D studies of cut mark micromorphology) despite quartzite tools being the most available (abundant) at the site (Leakey & Roe, 1994).

Such a pattern is interesting because our common understanding is that, relative abundance and total mass of lithic artifacts made from different materials, can be used an indicator of both; availability of those raw materials, and hominin preferences for those specific raw materials (Leakey, 1966; McHenry & de la Torre, 2018). Butchery actualistic studies (Jones, 1979; Key et al. 2020) show that both lava (basalt) and quartzite have advantageous 'butchery properties' over other raw material types. For example, basalt (lava) has a strong, durable cutting edge, and therefore can be used to create tools that last longer (durable) during butchery (Jones, 1979; Key et al. 2020), whereas, quartzite has the sharpest cutting edge, making it ideal for creating sharp butchery tools (Key et al. 2020). Based on this, it is impossible to use functional/practical attributes of these materials as an explanation for the preferential use of lava tools over the abundant quartzite tools at HEB site.

An alternative explanation would be looking at relative availability of raw material sources, where the distance of the raw material primary sources from the butchery site, can also influence raw material type usage and preferences (McHenry & de la Torre, 2018). Similar to effects of paleoclimate changes in Africa which led to patchiness of food and water resources, lithic tools raw material distributions across Olduvai would have subjected HEB hominins to landscape and predatory pressures associated with exploitation of resources that were widely distributed across the Olduvai Pleistocene landscape (Cachel et al. 1998; Leakey, 1966; McHenry & de la Torre, 2018; Santonja et al. 2014). This means that there would be conscious (budgeted) usage of raw material types depending on their availability (McHenry & de la Torre, 2018; Santonja et al. 2014).

At HEB site, primary source of quartzite raw material is located 15kms from the site (Enabor Soit hill), whereas, lava raw material types are further away, at least 19km (Lemagrut) and 22km (Engelosin). Although such proximity of quartzite primary source can explain abundance of quartzite tools at HEB, Researchers (Leakey & Roe, 1994; Njau et al. 2020) have also described HEB stratigraphy as comprising of alternating horizons of claystones and siltstones with occasional sandy, pebbly stream fill and lag deposits. These sedimentological properties are suggestive of shifting lake and stream positions, resulting from regionally driven palaeoenvironmental change (Njau et al. 2020, p.3). The riverine and lacustrine contexts are evidence of a stream running through HEB and draining into the Olduvai paleolake (Njau et al. 2020). This stream probably acted as a secondary raw material source, transporting lava from surrounding volcanic mountains. Presence of a stream transporting lava through HEB would make lava the most accessible raw material at HEB (proximity-wise) which can be used without budgetary constraints, whereas, quartzite would have been manufactured, but used sparingly accounting for the 19km distance from the source.

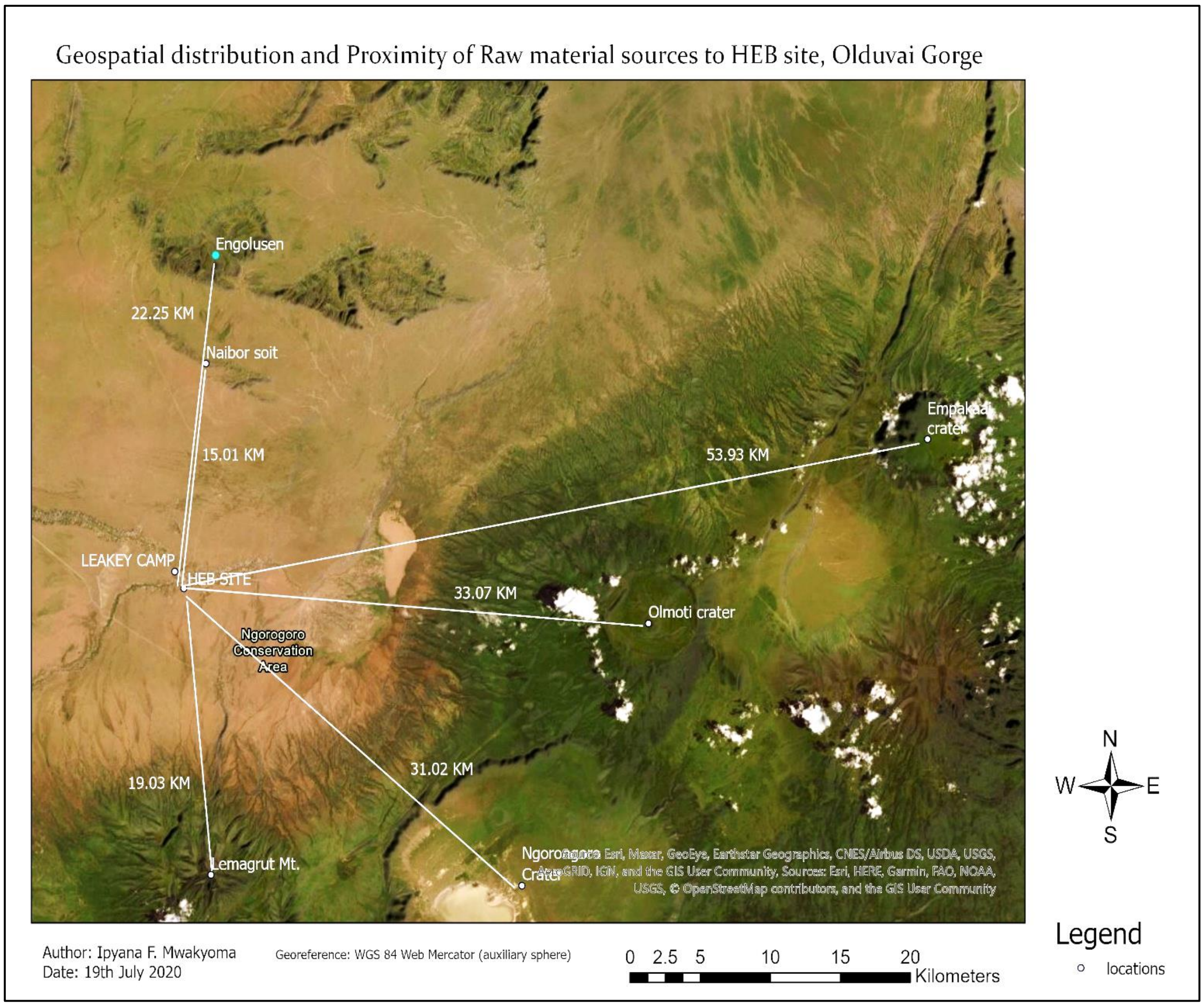


Figure 5. 2: GIS satellite image showing the spatial distribution and proximity of raw material sources from HEB site, Olduvai Gorge.

C: Diagnosing both raw material and technology types of ESA butchery tools at HEB

Quadratic discriminant analysis of cut mark measurements based on similarities in both the raw material and technological form of the tool that made those cut marks, classified cut marks with 68% accuracy. Keevil (2018) assessed that cut marks made by stone tools of the same technological form are more likely to preserve similar micromorphological features than cut marks made by tools of the same raw material type and that tool technological form influences cut mark morphology more than tool raw material type (p.93). This explains the varying accuracy levels and classification conflicts between the technology only, raw material only, and the combined (technology + raw material) models.

Out of the 20 archaeological samples from HEB, the combined (technology + raw material) model had identified 9 tools (45%) as lava flakes, 6 tools (30%) as lava bifaces, 2 tools (10%) as Quartzite Bifaces, 1 tool (5%) as a biface of unknown raw material, 1 tool (5%) as a flake of unknown raw, and 1 tool (5%) as a lava tool of unknown technology. This means that there are 10 (50%) flakes tools (regardless of their raw material types) and 9 (45%) bifaces (regardless of regardless of their raw material types). Though on a relatively lower margin, the combined (technology + raw material) model agrees with the 'technology only' model that more flake tools were used for butchery at HEB compared to bifaces. The combined (technology + raw material) model also agrees with the 'raw material only' model that tools made of lava were used more during butchery than other raw material types by classifying 16 tools (80%) of all cut marks as being created by lava tools (irrespective of their technology types). The rest were diagnosed as being created by quartzite tools (10%) and an unidentified/inconclusive raw material type (10%).

The combined (technology + raw material) classification also indicated several butchery behaviors including using the same tool multiple times to process a single carcass element.

Evidence for such behavior has been reported by researchers before including Keevil (2018), who reported a single tool being used to create four different cut mark traces on the same fossil bone element. In this study as well, three different cut marks located on midshaft section of a radius and positioned close and parallel to each other (HEBT4_L8_372-3a, HEBT4_L8_372-3a, and HEBT4_L8_372-4) were all diagnosed as being created by lava flake tool. Adjacent to these cut marks but on the same bone element, another cut mark was diagnosed as being created by lava biface tool (HEBT4_L8_372-1). Keevil (2018) proposed that, such pattern could have been created by either a butcher using a single tool multiple times to process a single carcass element, or a butcher or multiple butchers using several tools of the same form to process a single carcass element (p. 98). However, improving credibility of these assumptions would require 3D analysis of cut marks created by controlled actualistic studies focusing on butchery sequences, coupled with studies of macroscopic cut mark patterns on bones.

## 5.3 Limitation of the study and Future research prospects/direction

### *5.3.1 Limitations of the study*

The study relied on the ability of discriminant models to classify cut mark micro-morphometrics into specific tools types. However, the accuracy levels achieved by the discriminant models were average, and low compared to Keevil (2018) or other BSM discriminant studies using 3D methods (e.g. Pante et al. 2017). Efforts to achieve better classification accuracies were hampered by many factors, notably size of the sample dataset. The discriminant models in the study had a small sample size (n=276), which is relatively inadequate to train a statistical classifier.

Furthermore, the archaeological sample under study was also very small (n=20), which might limit the study's ability to accurately represent the whole HEB site. The archaeological sample was selected based on subjective criteria related to the state of cut mark preservation, therefore, interpretations made in the study could only be representative of a subset of butchery activities at HEB rather than the entirety of hominin butchery behavior at the site.

Also, the training dataset from (Keevil, 2018) was created in a controlled experiment that was designed to keep subjective butchery attributes constant by using a mechanized saw to create the cut marks. This means that subjective aspects of butchery activity, such as how tools were held during butchery, or the amount of force applied when defleshing the carcass were not considered when creating the training dataset used in the study. While this method is commendable for reducing bias and subjectivity, it does not truly reflect an actual butchery event that took place at HEB site, where different butchers probably held butchery tools differently, or applied different amount of force when defleshing a carcasses to create the archaeological cut marks (testing dataset) classified in this study. Even a single butcher can hold tools differently or use different amounts of force for every separate slashing event when processing a single carcass. How tools are held, and the force applied can influence cut mark micromorphological features like the angle and depth of the cut mark, all of which were included as important variables in this study's QDA classifiers.

Other challenges were related to 3D scanning archaeological specimens. For example, the dark coloration of fossilized bones affected visibility and light reflectance, which are crucial when using the optical profilometry. Dark color absorbs light, which can obstruct photographic visibility of the mark, leading to loss of data and lowering of the quality of 3-D cut mark models.

Also, the data used in this study regarding the frequency and distribution of ESA artifacts at HEB site, came from decades' old excavation records by Leakey & Roe (1994). While Leakey's accounts were useful, they were not from the same archaeological levels as the OGCP cut marks analyzed in this study. The OGCP have recovered more than 2500 artifacts from T4 & T5, that are directly associated and more contextually related to the archaeological cut marks used in this study. However, these artifacts have not yet been analyzed (Njau et al. 2020), and therefore could not be used in the study.

*5.3.2 Future research prospects and direction*

Based on the limitations of the study and results obtained, there are a lot of areas that needs improvement and further investigations. Methodologically, optical profilometry has the potential to develop into a more reliable quantitative method for studying BSMs. Its potential in diagnosing tool effector from trace marks, can be applied to taphonomic studies of fossil assemblages in sites where there are no artifacts found like Dikika, Ethiopia (McPherron et al. 2010). To achieve this, there is a need for further inter-analyst studies dedicated at improving optical profilometry measurement and analysis protocols (Pante et al. 2017). Creation of bigger cut mark database from controlled butchery experiments will further improve accuracies of the classification models used in 3D studies of cut marks.

Finally, since the research at HEB by OGCP (Olduvai Gorge Coring Project) is still on going, then, there is hope for better resolution of the interpretations made in this study by increasing the archaeological sample size. Independent analyses of the lithic artifacts recovered from HEB by OGCP, will further inform this and/or similar studies, and help build a comprehensive picture of *Homo erectus* butchery practices at HEB.

# CHAPTER 6 CONCLUSION

This study identifies the technology and raw material types of the early stone age (ESA) tools used by *H. erectus* for butchery at HEB site, Olduvai gorge, around 0.9 million years ago. The study expands upon previous BSM research on hominin feeding behavior by successfully applying the quadratic discriminant analysis (QDA) models developed by Keevil (2018). Results show that, *H. erectus* used both flakes and bifaces (hand axes) to butcher animals at HEB site. Also, the QDA model diagnosing raw material types, indicate that *H. erectus* preferably used lava (basalt and phonolite) tools for butchery, despite abundance of quartzite tools at the site. These results have implications on our understanding of *H. erectus* feeding behavior at HEB site, and how the preferential use of ESA tools influenced human evolution during the Pleistocene.

The study contributes to the body of knowledge on objective and quantifiable taphonomic methods of studying BSMs. This is because apart from being able to characterize the ESA tools used for butchery by *H. erectus* at HEB, the study also demonstrated the efficacy and replicability of the optical profilometry as a method for studying cut marks. This is important, because developing an objective and standardized method of studying BSMs, provides a platform for not only, making better assumptions about our past, but also the ability to scientifically test them.

This research demonstrated that 3D optical profilometric study of butchery marks at HEB indicate hominin tool use and choice, and that the tool frequencies diagnosed from the 3D optical profilometric study, are reflective of the technology and raw material distribution at HEB site. All technology QDA models classifying 3D cut mark micromorphological measurements obtained through optical profilometry indicate that hominins at HEB used flakes more than bifaces during butchery. This pattern is attributed to functional efficacy of flake in undertaking relatively small, precise cutting tasks (Key & Lycett, 2017). Biface tools were also used at HEB, probably to undertake specific type of tasks involving cutting relatively large and resistant portions of carcasses. This assessment is also supported by the proportional abundance of flake tools at HEB compared to bifaces (Leakey & Roe, 1994).

In terms of raw materials, QDA classification of 3D cut mark micro-morphometrics was not consistent with the known (Leakey & Roe, 1994) frequency and distribution of raw material types at HEB site. While QDA classification of HEB fossil cut mark micromorphology indicates that lava tools were mostly used to create those cut marks; it is quartzite tools and not lava, that made up the majority of stone tool artifacts recovered at HEB. This means that despite abundance of quartzite tools at HEB, hominins preferably used more lava tools during butchery. Raw material budgeting in relation to availability (proximity of raw material sources from HEB) can best explain this pattern. Sedimentological records (Leakey & Roe, 1994; Njau et al. 2020) indicates presence of a stream that probably acted as a secondary source of raw material, transporting lava from nearby volcanic mountains through HEB site. This means that there would be conscious (budgeted) usage of raw material types depending on their availability, and therefore lava (the most available) would be used more, while quartzite tools manufactured at the site would be used sparingly.

These findings have several implications in human evolution studies as characteristics of butchery tools and underlying choices on how they are used during butchery, is important in understanding how hominins mitigated costs of acquiring the high-caloric meat resources. In human evolutionary studies, meat in the diet of hominins is significant because it provided high nutritional returns (high energy/protein with low digestive costs) (Bunn, 2006; Pante, 2010; Pante, 2013; Ungar, 2006). However, this energetic advantage was usually kept in check by other factors such as the ‘costs’ of searching or acquiring and butchering that meat resource (Blumenschine & Pobiner, 2007; Shipman &Walker, 1989). This study contributes to our understanding of how hominin butchery behavior was instrumental in the acquisition and maximization of the metabolic advantages associated with meat diet (e.g. funding the evolution, and maintenance of a bigger brain).

.

REFERENCES

Altman, N., & Krzywinski, M. (2016). Analyzing outliers: influential or nuisance?

Ascher, R. (1961). Analogy in archaeological interpretation. *Southwestern journal of anthropology*, *17*(4), 317-325.

Behrensmeyer, A. K., & Kidwell, S. M. (1985). Taphonomy's contributions to paleobiology. *Paleobiology*, *11*(1), 105-119.

Bello, S. M., Parfitt, S. A., & Stringer, C. (2009). Quantitative micromorphological analyses of cut marks produced by ancient and modern handaxes. *Journal of Archaeological Science*, *36*(9), 1869-1880.

Bello, S. M., Parfitt, S. A., & Stringer, C. (2009). Quantitative micromorphological analyses of cut marks produced by ancient and modern handaxes. *Journal of Archaeological Science*, *36*(9), 1869-1880.

Bello, S. M., & Soligo, C. (2008). A new method for the quantitative analysis of cutmark micromorphology. *Journal of Archaeological Science*, *35*(6), 1542-1552.

Bello, S. M. (2011). New results from the examination of cut-marks using three-dimensional imaging. In *Developments in Quaternary Sciences* (Vol. 14, pp. 249-262). Elsevier.

Blatná, D. (2006). Outliers in regression. *Trutnov*, *30*, 1-6.

Blumenschine, R. J., & Selvaggio, M. M. (1988). Percussion marks on bone surfaces as a new diagnostic of hominid behavior. *Nature*, *333*(6175), 763-765.

Blumenschine, R. J. (1991). Hominid carnivory and foraging strategies, and the socio-economic function of early archaeological sites. *Philosophical Transactions of the Royal Society of London. Series B: Biological Sciences*, *334*(1270), 211-221.

Blumenschine, R. J. (1993). A carnivore's view of archaeological bone assemblages. *From bones to behavior*.

Blumenschine, R. J., Cavallo, J. A., & Capaldo, S. D. (1994). Competition for carcasses and early hominid behavioral ecology: A case study and conceptual framework. *Journal of Human Evolution*, *27*(1-3), 197-213.

Blumenschine, R. J. (1995). Percussion marks, tooth marks, and experimental determinations of the timing of hominid and carnivore access to long bones at FLK Zinjanthropus, Olduvai Gorge, Tanzania. *Journal of Human Evolution*, *29*(1), 21-51.

Blumenschine, R. J., & Selvaggio, M. M. (1988). Percussion marks on bone surfaces as a new diagnostic of hominid behavior. *Nature*, *333*(6175), 763-765.

Blumenschine, R. J., Marean, C. W., & Capaldo, S. D. (1996). Blind tests of inter-analyst correspondence and accuracy in the identification of cut marks, percussion marks, and carnivore tooth marks on bone surfaces. *Journal of archaeological science*, *23*(4), 493-507.

Blumenschine, R. J., Prassack, K. A., Kreger, C. D., & Pante, M. C. (2007). Carnivore tooth-marks, microbial bioerosion, and the invalidation of test of Oldowan hominin scavenging behavior. *Journal of Human Evolution*, *53*(4), 420-426.

Blumenschine, R. J., & Pobiner, B. L. (2007). Zooarchaeology and the ecology of Oldowan hominin carnivory. *Evolution of the human diet: the known, the unknown, and the unknowable*, 167-190.

Blumenschine, R. J., Masao, F. T., Tactikos, J. C., & Ebert, J. I. (2008). Effects of distance from stone source on landscape-scale variation in Oldowan artifact assemblages in the Paleo-Olduvai Basin, Tanzania. *Journal of Archaeological Science*, *35*(1), 76-86.

Boschin, F., & Crezzini, J. (2012). Morphometrical analysis on cut marks using a 3D digital microscope. *International Journal of Osteoarchaeology*, *22*(5), 549-562.

Braun, D. R., Pante, M., & Archer, W. (2016). Cut marks on bone surfaces: influences on variation in the form of traces of ancient behaviour. *Interface focus*, *6*(3), 20160006.

Braun, D. R., Harris, J. W., & Maina, D. N. (2009). Oldowan raw material procurement and use: evidence from the Koobi Fora Formation. *Archaeometry*, *51*(1), 26-42.

Brett, C. E., & Baird, G. C. (1986). Comparative taphonomy: a key to paleoenvironmental interpretation based on fossil preservation. *Palaios*, 207-227.

Bunn, H. T., Kroll, E. M., Ambrose, S. H., Behrensmeyer, A. K., Binford, L. R., Blumenschine, R. J., ... & Wymer, J. J. (1986). Systematic butchery by Plio/Pleistocene hominids at Olduvai Gorge, Tanzania [and comments and reply]. *Current Anthropology*, *27*(5), 431-452.

Bunn, H. T. (1986). Patterns of skeletal representation and hominid subsistence activities at Olduvai Gorge, Tanzania, and Koobi Fora, Kenya. *Journal of Human Evolution*, *15*(8), 673-690.

Bunn, H. T. (2001). *Hunting, power scavenging, and butchering by Hadza foragers and by Plio-Pleistocene Homo* (pp. 199-218). Meat-Eating and Human Evolution. Oxford University Press, Oxford.

Bunn, H. T., & Ezzo, J. A. (1993). Hunting and scavenging by Plio-Pleistocene hominids: nutritional constraints, archaeological patterns, and behavioural implications. *Journal of Archaeological Science*, *20*(4), 365-398.

Bunn, H. T. (2006). Meat made us human. *Evolution of the human diet: the known, the unknown, and the unknowable*, 191-211.

Capaldo, S. D. (1997). Experimental determinations of carcass processing by Plio-Pleistocene hominids and carnivores at FLK 22 (Zinjanthropus), Olduvai Gorge, Tanzania. *Journal of Human Evolution*, *33*(5), 555-597.

Cachel, S., Harris, J. W., Petraglia, M. D., & Korisettar, R. (1998). The lifeways of Homo erectus inferred from archaeology and evolutionary ecology: a perspective from East Africa. *Early human behaviour in global context: the rise and diversity of the lower Palaeolithic record*, 108-132.

Courtenay, L. A., Yravedra, J., Huguet, R., Ollé, A., Aramendi, J., Maté-González, M. Á., & González-Aguilera, D. (2019). New taphonomic advances in 3D digital microscopy: A morphological characterization of trampling marks. Quaternary International, 517, 55-66.

Courtenay, L. A., Huguet, R., González-Aguilera, D., & Yravedra, J. (2020). A hybrid geometric morphometric deep learning approach for cut and trampling mark classification. *Applied Sciences*, *10*(1), 150.

de la Torre, I. (2016). The origins of the Acheulean: past and present perspectives on a major transition in human evolution. *Philosophical Transactions of the Royal Society B: Biological Sciences*, *371*(1698), 20150245.

de la Torre, I., & Mora, R. (2014). The transition to the Acheulean in East Africa: an assessment of paradigms and evidence from Olduvai Gorge (Tanzania). *Journal of Archaeological Method and Theory*, *21*(4), 781-823.

de la Torre, I., & Mora, R. (2018). Technological behaviour in the early Acheulean of EF-HR (Olduvai Gorge, Tanzania). *Journal of human evolution*, *120*, 329-377.

De Juana, S., Galán, A. B., & Domínguez-Rodrigo, M. (2010). Taphonomic identification of cut marks made with lithic handaxes: an experimental study. *Journal of Archaeological Science*, *37*(8), 1841-1850.

Domínguez-Rodrigo, M., & Pickering, T. R. (2003). Early hominid hunting and scavenging: a zooarchaeological review. *Evolutionary Anthropology: Issues, News, and Reviews: Issues, News, and Reviews*, *12*(6), 275-282.

Domínguez-Rodrigo, M., & Barba, R. (2007). New estimates of tooth-mark and percussion-mark frequencies at the FLK Zinjanthropus level: the carn. In *Deconstructing Olduvai: A Taphonomic Study of the Bed I Sites* (pp. 39-74). Springer, Dordrecht.

Domínguez-Rodrigo, M. (2008). Conceptual premises in experimental design and their bearing on the use of analogy: an example from experiments on cut marks. *World Archaeology*, *40*(1), 67-82.

Domínguez-Rodrigo, M., De Juana, S., Galan, A. B., & Rodríguez, M. (2009). A new protocol to differentiate trampling marks from butchery cut marks. *Journal of Archaeological Science*, *36*(12), 2643-2654.

Domínguez-Rodrigo, M., Bunn, H. T., & Yravedra, J. (2014). A critical re-evaluation of bone surface modification models for inferring fossil hominin and carnivore interactions through a multivariate approach: application to the FLK Zinj archaeofaunal assemblage (Olduvai Gorge, Tanzania). *Quaternary International*, *322*, 32-43.

Domínguez-Rodrigo, M., Bunn, H. T., Mabulla, A. Z., Baquedano, E., Uribelarrea, D., Pérez-González, A., ... & Barba, R. (2014). On meat eating and human evolution: A taphonomic analysis of BK4b (Upper Bed II, Olduvai Gorge, Tanzania), and its bearing on hominin megafaunal consumption. *Quaternary International*, *322*, 129-152.

Egeland, C. P., & Domínguez-Rodrigo, M. (2008). Taphonomic perspectives on hominid site use and foraging strategies during Bed II times at Olduvai Gorge, Tanzania. *Journal of human evolution*, *55*(6), 1031-1052.

Egeland, C. P., Fadem, C. M., Byerly, R. M., Henderson, C., Fitzgerald, C., Mabulla, A. Z., ... & Gidna, A. (2019). Geochemical and physical characterization of lithic raw materials in the Olduvai Basin, Tanzania. *Quaternary International*, *526*, 99-115.

Ferraro, J. V., Plummer, T. W., Pobiner, B. L., Oliver, J. S., Bishop, L. C., Braun, D. R., ... & Hertel, F. (2013). Earliest archaeological evidence of persistent hominin carnivory. *PloS one*, *8*(4), e62174.

Fisher, J. W. (1995). Bone surface modifications in zooarchaeology. *Journal of Archaeological method and theory*, *2*(1), 7-68.

Foley, R. A. (2001). The evolutionary consequences of increased carnivory in hominids. *Meat-eating and human evolution*, 305-331.

Freestone, I. C., & Middleton, A. P. (1987). Mineralogical applications of the analytical SEM in archaeology. *Mineralogical Magazine*, *51*(359), 21-31.

Frahm, E. (2014). Scanning electron microscopy (SEM): Applications in Archaeology. *Encyclopedia of Global Archaeology*, 6487-6495.

Galán, A. B., & Domínguez-Rodrigo, M. (2014). Testing the efficiency of simple flakes, retouched flakes and small handaxes during butchery. *Archaeometry*, *56*(6), 1054-1074.

Gifford-Gonzalez, D. (1991). Bones are not enough: analogues, knowledge, and interpretive strategies in zooarchaeology. *Journal of Anthropological Archaeology*, *10*(3), 215-254.

González, M. Á. M., Yravedra, J., González-Aguilera, D., Palomeque-González, J. F., & Domínguez-Rodrigo, M. (2015). Micro-photogrammetric characterization of cut marks on bones. *Journal of Archaeological Science*, *62*, 128-142.

Greenfield, H. J. (2006). Slicing cut marks on animal bones: diagnostics for identifying stone tool type and raw material. *Journal of Field Archaeology*, *31*(2), 147-163.

Gumrukcu, M. (n.d.). *Assessing the effects of fluvial abrasion on bone surface modifications using high-resolution 3-D scanning*. Colorado State University. Libraries.

Gümrükçü, M., & Pante, M. C. (2018). Assessing the effects of fluvial abrasion on bone surface modifications using high-resolution 3-D scanning. *Journal of Archaeological Science: Reports*, *21*, 208-221.

Hawkes, K., O´Connell, J. F., & Blurton Jones, N. G. (1991). Hunting income patterns among the Hadza: big game, common goods, foraging goals and the evolution of the human diet.

*Philosophical Transactions of the Royal Society of London. Series B: Biological Sciences*, *334*(1270), 243-251.

Hay, R. L. (1976). *Geology of the Olduvai Gorge*. Рипол Классик.

Https://www.sensofar.com/metrology/products/sneox/

Isler, K., & Van Schaik, C. P. (2014). How humans evolved large brains: comparative evidence. *Evolutionary Anthropology: Issues, News, and Reviews*, *23*(2), 65-75.

Jones, P. R. (1981). Experimental implement manufacture and use; a case study from Olduvai Gorge, Tanzania. *Philosophical Transactions of the Royal Society of London. B, Biological Sciences*, *292*(1057), 189-195.

Jones, P. R. (1980). Experimental butchery with modern stone tools and its relevance for Palaeolithic archaeology. *World Archaeology*, *12*(2), 153-165.

Jones, P. R. (1979). Effects of raw materials on biface manufacture. *Science*, *204*(4395), 835-836.

Jobson, R. W. (1986). Stone tool morphology and rabbit butchering. *Lithic Technology*, *15*(1), 9-20.

Keevil, T., Pante, M., Glantz, M., & Lacy, M. (2018). *Inferring Early Stone Age Tool Technology and Raw Material from Cut Mark Micromorphology Using High-Resolution 3-D Scanning with Applications to Middle Bed II, Olduvai Gorge, Tanzania* (ProQuest Dissertations Publishing). Retrieved from http://search.proquest.com/docview/2055364067/

Key, A. J., Proffitt, T., Stefani, E., & Lycett, S. J. (2016). Looking at handaxes from another angle: Assessing the ergonomic and functional importance of edge form in Acheulean bifaces. *Journal of Anthropological Archaeology*, *44*, 43-55.

Key, A. J., & Lycett, S. J. (2017). Reassessing the production of handaxes versus flakes from a functional perspective. *Archaeological and Anthropological Sciences*, *9*(5), 737-753.

Key, A., Proffitt, T., & de la Torre, I. (2020). Raw material optimization and stone tool engineering in the Early Stone Age of Olduvai Gorge (Tanzania). *Journal of the Royal Society Interface*, *17*(162), 20190377.

Key, A. J., & Lycett, S. J. (2017). Reassessing the production of handaxes versus flakes from a functional perspective. *Archaeological and Anthropological Sciences*, *9*(5), 737-753.

Kimura, Y. (1999). Tool-using strategies by early hominids at Bed II, Olduvai Gorge, Tanzania. *Journal of Human Evolution*, *37*(6), 807-831.

Kohn, M., & Mithen, S. (1999). Handaxes: products of sexual selection?. *ANTIQUITY-OXFORD-*, *73*, 518-526.

Leakey, L. S., Tobias, P. V., & Napier, J. R. (1964). A new species of the genus Homo from Olduvai Gorge. *Nature*, *202*(4927), 7-9.

Leakey, M. D. (1966). A review of the Oldowan culture from Olduvai Gorge, Tanzania. *Nature*, *210*(5035), 462-466.

Leakey, M. D. (1971). *Olduvai Gorge: Volume 3, excavations in beds I and II, 1960-1963* (Vol. 3). Cambridge University Press.

Leakey, M., & Roe, D. (1995). *Olduvai Gorge: volume 5, excavations in beds III, IV and the Masek beds* (Vol. 5). Cambridge University Press.

Lyman, R. L., & Lyman, C. (1994). *Vertebrate taphonomy*. Cambridge University Press.

González, M. Á. M., Yravedra, J., González-Aguilera, D., Palomeque-González, J. F., & Domínguez-Rodrigo, M. (2015). Micro-photogrammetric characterization of cut marks on bones. *Journal of Archaeological Science*, *62*, 128-142.

Maté-González, M. Á., Palomeque-González, J. F., Yravedra, J., González-Aguilera, D., & Domínguez-Rodrigo, M. (2018). Micro-photogrammetric and morphometric differentiation of cut marks on bones using metal knives, quartzite, and flint flakes. *Archaeological and Anthropological Sciences*, *10*(4), 805-816.

Maté-González, M. Á., Yravedra, J., Martín-Perea, D. M., Palomeque-González, J., San-Juan-Blazquez, M., Estaca-Gómez, V., ... & Domínguez-Rodrigo, M. (2018). Flint and quartzite: distinguishing raw material through bone cut marks. *Archaeometry*, *60*(3), 437-452.

Machin, A. J., Hosfield, R. T., & Mithen, S. J. (2007). Why are some handaxes symmetrical? Testing the influence of handaxe morphology on butchery effectiveness. *Journal of Archaeological Science*, *34*(6), 883-893.

Marshall, F. (1986). Implications of bone modification in a Neolithic faunal assemblage for the study of early hominid butchery and subsistence practices. *Journal of Human Evolution*, *15*(8), 661-672.

McHenry, L. J., & de la Torre, I. (2018). Hominin raw material procurement in the Oldowan-Acheulean transition at Olduvai Gorge. *Journal of human evolution*, *120*, 378-401.

McCall, G. S. (2005). An experimental examination of the potential function of Early Stone Age tool technology and implications for subsistence behavior. *Lithic Technology*, *30*(1), 29-43.

McPherron, S. P., Alemseged, Z., Marean, C. W., Wynn, J. G., Reed, D., Geraads, D., ... & Béarat, H. A. (2010). Evidence for stone-tool-assisted consumption of animal tissues before 3.39 million years ago at Dikika, Ethiopia. *Nature*, *466*(7308), 857-860.

Mithen, S. (2003). Handaxes: the first aesthetic artefacts. In *Evolutionary aesthetics* (pp. 261-275). Springer, Berlin, Heidelberg.

Monahan, C. M. (1996). New zooarchaeological data from Bed II, Olduvai Gorge, Tanzania: implications for hominid behavior in the Early Pleistocene. *Journal of Human Evolution*, *31*(2), 93-128.

Muttart, M., Pante, M., Boone, R., & LaBelle, J. (2017). *Taxonomic Distinctions in the 3D Micromorphology of Tooth Marks with Application to Feeding Traces from Middle Bed II, Olduvai Gorge, Tanzania* [ProQuest Dissertations Publishing]. http://search.proquest.com/docview/1961606316/

Njau, J., Herrmann, E. W., Ruck, L., Pante, M., Farrugia, P., Toth, N., ... & Stanistreet, I. G. (2020). Core stratigraphy constrains Bed IV archaeological record at HEB site, Olduvai Gorge, Tanzania. *Palaeogeography, Palaeoclimatology, Palaeoecology*, 109773.

O'Connell, J. F., Hawkes, K., & Jones, N. B. (1988). Hadza scavenging: Implications for Plio/Pleistocene hominid subsistence. *Current Anthropology*, *29*(2), 356-363.

O'Connell, J. F., Hawkes, K., & Jones, N. B. (1988). Hadza hunting, butchering, and bone transport and their archaeological implications. *Journal of Anthropological research*, *44*(2), 113-161.

Oliver, J. S. (1994). Estimates of hominid and carnivore involvement in the FLK Zinjanthropus fossil assemblage: some socioecological implications. *Journal of Human Evolution*, *27*(1-3), 267-294.

Olsen, S. L. (1988). Applications of scanning electron microscopy in archaeology. In *Advances in Electronics and Electron Physics* (Vol. 71, pp. 357-380). Academic Press.

Organista, E., Pernas-Hernández, M., Gidna, A., Yravedra, J., & Domínguez-Rodrigo, M. (2016). An experimental lion-to-hammerstone model and its relevance to understand hominin-carnivore interactions in the archeological record. *Journal of Archaeological Science*, *66*, 69-77.

Otárola-Castillo, E., Torquato, M. G., Hawkins, H. C., James, E., Harris, J. A., Marean, C. W., ... & Thompson, J. C. (2018). Differentiating between cutting actions on bone using 3D geometric morphometrics and Bayesian analyses with implications to human evolution. *Journal of Archaeological Science*, *89*, 56-67.

Pante, M. C., Blumenschine, R. J., Capaldo, S. D., & Scott, R. S. (2012). Validation of bone surface modification models for inferring fossil hominin and carnivore feeding interactions, with reapplication to FLK 22, Olduvai Gorge, Tanzania. *Journal of human evolution*, *63*(2), 395-407.

Pante, M. C. (2013). The larger mammal fossil assemblage from JK2, Bed III, Olduvai Gorge, Tanzania: implications for the feeding behavior of Homo erectus. *Journal of human evolution*, *64*(1), 68-82.

Pante, M. C., Scott, R. S., Blumenschine, R. J., & Capaldo, S. D. (2015). Revalidation of bone surface modification models for inferring fossil hominin and carnivore feeding interactions. *Quaternary International*, *355*, 164-168.

Pante, M. C., Muttart, M. V., Keevil, T. L., Blumenschine, R. J., Njau, J. K., & Merritt, S. R. (2017). A new high-resolution 3-D quantitative method for identifying bone surface modifications with implications for the Early Stone Age archaeological record. *Journal of human evolution*, *102*, 1-11.

Pante, M. C., Njau, J. K., Hensley-Marschand, B., Keevil, T. L., Martín-Ramos, C., Peters, R. F., & de la Torre, I. (2018). The carnivorous feeding behavior of early Homo at HWK EE, Bed II, Olduvai Gorge, Tanzania. *Journal of human evolution*, *120*, 215-235.

Pante, M. C., & de la Torre, I. (2018). A hidden treasure of the Lower Pleistocene at Olduvai Gorge, Tanzania: the Leakey HWK EE assemblage. *Journal of Human Evolution*, *120*, 114-139.

Parkinson, J. A. (2013). *A GIS image analysis approach to documenting Oldowan hominin carcass acquisition: Evidence from Kanjera South, FLK Zinj, and neotaphonomic models of carnivore bone destruction*. City University of New York.

Parkinson, J. A. (2018). Revisiting the hunting-versus-scavenging debate at FLK Zinj: A GIS spatial analysis of bone surface modifications produced by hominins and carnivores in the FLK 22 assemblage, Olduvai Gorge, Tanzania. *Palaeogeography, Palaeoclimatology, Palaeoecology*, *511*, 29-51.

Pate, F. (1994). Bone Chemistry and Paleodiet. *Journal of Archaeological Method and Theory, 1*(2), 161-209.

Pickering, T. R., & Egeland, C. P. (2006). Experimental patterns of hammerstone percussion damage on bones: implications for inferences of carcass processing by humans. *Journal of archaeological Science*, *33*(4), 459-469.

Potts, R. (2017). *Early Hominid Activities at Olduvai: Foundations of Human Behavior*. Routledge.

Potts, R., & Shipman, P. (1981). Cutmarks made by stone tools on bones from Olduvai Gorge, Tanzania. *Nature*, *291*(5816), 577-580.

Prassack, K., & Pante, M. C. (2007). Carnivore tooth-marks, microbial bioerosion, and the invalidation of Domínguez-Rodrigo and Barba's (2006) test of... *Journal of Human Evolution*, *53*, 420e426.

Roche, H., Blumenschine, R. J., & Shea, J. J. (2009). Origins and adaptations of early Homo: what archeology tells us. In *The First Humans–Origin and Early Evolution of the Genus Homo* (pp. 135-147). Springer, Dordrecht.

Sánchez-Yustos, P., Diez-Martín, F., Domínguez-Rodrigo, M., Fraile, C., Duque, J., Uribelarrea, D., ... & Baquedano, E. (2016). Techno-economic human behavior in a context of recurrent megafaunal exploitation at 1.3 Ma. Evidence from BK4b (Upper Bed II, Olduvai Gorge, Tanzania). *Journal of Archaeological Science: Reports*, *9*, 386-404.

Santonja, M., Panera, J., Rubio-Jara, S., Pérez-González, A., Uribelarrea, D., Domínguez-Rodrigo, M., ... & Baquedano, E. (2014). Technological strategies and the economy of raw materials in the TK (Thiongo Korongo) lower occupation, Bed II, Olduvai Gorge, Tanzania. *Quaternary International*, *322*, 181-208.

Selvaggio, M. M. (1994). Carnivore tooth marks and stone tool butchery marks on scavenged bones: archaeological implications. *Journal of Human Evolution*, *27*(1-3), 215-228.

Selvaggio, M. M., & Wilder, J. (2001). Identifying the involvement of multiple carnivore taxa with archaeological bone assemblages. *Journal of Archaeological Science*, *28*(5), 465-470.

Sept, J. (1992). Archaeological evidence and ecological perspectives for reconstructing early hominid subsistence behavior. *Archaeological Method and Theory*, *4*, 1-56.

Shipman, P., & Rose, J. (1983). Early hominid hunting, butchering, and carcass-processing behaviors: approaches to the fossil record. *Journal of anthropological Archaeology*, *2*(1), 57-98.

Shipman, P. (1986). Studies of hominid—Faunal interactions at Olduvai Borge. *Journal of Human Evolution*, *15*(8), 691-706.

Shipman, P., & Walker, A. (1989). The costs of becoming a predator. *Journal of Human Evolution*, *18*(4), 373-392.

Sikes, N. E. (1994). Early hominid habitat preferences in East Africa: paleosol carbon isotopic evidence. *Journal of Human Evolution*, *27*(1-3), 25-45.

Stiner, M. C. (1990). The use of mortality patterns in archaeological studies of hominid predatory adaptations. *Journal of anthropological archaeology*, *9*(4), 305-351.

Srivastava, S., Gupta, M. R., & Frigyik, B. A. (2007). Bayesian quadratic discriminant analysis. *Journal of Machine Learning Research*, *8*(Jun), 1277-1305.

Toth, N. (1985). The Oldowan reassessed: a close look at early stone artifacts. *Journal of Archaeological Science*, *12*(2), 101-120.

Ungar, P. S., Grine, F. E., & Teaford, M. F. (2006). Diet in early Homo: a review of the evidence and a new model of adaptive versatility. *Annu. Rev. Anthropol.*, *35*, 209-228.

Ungar, P. S. (Ed.). (2006). *Evolution of the human diet: the known, the unknown, and the unknowable*. Oxford University Press.

Yravedra, J., Maté-González, M. Á., Palomeque-González, J. F., Aramendi, J., Estaca-Gómez, V., San Juan Blazquez, M., ... & Cobo-Sánchez, L. (2017). A new approach to raw material use in the exploitation of animal carcasses at BK (Upper Bed II, Olduvai Gorge, Tanzania): a micro-photogrammetric and geometric morphometric analysis of fossil cut marks. *Boreas*, *46*(4), 860-873

# APPENDIX A - RAW MEASUREMENTS FROM ARCHAEOLOGICAL CUT MARKS

| ID | SURFACE (3D) | VOLUME (3D) | MAX DEPTH (3D) | MEAN DEPTH (3D) | MAX LENGTH (3D) | MAX WIDTH (3D) | MAX DEPTH (PRFD) | AREA (PRFD) | WIDTH (PRFD) | RA (PRFD) | WA (PRFD) | ANGLE (PRFD) | RADIUS (PRFD) |
|---|---|---|---|---|---|---|---|---|---|---|---|---|---|
| T4_L7_195-1 | 300183 | 5834020 | 47.1881 | 19.4349 | 2539.55 | 111.749 | 35.8637 | 2528.92 | 115.92 | 0.294518 | 7.74718 | 110.008 | 62.28 |
| T4_L7_232-1 | 474588 | 13782648 | 74.7634 | 29.0413 | 7640.98 | 118.895 | 35.8055 | 2135.87 | 126.96 | 0.414595 | 10.1616 | 108.971 | 64.1616 |
| T4_L8_147-1 | 1087062 | 45668936 | 93.4347 | 42.0113 | 6095.1 | 152.852 | 27.497 | 1879.97 | 121.44 | 0.276911 | 6.38159 | 127.587 | 75.1457 |
| T4_L8_188-1 | 1565843 | 49729211 | 67.4741 | 31.7587 | 8435.95 | 157.321 | 17.0053 | 1858.7 | 190.44 | 0.544015 | 2.46493 | 157.145 | 255.435 |
| T4_L8_223-1 | 816188 | 30237068 | 85.7362 | 37.0467 | 3508.63 | 348.606 | 62.0964 | 12687.6 | 339.48 | 0.738591 | 12.3852 | 135.889 | 277.298 |
| T4_L8_232-1 | 602320 | 18273256 | 65.6348 | 30.3381 | 3849.657 | 302.037 | 20.6981 | 3904.69 | 303.6 | 0.564427 | 8.61632 | 166.817 | 786.603 |
| T4_L8_294-2 | 1643627 | 53009116 | 99.7602 | 32.2513 | 11973.73 | 391.364 | 36.0956 | 6312.76 | 320.16 | 0.877583 | 7.12864 | 154.059 | 377.918 |
| T4_L8_351-1 | 192394 | 2100125 | 30.8955 | 10.9158 | 1928.99 | 149.236 | 7.24122 | 470.976 | 118.68 | 0.0823033 | 1.76134 | 163.068 | 346.759 |
| T4_L8_351-2 | 186445 | 5050305 | 48.4657 | 27.0874 | 2281.32 | 42.5574 | 26.8265 | 1809.04 | 179.4 | 2.05597 | 5.04801 | 145.203 | 212.813 |
| T4_L8_359-1a | 119231 | 5163297 | 81.8146 | 43.3051 | 1937.13 | 104.545 | 25.2297 | 1245.68 | 96.6 | 0.385071 | 5.7554 | 124.263 | 58.8 |
| T4_L8_359-1b | 150771 | 6699224 | 71.565 | 44.433 | 1600.81 | 131.129 | 6.0788 | 277.968 | 74.52 | 0.167872 | 0.814142 | 158.951 | 207.993 |
| T4_L8_359-2 | 1248612 | 105938389 | 138.601 | 84.8449 | 7546.16 | 261.971 | 56.8211 | 9608.18 | 336.72 | 1.45812 | 15.7521 | 138.991 | 342.403 |
| T4_L8_359-2b | 1508529 | 56691582 | 77.4564 | 37.5807 | 7726.51 | 264.026 | 54.5429 | 8127.38 | 267.72 | 1.35748 | 10.5876 | 133.242 | 185.131 |
| T4_L8_372-1 | 359608 | 6167786 | 47.5549 | 17.1514 | 2909.76 | 149.969 | 14.6919 | 1293.83 | 129.72 | 0.157227 | 2.90791 | 151.979 | 144.831 |
| T4_L8_372-3a | 1480728 | 44085766 | 88.9944 | 29.773 | 9829.04 | 180.036 | 52.6124 | 7396.3 | 273.24 | 1.17628 | 9.85654 | 133.829 | 193.533 |
| T4_L8_372-3b | 761257 | 16156721 | 60.2608 | 21.2237 | 10140.961 | 135.649 | 39.2008 | 3822 | 195.96 | 2.03186 | 5.51971 | 136.111 | 144.656 |
| T4_L8_372-4 | 552798 | 8352982 | 45.7256 | 15.1104 | 6598.82 | 93.8606 | 29.9489 | 3376.02 | 231.84 | 1.05802 | 5.0888 | 148.234 | 229.731 |
| T4_L8_373-2 | 1821920 | 57638743 | 137.52 | 31.6363 | 11346.1 | 382.974 | 111.918 | 44159.3 | 687.24 | 3.26785 | 14.5313 | 144.809 | 634.465 |
| T4_L8_391-1 | 469328 | 14447206 | 60.8351 | 30.7828 | 5626.39 | 111.885 | 29.2453 | 2389.84 | 154.56 | 0.418201 | 6.25504 | 137.542 | 117.499 |
| T4_L8_468-2 | 120084 | 1142406 | 26.8369 | 9.5134 | 1925.529 | 93.9714 | 13.2971 | 933.88 | 118.68 | 0.458641 | 3.09233 | 160.019 | 185.845 |

APPENDIX B – DISTRIBUTIONS OF ALL 12 INDIVIDUAL NUMERIC VARIABLES FROM A JOINT EXPERIMENTAL & ARCHAEOLOGICAL DATASET TABLE

### SA distribution

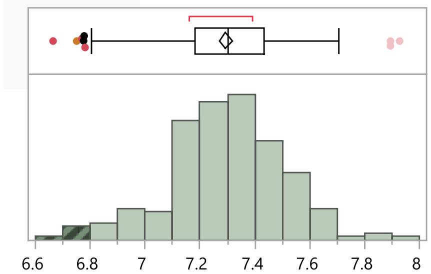


### Quantile

| | | |
|---|---|---|
| 100.0 % | maximum | 7.927204268 |
| 99.5% | | 7.9147131526 |
| 97.5% | | 7.6418541046 |
| 90.0% | | 7.5573253895 |
| 75.0% | quartile | 7.435424376 |
| 50.0% | median | 7.3026589265 |
| 25.0% | quartile | 7.182044099 |
| 10.0% | | 7.030748901 |
| 2.5% | | 6.8005231753 |
| 0.5% | | 6.6974797975 |
| 0.0% | minimum | 6.665170075 |

### Summary statistics

| | |
|---|---|
| Mean | 7.2947029 |
| Std Dev | 0.2074181 |
| Std Err Mean | 0.0125306 |
| Upper 95% Mean | 7.3193718 |
| Lower 95% Mean | 7.270034 |
| N | 274 |

### Volume distribution

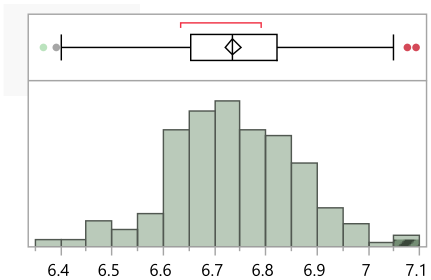


### Quantile

| | | |
|---|---|---|
| 100.0 % | maximum | 7.093108118 |
| 99.5% | | 7.0867420381 |
| 97.5% | | 6.973345031 |
| 90.0% | | 6.8822455975 |
| 75.0% | quartile | 6.8222655423 |
| 50.0% | median | 6.734887987 |
| 25.0% | quartile | 6.6533830963 |
| 10.0% | | 6.5990371905 |
| 2.5% | | 6.4647655863 |
| 0.5% | | 6.3755230659 |
| 0.0% | minimum | 6.366105653 |

### Summary statistics

| | |
|---|---|
| Mean | 6.7357912 |
| Std Dev | 0.1233461 |
| Std Err Mean | 0.0074516 |
| Upper 95% Mean | 6.7504611 |
| Lower 95% Mean | 6.7211213 |
| N | 274 |

### MDP distribution

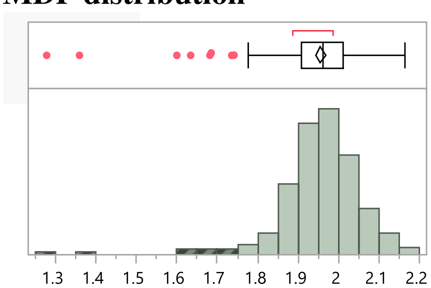


### Quantile

| | | |
|---|---|---|
| 100.0 % | maximum | 2.165598913 |
| 99.5% | | 2.1620712419 |
| 97.5% | | 2.1293000016 |
| 90.0% | | 2.061756924 |
| 75.0% | quartile | 2.0122597893 |
| 50.0% | median | 1.96008517 |
| 25.0% | quartile | 1.9065134755 |
| 10.0% | | 1.8619383225 |
| 2.5% | | 1.7293738 |
| 0.5% | | 1.3088534336 |
| 0.0% | minimum | 1.278462567 |

### Summary statistics

| | |
|---|---|
| Mean | 1.9555624 |
| Std Dev | 0.1014617 |
| Std Err Mean | 0.0061295 |
| Upper 95% Mean | 1.9676296 |
| Lower 95% Mean | 1.9434953 |
| N | 274 |

## MEAN distribution

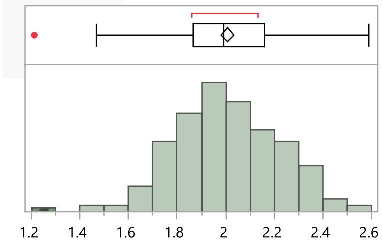


### Quantile

| | | |
|---|---|---|
| 100.0 % | maximum | 2.589813214 |
| 99.5% | | 2.5770576779 |
| 97.5% | | 2.4013895318 |
| 90.0% | | 2.2959868695 |
| 75.0% | quartile | 2.1567632235 |
| 50.0% | median | 1.992657188 |
| 25.0% | quartile | 1.8641258063 |
| 10.0% | | 1.746029881 |
| 2.5% | | 1.6126152116 |
| 0.5% | | 1.3085482783 |
| 0.0% | minimum | 1.213010387 |

### Summary statistics

| | |
|---|---|
| Mean | 2.0061532 |
| Std Dev | 0.2114941 |
| Std Err Mean | 0.0127768 |
| Upper 95% Mean | 2.0313068 |
| Lower 95% Mean | 1.9809996 |
| N | 274 |

## ML distribution

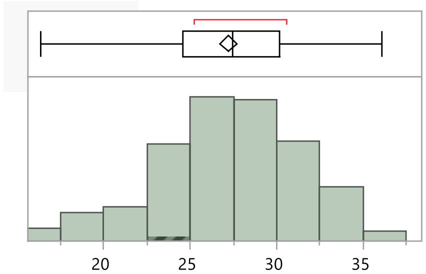


### Quantile

| | | |
|---|---|---|
| 100.0 % | maximum | 36.12087072 |
| 99.5% | | 35.998929908 |
| 97.5% | | 34.50304812 |
| 90.0% | | 32.736764805 |
| 75.0% | quartile | 30.207791973 |
| 50.0% | median | 27.478374255 |
| 25.0% | quartile | 24.565225998 |
| 10.0% | | 21.74853287 |
| 2.5% | | 17.958831068 |
| 0.5% | | 16.332482608 |
| 0.0% | minimum | 16.33110239 |

### Summary statistics

| | |
|---|---|
| Mean | 27.205057 |
| Std Dev | 4.144373 |
| Std Err Mean | 0.2503707 |
| Upper 95% Mean | 27.69796 |
| Lower 95% Mean | 26.712154 |
| N | 274 |

## MW distribution

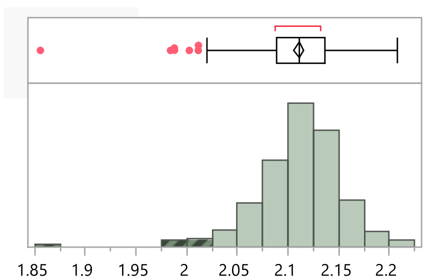


### Quantile

| | | |
|---|---|---|
| 100.0 % | maximum | 2.20839956 |
| 99.5% | | 2.2065978001 |
| 97.5% | | 2.1814980628 |
| 90.0% | | 2.1566131235 |
| 75.0% | quartile | 2.1369164178 |
| 50.0% | median | 2.1114713915 |
| 25.0% | quartile | 2.0891518838 |
| 10.0% | | 2.0624070785 |
| 2.5% | | 2.011501999 |
| 0.5% | | 1.9037010199 |
| 0.0% | minimum | 1.855543671 |

### Summary statistics

| | |
|---|---|
| Mean | 2.1106702 |
| Std Dev | 0.0412742 |
| Std Err Mean | 0.0024935 |
| Upper 95% Mean | 2.1155791 |
| Lower 95% Mean | 2.1057614 |
| N | 274 |

**RA distribution**

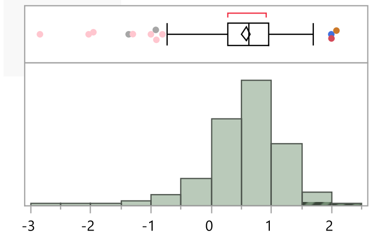


**Quantile**

| | | |
|---|---|---|
| 100.0 % | maximum | 2.078824893 |
| 99.5% | | 2.0479172239 |
| 97.5% | | 1.6508587136 |
| 90.0% | | 1.246207736 |
| 75.0% | quartile | 0.9501861933 |
| 50.0% | median | 0.6315135765 |
| 25.0% | quartile | 0.270034122 |
| 10.0% | | -0.118695424 |
| 2.5% | | -0.931483718 |
| 0.5% | | -2.542247909 |
| 0.0% | minimum | -2.845509951 |

**Summary statistics**

| | |
|---|---|
| Mean | 0.5755458 |
| Std Dev | 0.6349462 |
| Std Err Mean | 0.0383585 |
| Upper 95% Mean | 0.6510619 |
| Lower 95% Mean | 0.5000297 |
| N | 274 |

**ANG distribution**

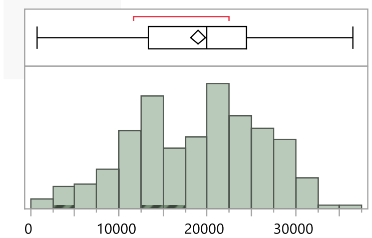


**Quantile**

| | | |
|---|---|---|
| 100.0 % | maximum | 36430.34266 |
| 99.5% | | 35413.180345 |
| 97.5% | | 31646.424866 |
| 90.0% | | 28586.06684 |
| 75.0% | quartile | 24423.56272 |
| 50.0% | median | 19880.96859 |
| 25.0% | quartile | 13286.200535 |
| 10.0% | | 9352.3097705 |
| 2.5% | | 4061.366876 |
| 0.5% | | 1134.4837346 |
| 0.0% | minimum | 719.9908115 |

**Summary statistics**

| | |
|---|---|
| Mean | 18954.66 |
| Std Dev | 7304.0657 |
| Std Err Mean | 441.25474 |
| Upper 95% Mean | 19823.354 |
| Lower 95% Mean | 18085.965 |
| N | 274 |

**AREA distribution**

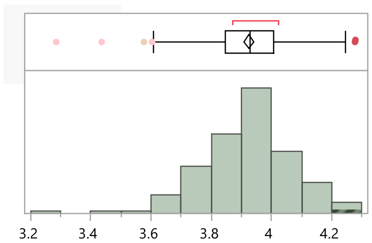


**Quantile**

| | | |
|---|---|---|
| 100.0 % | maximum | 4.278973665 |
| 99.5% | | 4.2783868669 |
| 97.5% | | 4.2149559905 |
| 90.0% | | 4.1075069515 |
| 75.0% | quartile | 4.0060925795 |
| 50.0% | median | 3.927404787 |
| 25.0% | quartile | 3.8452828963 |
| 10.0% | | 3.741784958 |
| 2.5% | | 3.6383763706 |
| 0.5% | | 3.3413576521 |
| 0.0% | minimum | 3.284687429 |

**Summary statistics**

| | |
|---|---|
| Mean | 3.924102 |
| Std Dev | 0.1408296 |
| Std Err Mean | 0.0085078 |
| Upper 95% Mean | 3.9408513 |
| Lower 95% Mean | 3.9073527 |
| N | 274 |

## RAD distribution

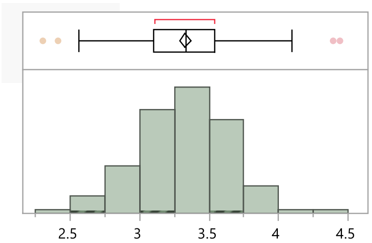


### Quantile

| | | |
|---|---|---|
| 100.0 % | maximum | 4.441409655 |
| 99.5% | | 4.4230030946 |
| 97.5% | | 3.9417285155 |
| 90.0% | | 3.7335255575 |
| 75.0% | quartile | 3.5372445083 |
| 50.0% | median | 3.3353395555 |
| 25.0% | quartile | 3.1036234153 |
| 10.0% | | 2.898753575 |
| 2.5% | | 2.6354152594 |
| 0.5% | | 2.342211411 |
| 0.0% | minimum | 2.301245247 |

### Summary statistics

| | |
|---|---|
| Mean | 3.3253174 |
| Std Dev | 0.3330523 |
| Std Err Mean | 0.0201204 |
| Upper 95% Mean | 3.3649284 |
| Lower 95% Mean | 3.2857065 |
| N | 274 |

## W distribution

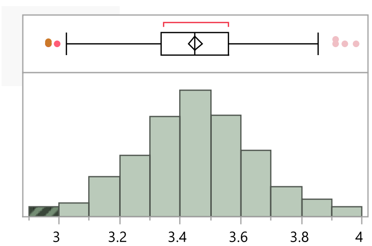


### Quantile

| | | |
|---|---|---|
| 100.0 % | maximum | 3.980552648 |
| 99.5% | | 3.966635984 |
| 97.5% | | 3.8469622165 |
| 90.0% | | 3.689675958 |
| 75.0% | quartile | 3.5589827438 |
| 50.0% | median | 3.447836328 |
| 25.0% | quartile | 3.3387415943 |
| 10.0% | | 3.193159666 |
| 2.5% | | 3.053129072 |
| 0.5% | | 2.964667834 |
| 0.0% | minimum | 2.964667834 |

### Summary statistics

| | |
|---|---|
| Mean | 3.4489501 |
| Std Dev | 0.1917598 |
| Std Err Mean | 0.0115846 |
| Upper 95% Mean | 3.4717567 |
| Lower 95% Mean | 3.4261435 |
| N | 274 |

## MD distribution

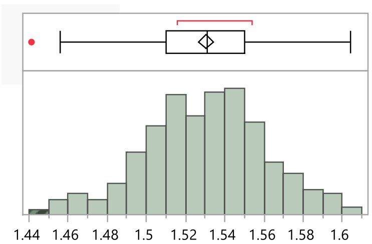


### Quantile

| | | |
|---|---|---|
| 100.0 % | maximum | 1.603917507 |
| 99.5% | | 1.603213686 |
| 97.5% | | 1.5933913284 |
| 90.0% | | 1.5698896335 |
| 75.0% | quartile | 1.550394012 |
| 50.0% | median | 1.530867138 |
| 25.0% | quartile | 1.5099545538 |
| 10.0% | | 1.4929516605 |
| 2.5% | | 1.4624389778 |
| 0.5% | | 1.4469688054 |
| 0.0% | minimum | 1.441356474 |

### Summary statistics

| | |
|---|---|
| Mean | 1.5304207 |
| Std Dev | 0.0305904 |
| Std Err Mean | 0.001848 |
| Upper 95% Mean | 1.5340589 |
| Lower 95% Mean | 1.5267825 |
| N | 274 |

APPENDIX C – DISCRIMINANT SCORES OF THE QDA MODEL FOR RAW MATERIAL CLASSIFICATION

| Row | Actual | Predicted | Prob (Pred) | Others |
|---|---|---|---|---|
| 1 | HEBT4_L7_232-1 | BASALT | 0.8915 | QUARTZITE 0.11 |
| 2 | HEBT4_L8_147-1 | QUARTZITE | 0.5114 | BASALT 0.49 |
| 3 | HEBT4_L8_223-1 | QUARTZITE | 0.7246 | BASALT 0.16 CHERT 0.12 |
| 4 | HEBT4_L8_294-2 | BASALT | 0.7848 | QUARTZITE 0.21 |
| 5 | HEBT4_L8_359-2 | QUARTZITE | 0.9020 | BASALT 0.25 QUARTZITE 0.22 |
| 6 | HEBT4_L8_359-2b | QUARTZITE | 0.5274 | BASALT 0.23 CHERT 0.24 |
| 7 | HEBT4_L8_372-3a | QUARTZITE | 0.5209 | BASALT 0.39 |
| 8 | HEBT4_L8_372-3b | QUARTZITE | 0.4306 | BASALT 0.40 CHERT 0.17 |
| 9 | HEBT4_L8_373-2 | CHERT | 0.9272 | BASALT 0.23 QUARTZITE 0.38 |
| 10 | HEBT4_L7_195-1 | BASALT | 0.6092 | QUARTZITE 0.37 |
| 11 | HEBT4_L8_351-2 | CHERT | 0.9933 | |
| 12 | HEBT4_L8_372-4 | QUARTZITE | 0.5055 | BASALT 0.34 CHERT 0.16 |
| 13 | HEBT4_L8_391-1 | BASALT | 0.9155 | CHERT 0.12 |
| 14 | HEBT4_L8_359-1a | BASALT | 0.9219 | |
| 15 | HEBT4_L8_188-1 | BASALT | 0.9714 | |
| 16 | HEBT4_L8_232-1 | BASALT | 0.9558 | |
| 17 | HEBT4_L8_351-1 | BASALT | 1.0000 | |
| 18 | HEBT4_L8_372-1 | BASALT | 0.9839 | |
| 19 | HEBT4_L8_468-2 | BASALT | 0.9652 | |
| 20 | HEBT4_L8_359-1b | BASALT | 1.0000 | |
| 21 | QUARTZITE | CHERT | 0.6492 | BASALT 0.17 CHERT 0.39 |
| 22 | QUARTZITE | QUARTZITE | 0.5471 | BASALT 0.24 CHERT 0.21 |
| 23 | QUARTZITE | QUARTZITE | 0.7192 | BASALT 0.16 CHERT 0.12 |
| 24 | QUARTZITE | BASALT | 0.6280 | CHERT 0.17 |
| 25 | QUARTZITE | QUARTZITE | 0.6843 | BASALT 0.31 |
| 26 | QUARTZITE | BASALT | 0.4969 | CHERT 0.21 |
| 27 | QUARTZITE | CHERT | 0.6950 | BASALT 0.13 |
| 28 | QUARTZITE | CHERT | 0.5949 | BASALT 0.35 |
| 29 | QUARTZITE | QUARTZITE | 0.4548 | BASALT 0.34 CHERT 0.21 |
| 30 | QUARTZITE | QUARTZITE | 0.5488 | BASALT 0.16 CHERT 0.29 |
| 31 | QUARTZITE | CHERT | 0.4776 | BASALT 0.24 |
| 32 | QUARTZITE | QUARTZITE | 0.5129 | BASALT 0.12 CHERT 0.37 |
| 33 | QUARTZITE | CHERT | 0.5212 | BASALT 0.11 |
| 34 | QUARTZITE | BASALT | 0.4057 | CHERT 0.23 |
| 35 | QUARTZITE | QUARTZITE | 0.5603 | BASALT 0.24 CHERT 0.20 |
| 36 | QUARTZITE | CHERT | 0.5701 | BASALT 0.16 |
| 37 | QUARTZITE | CHERT | 0.4657 | BASALT 0.29 |
| 38 | QUARTZITE | QUARTZITE | 0.4195 | BASALT 0.21 CHERT 0.37 |
| 39 | QUARTZITE | QUARTZITE | 0.3926 | BASALT 0.22 CHERT 0.38 |
| 40 | QUARTZITE | BASALT | 0.3950 | CHERT 0.22 |
| 41 | QUARTZITE | BASALT | 0.5099 | CHERT 0.24 |
| 42 | QUARTZITE | BASALT | 0.7038 | CHERT 0.10 |
| 43 | QUARTZITE | BASALT | 0.7323 | CHERT 0.11 |
| 44 | QUARTZITE | BASALT | 0.5604 | BASALT 0.37 CHERT 0.19 |
| 45 | QUARTZITE | BASALT | 0.5333 | CHERT 0.24 |

| Row | Actual | Predicted | Prob (Pred) | Others |
|---|---|---|---|---|
| 46 | QUARTZITE | QUARTZITE | 0.6780 | BASALT 0.29 |
| 47 | QUARTZITE | QUARTZITE | 0.8725 | BASALT 0.37 CHERT 0.13 |
| 48 | QUARTZITE | CHERT | 0.5762 | CHERT 0.26 |
| 49 | QUARTZITE | QUARTZITE | 0.8298 | CHERT 0.15 |
| 50 | QUARTZITE | QUARTZITE | 0.8192 | CHERT 0.13 |
| 51 | QUARTZITE | QUARTZITE | 0.8790 | CHERT 0.11 |
| 52 | QUARTZITE | CHERT | 0.6671 | CHERT 0.38 |
| 53 | QUARTZITE | QUARTZITE | 0.6420 | CHERT 0.35 |
| 54 | QUARTZITE | CHERT | 0.8425 | |
| 55 | QUARTZITE | BASALT | 0.4954 | CHERT 0.14 |
| 56 | QUARTZITE | BASALT | 0.6630 | CHERT 0.16 |
| 57 | QUARTZITE | BASALT | 0.5979 | |
| 58 | QUARTZITE | BASALT | 0.5410 | CHERT 0.36 |
| 59 | QUARTZITE | BASALT | 0.5078 | CHERT 0.18 |
| 60 | QUARTZITE | BASALT | 0.5406 | CHERT 0.37 |
| 61 | QUARTZITE | BASALT | 0.6329 | CHERT 0.17 |
| 62 | QUARTZITE | BASALT | 0.6955 | CHERT 0.11 |
| 63 | QUARTZITE | BASALT | 0.5193 | CHERT 0.10 |
| 64 | QUARTZITE | BASALT | 0.6682 | CHERT 0.16 |
| 65 | QUARTZITE | QUARTZITE | 0.6093 | BASALT 0.19 CHERT 0.20 |
| 66 | QUARTZITE | BASALT | 0.7249 | CHERT 0.15 |
| 67 | QUARTZITE | BASALT | 0.6065 | CHERT 0.14 |
| 68 | QUARTZITE | BASALT | 0.5244 | CHERT 0.15 |
| 69 | BASALT | BASALT | 0.8559 | CHERT 0.12 |
| 70 | BASALT | BASALT | 0.6593 | QUARTZITE 0.26 |
| 71 | BASALT | BASALT | 0.7056 | CHERT 0.24 |
| 72 | BASALT | BASALT | 0.8616 | CHERT 0.16 QUARTZITE 0.17 |
| 73 | BASALT | BASALT | 0.9255 | CHERT 0.13 QUARTZITE 0.21 |
| 74 | BASALT | BASALT | 0.8817 | CHERT 0.12 QUARTZITE 0.14 |
| 75 | BASALT | BASALT | 0.7247 | CHERT 0.12 QUARTZITE 0.15 |
| 76 | BASALT | BASALT | 0.6595 | CHERT 0.14 QUARTZITE 0.20 |
| 77 | BASALT | BASALT | 0.9744 | CHERT 0.17 QUARTZITE 0.24 |
| 78 | BASALT | BASALT | 0.9329 | CHERT 0.16 QUARTZITE 0.19 |
| 79 | BASALT | QUARTZITE | 0.5963 | CHERT 0.20 |
| 80 | BASALT | BASALT | 0.7751 | CHERT 0.11 QUARTZITE 0.11 |
| 81 | BASALT | BASALT | 0.7705 | CHERT 0.21 |
| 82 | BASALT | CHERT | 0.4961 | QUARTZITE 0.20 |
| 83 | BASALT | BASALT | 0.9514 | CHERT 0.12 QUARTZITE 0.20 |
| 84 | BASALT | BASALT | 0.6407 | CHERT 0.18 QUARTZITE 0.18 |
| 85 | BASALT | BASALT | 0.9888 | CHERT 0.16 |
| 86 | BASALT | BASALT | 0.3956 | CHERT 0.31 QUARTZITE 0.29 |
| 87 | BASALT | BASALT | 0.8950 | CHERT 0.32 |
| 88 | BASALT | BASALT | 0.8954 | CHERT 0.15 QUARTZITE 0.26 |
| 89 | BASALT | BASALT | 0.6790 | CHERT 0.14 QUARTZITE 0.19 |
| 90 | BASALT | BASALT | 0.7374 | CHERT 0.24 |
| 91 | BASALT | BASALT | 0.6997 | CHERT 0.17 QUARTZITE 0.13 |
| 92 | BASALT | BASALT | 0.9437 | QUARTZITE 0.28 |
| 93 | BASALT | BASALT | 0.9110 | CHERT 0.16 |
| 94 | BASALT | BASALT | 0.8127 | QUARTZITE 0.11 |
| 95 | BASALT | BASALT | 0.8613 | CHERT 0.10 |
| 96 | BASALT | BASALT | 0.5964 | CHERT 0.14 QUARTZITE 0.27 |
| 97 | BASALT | BASALT | 0.8789 | CHERT 0.11 QUARTZITE 0.20 |

| Row | Actual | Predicted | Prob (Pred) | Others |
|---|---|---|---|---|
| 98 | BASALT | BASALT | 0.6166 | CHERT 0.29 |
| 99 | BASALT | CHERT | 0.5879 | QUARTZITE 0.19 |
| 100 | BASALT | BASALT | 0.6503 | CHERT 0.22 QUARTZITE 0.13 |
| 101 | BASALT | QUARTZITE | 0.4784 | CHERT 0.21 |
| 102 | BASALT | BASALT | 0.7154 | CHERT 0.19 |
| 103 | BASALT | BASALT | 0.7987 | QUARTZITE 0.19 |
| 104 | BASALT | QUARTZITE | 0.7288 | QUARTZITE 0.47 |
| 105 | BASALT | BASALT | 0.7945 | QUARTZITE 0.19 |
| 106 | BASALT | BASALT | 0.7004 | CHERT 0.12 QUARTZITE 0.18 |
| 107 | BASALT | BASALT | 0.5260 | CHERT 0.45 |
| 108 | BASALT | BASALT | 0.5189 | CHERT 0.46 |
| 109 | BASALT | BASALT | 0.6185 | CHERT 0.37 |
| 110 | BASALT | BASALT | 0.9433 | QUARTZITE 0.17 |
| 111 | BASALT | QUARTZITE | 0.5430 | CHERT 0.17 |
| 112 | BASALT | BASALT | 0.7104 | CHERT 0.15 QUARTZITE 0.14 |
| 113 | BASALT | BASALT | 0.8532 | CHERT 0.14 |
| 114 | BASALT | BASALT | 0.5752 | CHERT 0.29 QUARTZITE 0.14 |
| 115 | BASALT | BASALT | 0.6895 | CHERT 0.16 QUARTZITE 0.16 |
| 116 | BASALT | BASALT | 0.5110 | QUARTZITE 0.48 |
| 117 | CHERT | CHERT | 0.8251 | BASALT 0.16 |
| 118 | CHERT | CHERT | 0.8646 | BASALT 0.13 |
| 119 | CHERT | BASALT | 0.5572 | QUARTZITE 0.10 |
| 120 | CHERT | BASALT | 0.6161 | QUARTZITE 0.14 |
| 121 | CHERT | BASALT | 0.4493 | QUARTZITE 0.18 |
| 122 | CHERT | BASALT | 0.9053 | BASALT 0.31 |
| 123 | CHERT | BASALT | 0.8067 | QUARTZITE 0.19 |
| 124 | CHERT | QUARTZITE | 0.5177 | BASALT 0.32 |
| 125 | CHERT | BASALT | 0.5265 | |
| 126 | CHERT | CHERT | 0.7471 | BASALT 0.24 |
| 127 | CHERT | CHERT | 0.9927 | QUARTZITE 0.12 |
| 128 | CHERT | CHERT | 0.9451 | QUARTZITE 0.12 |
| 129 | CHERT | BASALT | 0.7642 | QUARTZITE 0.35 |
| 130 | CHERT | BASALT | 0.5748 | QUARTZITE 0.15 |
| 131 | CHERT | BASALT | 0.4750 | QUARTZITE 0.15 |
| 132 | CHERT | BASALT | 0.4642 | QUARTZITE 0.25 |
| 133 | CHERT | BASALT | 0.4134 | QUARTZITE 0.37 |
| 134 | CHERT | CHERT | 0.4995 | BASALT 0.36 QUARTZITE 0.14 |
| 135 | CHERT | CHERT | 0.9487 | QUARTZITE 0.17 |
| 136 | CHERT | CHERT | 0.3517 | BASALT 0.34 QUARTZITE 0.31 |
| 137 | CHERT | CHERT | 0.9367 | BASALT 0.16 |
| 138 | CHERT | CHERT | 0.9923 | QUARTZITE 0.12 |
| 139 | CHERT | CHERT | 0.4808 | BASALT 0.47 |
| 140 | CHERT | BASALT | 0.6929 | BASALT 0.31 QUARTZITE 0.27 |
| 141 | CHERT | BASALT | 0.3870 | QUARTZITE 0.29 |
| 142 | CHERT | CHERT | 0.7887 | BASALT 0.21 |
| 143 | CHERT | BASALT | 0.6283 | QUARTZITE 0.14 |
| 144 | CHERT | BASALT | 0.5289 | QUARTZITE 0.22 |
| 145 | CHERT | BASALT | 0.5815 | BASALT 0.33 QUARTZITE 0.29 |
| 146 | CHERT | CHERT | 0.8497 | BASALT 0.14 |
| 147 | CHERT | BASALT | 0.5649 | QUARTZITE 0.22 |
| 148 | CHERT | BASALT | 0.6267 | QUARTZITE 0.16 |
| 149 | CHERT | BASALT | 0.5886 | QUARTZITE 0.16 |

| Row | Actual | Predicted | Prob (Pred) | Others |
|---|---|---|---|---|
| 150 | CHERT | CHERT | 0.7217 | BASALT 0.28 |
| 151 | CHERT | CHERT | 0.5332 | BASALT 0.46 |
| 152 | CHERT | BASALT | 0.4902 | QUARTZITE 0.24 |
| 153 | CHERT | BASALT | 0.5483 | QUARTZITE 0.27 |
| 154 | CHERT | BASALT | 0.5636 | QUARTZITE 0.20 |
| 155 | CHERT | CHERT | 0.6340 | BASALT 0.35 |
| 156 | CHERT | QUARTZITE | 0.3958 | BASALT 0.31 |
| 157 | CHERT | CHERT | 0.5140 | BASALT 0.44 |
| 158 | CHERT | BASALT | 0.4657 | QUARTZITE 0.25 |
| 159 | CHERT | CHERT | 0.6029 | QUARTZITE 0.34 |
| 160 | CHERT | QUARTZITE | 0.5717 | BASALT 0.13 QUARTZITE 0.39 |
| 161 | CHERT | BASALT | 0.5935 | QUARTZITE 0.14 |
| 162 | CHERT | CHERT | 0.5655 | BASALT 0.15 QUARTZITE 0.28 |
| 163 | CHERT | CHERT | 0.5635 | QUARTZITE 0.38 |
| 164 | CHERT | CHERT | 0.7246 | BASALT 0.20 |
| 165 | CHERT | BASALT | 0.4737 | BASALT 0.28 |
| 166 | BASALT | BASALT | 0.5395 | CHERT 0.25 QUARTZITE 0.21 |
| 167 | BASALT | BASALT | 0.7799 | CHERT 0.12 |
| 168 | BASALT | BASALT | 0.8272 | CHERT 0.12 |
| 169 | BASALT | BASALT | 0.6199 | CHERT 0.33 |
| 170 | BASALT | BASALT | 0.4145 | CHERT 0.24 QUARTZITE 0.35 |
| 171 | BASALT | QUARTZITE | 0.3386 | CHERT 0.33 |
| 172 | BASALT | BASALT | 0.7809 | CHERT 0.18 |
| 173 | BASALT | BASALT | 0.4583 | CHERT 0.30 QUARTZITE 0.24 |
| 174 | BASALT | BASALT | 0.7467 | CHERT 0.17 |
| 175 | BASALT | BASALT | 0.7419 | CHERT 0.24 |
| 176 | BASALT | BASALT | 0.7968 | CHERT 0.13 |
| 177 | BASALT | BASALT | 0.8069 | CHERT 0.15 QUARTZITE 0.20 |
| 178 | BASALT | BASALT | 0.6174 | CHERT 0.15 QUARTZITE 0.23 |
| 179 | BASALT | BASALT | 0.4949 | QUARTZITE 0.42 |
| 180 | BASALT | BASALT | 0.6960 | QUARTZITE 0.22 |
| 181 | BASALT | BASALT | 0.7186 | CHERT 0.13 QUARTZITE 0.15 |
| 182 | BASALT | BASALT | 0.6829 | CHERT 0.31 |
| 183 | BASALT | QUARTZITE | 0.4782 | CHERT 0.23 |
| 184 | BASALT | BASALT | 0.4380 | CHERT 0.42 QUARTZITE 0.14 |
| 185 | BASALT | QUARTZITE | 0.5061 | CHERT 0.28 |
| 186 | BASALT | CHERT | 0.4704 | CHERT 0.34 |
| 187 | BASALT | BASALT | 0.4357 | CHERT 0.18 QUARTZITE 0.38 |
| 188 | BASALT | BASALT | 0.6878 | CHERT 0.24 |
| 189 | BASALT | BASALT | 0.7691 | QUARTZITE 0.21 |
| 190 | BASALT | BASALT | 0.5136 | CHERT 0.40 |
| 191 | BASALT | BASALT | 0.6354 | CHERT 0.30 |
| 192 | BASALT | BASALT | 0.6429 | CHERT 0.35 |
| 193 | BASALT | BASALT | 0.6235 | CHERT 0.20 QUARTZITE 0.17 |
| 194 | BASALT | BASALT | 0.5183 | CHERT 0.14 QUARTZITE 0.34 |
| 195 | BASALT | BASALT | 0.8311 | CHERT 0.33 |
| 196 | BASALT | BASALT | 0.6924 | CHERT 0.16 QUARTZITE 0.15 |
| 197 | BASALT | BASALT | 0.8333 | CHERT 0.15 |
| 198 | BASALT | BASALT | 0.8284 | QUARTZITE 0.16 |
| 199 | BASALT | BASALT | 0.5925 | CHERT 0.40 |
| 200 | BASALT | QUARTZITE | 0.5330 | CHERT 0.33 |
| 201 | BASALT | BASALT | 0.4177 | CHERT 0.34 QUARTZITE 0.24 |

| Row | Actual | Predicted | Prob (Pred) | Others |
|---|---|---|---|---|
| 202 | BASALT | BASALT | 0.7817 | CHERT 0.16 |
| 203 | BASALT | BASALT | 0.5524 | CHERT 0.11 QUARTZITE 0.34 |
| 204 | BASALT | BASALT | 0.5067 | CHERT 0.18 QUARTZITE 0.31 |
| 205 | BASALT | BASALT | 0.8130 | CHERT 0.13 |
| 206 | BASALT | BASALT | 0.4033 | CHERT 0.36 QUARTZITE 0.24 |
| 207 | BASALT | BASALT | 0.5137 | CHERT 0.46 |
| 208 | BASALT | BASALT | 0.6270 | CHERT 0.32 |
| 209 | BASALT | BASALT | 0.7055 | QUARTZITE 0.28 |
| 210 | BASALT | BASALT | 0.6292 | CHERT 0.37 |
| 211 | BASALT | BASALT | 0.6075 | CHERT 0.12 QUARTZITE 0.27 |
| 212 | BASALT | BASALT | 0.6798 | CHERT 0.16 QUARTZITE 0.16 |
| 213 | CHERT | CHERT | 0.8200 | QUARTZITE 0.13 |
| 214 | CHERT | CHERT | 0.8866 | QUARTZITE 0.10 |
| 215 | CHERT | CHERT | 0.9985 | QUARTZITE 0.34 |
| 216 | CHERT | CHERT | 0.7645 | BASALT 0.21 |
| 217 | CHERT | CHERT | 0.6653 | QUARTZITE 0.25 |
| 218 | CHERT | BASALT | 0.3748 | QUARTZITE 0.34 |
| 219 | CHERT | CHERT | 0.9839 | QUARTZITE 0.40 |
| 220 | CHERT | CHERT | 0.9229 | BASALT 0.11 |
| 221 | CHERT | CHERT | 0.8706 | QUARTZITE 0.11 |
| 222 | CHERT | CHERT | 0.7237 | QUARTZITE 0.25 |
| 223 | CHERT | CHERT | 0.9212 | BASALT 0.21 QUARTZITE 0.30 |
| 224 | CHERT | CHERT | 0.9720 | BASALT 0.14 QUARTZITE 0.23 |
| 225 | CHERT | BASALT | 0.7418 | QUARTZITE 0.30 |
| 226 | CHERT | BASALT | 0.5550 | QUARTZITE 0.28 |
| 227 | CHERT | BASALT | 0.7565 | QUARTZITE 0.30 |
| 228 | CHERT | QUARTZITE | 0.5110 | BASALT 0.20 |
| 229 | CHERT | QUARTZITE | 0.4881 | BASALT 0.10 |
| 230 | CHERT | BASALT | 0.5765 | QUARTZITE 0.35 |
| 231 | CHERT | CHERT | 0.8069 | QUARTZITE 0.19 |
| 232 | CHERT | CHERT | 0.7699 | QUARTZITE 0.23 |
| 233 | CHERT | CHERT | 1.0000 | |
| 234 | CHERT | CHERT | 0.8919 | QUARTZITE 0.10 |
| 235 | CHERT | CHERT | 0.7696 | QUARTZITE 0.18 |
| 236 | CHERT | CHERT | 0.7996 | QUARTZITE 0.15 |
| 237 | CHERT | CHERT | 0.7777 | QUARTZITE 0.14 |
| 238 | CHERT | BASALT | 0.6293 | BASALT 0.36 QUARTZITE 0.26 |
| 239 | CHERT | BASALT | 0.6744 | QUARTZITE 0.29 |
| 240 | CHERT | BASALT | 0.6818 | QUARTZITE 0.23 |
| 241 | CHERT | CHERT | 1.0000 | |
| 242 | CHERT | BASALT | 0.5994 | BASALT 0.28 QUARTZITE 0.26 |
| 243 | CHERT | CHERT | 0.6510 | BASALT 0.30 |
| 244 | CHERT | CHERT | 0.6672 | QUARTZITE 0.24 |
| 245 | CHERT | CHERT | 0.6829 | BASALT 0.21 QUARTZITE 0.10 |
| 246 | CHERT | CHERT | 0.4633 | BASALT 0.24 QUARTZITE 0.30 |
| 247 | CHERT | CHERT | 0.5400 | BASALT 0.25 QUARTZITE 0.21 |
| 248 | CHERT | CHERT | 0.7791 | BASALT 0.19 |
| 249 | BASALT | BASALT | 0.7535 | CHERT 0.17 |
| 250 | BASALT | CHERT | 0.7602 | QUARTZITE 0.34 |
| 251 | BASALT | BASALT | 0.9897 | CHERT 0.20 QUARTZITE 0.33 |
| 252 | BASALT | BASALT | 0.5558 | CHERT 0.21 QUARTZITE 0.23 |
| 253 | BASALT | QUARTZITE | 0.5473 | QUARTZITE 0.35 |

| Row | Actual | Predicted | Prob (Pred) | Others |
|---|---|---|---|---|
| 254 | BASALT | BASALT | 0.8743 | CHERT 0.12 |
| 255 | BASALT | BASALT | 0.4419 | CHERT 0.24 QUARTZITE 0.32 |
| 256 | BASALT | BASALT | 0.8664 | CHERT 0.13 |
| 257 | BASALT | CHERT | 0.5194 | QUARTZITE 0.21 |
| 258 | BASALT | QUARTZITE | 0.4212 | CHERT 0.35 |
| 259 | BASALT | BASALT | 0.8587 | QUARTZITE 0.14 |
| 260 | CHERT | CHERT | 0.8813 | BASALT 0.12 |
| 261 | BASALT | BASALT | 0.7255 | CHERT 0.25 |
| 262 | BASALT | BASALT | 0.9491 | CHERT 0.21 |
| 263 | BASALT | QUARTZITE | 0.8537 | QUARTZITE 0.19 |
| 264 | BASALT | BASALT | 0.8789 | CHERT 0.12 |
| 265 | BASALT | BASALT | 0.5171 | CHERT 0.47 |
| 266 | BASALT | BASALT | 0.7674 | CHERT 0.23 |
| 267 | CHERT | CHERT | 0.9995 | QUARTZITE 0.26 |
| 268 | CHERT | CHERT | 0.9996 | QUARTZITE 0.25 |
| 269 | QUARTZITE | BASALT | 0.8570 | BASALT 0.19 CHERT 0.39 |
| 270 | BASALT | CHERT | 0.9540 | QUARTZITE 0.30 |
| 271 | CHERT | CHERT | 0.9804 | BASALT 0.16 |
| 272 | QUARTZITE | QUARTZITE | 0.8536 | BASALT 0.15 |
| 273 | BASALT | BASALT | 0.5994 | QUARTZITE 0.38 |
| 274 | CHERT | CHERT | 0.9776 | QUARTZITE 0.31 |
| 275 | BASALT | CHERT | 0.5529 | QUARTZITE 0.16 |
| 276 | BASALT | BASALT | 0.9787 | CHERT 0.12 |

'*' indicates misclassified
"~" indicates excluded row

APPENDIX D – DISCRIMINANT SCORES OF THE QDA MODEL FOR TECHNOLOGY CLASSIFICATION

| Row | Actual | SqDist (Actual) | Prob (Actual) | -Log (Prob) | Predicted | Prob (Pred) | Others |
|---|---|---|---|---|---|---|---|
| 1 | HEBT4_L7_232-1 | . | . | . | NR | 0.9992 | |
| 2 | HEBT4_L8_147-1 | . | . | . | NR | 0.9998 | |
| 3 | HEBT4_L8_223-1 | . | . | . | BF | 0.9524 | |
| 4 | HEBT4_L8_294-2 | . | . | . | NR | 0.6533 | BF 0.35 |
| 5 | HEBT4_L8_359-2 | . | . | . | NR | 0.9311 | |
| 6 | HEBT4_L8_359-2b | . | . | . | BF | 0.8437 | NR 0.16 |
| 7 | HEBT4_L8_372-3a | . | . | . | NR | 0.8639 | BF 0.14 |
| 8 | HEBT4_L8_372-3b | . | . | . | NR | 0.9952 | |
| 9 | HEBT4_L8_373-2 | . | . | . | BF | 0.9001 | |
| 10 | HEBT4_L7_195-1 | . | . | . | NR | 0.8556 | BF 0.14 |
| 11 | HEBT4_L8_351-2 | . | . | . | NR | 1.0000 | |
| 12 | HEBT4_L8_372-4 | . | . | . | NR | 0.9999 | |
| 13 | HEBT4_L8_391-1 | . | . | . | NR | 0.9892 | |
| 14 | HEBT4_L8_359-1a | . | . | . | NR | 0.9997 | |
| 15 | HEBT4_L8_188-1 | . | . | . | NR | 0.9960 | |
| 16 | HEBT4_L8_232-1 | . | . | . | BF | 0.6835 | NR 0.32 |
| 17 | HEBT4_L8_351-1 | . | . | . | NR | 0.9978 | |
| 18 | HEBT4_L8_372-1 | . | . | . | NR | 0.9538 | |
| 19 | HEBT4_L8_468-2 | . | . | . | NR | 0.9952 | |
| 20 | HEBT4_L8_359-1b | . | . | . | NR | 1.0000 | |
| 21 | BF | -28.0366 | 0.9943 | 0.006 | BF | 0.9943 | |
| 22 | BF | -31.2941 | 0.7485 | 0.290 | BF | 0.7485 | NR 0.25 |
| 23 | BF | -26.6395 | 0.9045 | 0.100 | BF | 0.9045 | |
| 24 | BF | -32.0300 | 0.8710 | 0.138 | BF | 0.8710 | NR 0.13 |
| 25 | BF | -24.3211 | 0.7198 | 0.329 | BF | 0.7198 | NR 0.28 |
| 26 | BF | -32.0894 | 0.8417 | 0.172 | BF | 0.8417 | NR 0.16 |
| 27 | BF | -34.0628 | 0.9768 | 0.023 | BF | 0.9768 | |
| 28 | BF | -32.3026 | 0.0924 | 2.382 | FLAKE | 0.8825 | |
| 29 | BF | -28.9625 | 0.8921 | 0.114 | BF | 0.8921 | NR 0.11 |
| 30 | BF | -18.8561 | 0.8272 | 0.190 | BF | 0.8272 | NR 0.17 |
| 31 | BF | -23.3865 | 0.4503 | 0.798 | NR | 0.5497 | |
| 32 | BF | -31.6426 | 0.5735 | 0.556 | BF | 0.5735 | NR 0.41 |
| 33 | BF | -34.9046 | 0.4204 | 0.867 | FLAKE | 0.4910 | |
| 34 | BF | -30.4402 | 0.3669 | 1.003 | NR | 0.6331 | |
| 35 | BF | -22.0484 | 0.9733 | 0.027 | BF | 0.9733 | |
| 36 | BF | -30.8452 | 0.9504 | 0.051 | BF | 0.9504 | |
| 37 | BF | -33.4005 | 0.6654 | 0.407 | BF | 0.6654 | NR 0.33 |
| 38 | BF | -28.0851 | 0.9355 | 0.067 | BF | 0.9355 | |
| 39 | BF | -31.6544 | 0.8050 | 0.217 | BF | 0.8050 | NR 0.16 |
| 40 | BF | -33.1881 | 0.8980 | 0.108 | BF | 0.8980 | NR 0.10 |
| 41 | BF | -32.9398 | 0.2273 | 1.482 | NR | 0.7725 | |
| 42 | BF | -26.4572 | 0.3021 | 1.197 | CORE | 0.4795 | NR 0.22 |
| 43 | BF | -26.9311 | 0.9690 | 0.031 | BF | 0.9690 | |
| 44 | BF | -21.0075 | 0.0204 | 3.892 | CORE | 0.9514 | |
| 45 | NR | -32.0962 | 0.9770 | 0.023 | NR | 0.9770 | |

| Row | Actual | SqDist (Actual) | Prob (Actual) | -Log (Prob) | Predicted | Prob (Pred) | Others |
|---|---|---|---|---|---|---|---|
| 46 | NR | -23.8099 | 0.6608 | 0.414 | NR | 0.6608 | BF 0.34 |
| 47 | NR | -21.6870 | 0.5968 | 0.516 | NR | 0.5968 | BF 0.40 |
| 48 | NR | -12.2595 | 0.9806 | 0.020 | NR | 0.9806 | |
| 49 | NR | -21.4587 | 0.2435 | 1.413 | BF | 0.7565 | |
| 50 | NR | -11.9448 | 1.0000 | 0.000 | NR | 1.0000 | |
| 51 | NR | -11.8649 | 0.9999 | 0.000 | NR | 0.9999 | |
| 52 | NR | -23.5961 | 0.0415 | 3.181 | BF | 0.8140 | CORE 0.14 |
| 53 | NR | -20.9633 | 0.9506 | 0.051 | NR | 0.9506 | |
| 54 | NR | -18.1335 | 0.2382 | 1.435 | BF | 0.7444 | |
| 55 | NR | -30.8074 | 0.4115 | 0.888 | BF | 0.5885 | |
| 56 | NR | -34.5473 | 0.7517 | 0.285 | NR | 0.7517 | BF 0.24 |
| 57 | NR | -25.5223 | 0.9493 | 0.052 | NR | 0.9493 | |
| 58 | NR | -26.0888 | 0.0521 | 2.954 | BF | 0.9477 | |
| 59 | NR | -31.4385 | 0.9918 | 0.008 | NR | 0.9918 | |
| 60 | NR | -31.2873 | 0.8703 | 0.139 | NR | 0.8703 | BF 0.13 |
| 61 | NR | -34.7316 | 0.8380 | 0.177 | NR | 0.8380 | BF 0.16 |
| 62 | NR | -33.8454 | 0.8117 | 0.209 | NR | 0.8117 | BF 0.19 |
| 63 | NR | -30.6375 | 0.8553 | 0.156 | NR | 0.8553 | BF 0.14 |
| 64 | NR | -28.3342 | 0.5457 | 0.606 | NR | 0.5457 | BF 0.45 |
| 65 | NR | 42.7756 | 0.0000 | 12.503 | CORE | 0.9961 | |
| 66 | NR | -35.9751 | 0.4488 | 0.801 | BF | 0.5497 | |
| 67 | NR | -32.4785 | 0.4698 | 0.755 | BF | 0.5202 | |
| 68 | NR | -32.9285 | 0.8647 | 0.145 | NR | 0.8647 | BF 0.14 |
| 69 | BF | -31.6993 | 0.8610 | 0.150 | BF | 0.8610 | NR 0.14 |
| 70 | BF | -23.0524 | 0.9321 | 0.070 | BF | 0.9321 | |
| 71 | BF | -31.1723 | 0.7860 | 0.241 | BF | 0.7860 | NR 0.21 |
| 72 | BF | -33.0252 | 0.5681 | 0.566 | BF | 0.5681 | NR 0.43 |
| 73 | BF | -29.2910 | 0.8625 | 0.148 | BF | 0.8625 | NR 0.14 |
| 74 | BF | -24.2048 | 0.6375 | 0.450 | BF | 0.6375 | NR 0.36 |
| 75 | BF | -34.0783 | 0.8091 | 0.212 | BF | 0.8091 | NR 0.19 |
| 76 | BF | -36.6676 | 0.5654 | 0.570 | BF | 0.5654 | NR 0.43 |
| 77 | BF | -23.7537 | 0.7422 | 0.298 | BF | 0.7422 | NR 0.26 |
| 78 | BF | -31.2248 | 0.7903 | 0.235 | BF | 0.7903 | NR 0.21 |
| 79 | BF | -9.9458 | 0.0031 | 5.762 | NR | 0.9969 | |
| 80 | BF | -31.7936 | 0.7932 | 0.232 | BF | 0.7932 | NR 0.21 |
| 81 | BF | -28.4383 | 0.7994 | 0.224 | BF | 0.7994 | NR 0.20 |
| 82 | BF | -29.8722 | 0.9369 | 0.065 | BF | 0.9369 | |
| 83 | BF | -12.4378 | 0.8439 | 0.170 | BF | 0.8439 | NR 0.16 |
| 84 | BF | -34.0759 | 0.6743 | 0.394 | BF | 0.6743 | NR 0.33 |
| 85 | BF | -12.2859 | 0.2046 | 1.586 | NR | 0.7954 | |
| 86 | BF | -33.8764 | 0.9010 | 0.104 | BF | 0.9010 | |
| 87 | BF | -24.9508 | 0.5858 | 0.535 | BF | 0.5858 | NR 0.41 |
| 88 | BF | -32.8391 | 0.8048 | 0.217 | BF | 0.8048 | NR 0.20 |
| 89 | BF | -29.3327 | 0.2641 | 1.332 | NR | 0.7359 | |
| 90 | BF | -29.2687 | 0.6240 | 0.472 | BF | 0.6240 | NR 0.38 |
| 91 | BF | -23.7819 | 0.8793 | 0.129 | BF | 0.8793 | NR 0.12 |
| 92 | BF | -15.7913 | 0.6700 | 0.401 | BF | 0.6700 | NR 0.33 |
| 93 | NR | -26.8911 | 0.7408 | 0.300 | NR | 0.7408 | BF 0.26 |
| 94 | NR | -27.3595 | 0.9509 | 0.050 | NR | 0.9509 | |
| 95 | NR | -30.0014 | 0.9351 | 0.067 | NR | 0.9351 | |
| 96 | NR | -29.9535 | 0.4744 | 0.746 | BF | 0.5256 | |
| 97 | NR | -18.3195 | 0.5087 | 0.676 | NR | 0.5087 | BF 0.49 |

| Row | Actual | SqDist (Actual) | Prob (Actual) | -Log (Prob) | Predicted | Prob (Pred) | Others |
|---|---|---|---|---|---|---|---|
| 98 | NR | -31.7087 | 0.8963 | 0.109 | NR | 0.8963 | BF 0.10 |
| 99 | NR | -26.4541 | 0.8182 | 0.201 | NR | 0.8182 | BF 0.18 |
| 100 | NR | -34.6955 | 0.8649 | 0.145 | NR | 0.8649 | BF 0.14 |
| 101 | NR | -30.7602 | 0.9748 | 0.026 | NR | 0.9748 | |
| 102 | NR | -24.2919 | 0.0336 | 3.392 | BF | 0.9664 | |
| 103 | NR | -22.8731 | 0.5636 | 0.573 | NR | 0.5636 | BF 0.44 |
| 104 | NR | -24.7150 | 0.9088 | 0.096 | NR | 0.9088 | |
| 105 | NR | -28.5945 | 0.9417 | 0.060 | NR | 0.9417 | |
| 106 | NR | -32.6661 | 0.7017 | 0.354 | NR | 0.7017 | BF 0.30 |
| 107 | NR | -26.2730 | 0.7195 | 0.329 | NR | 0.7195 | BF 0.25 |
| 108 | NR | -30.1303 | 0.7577 | 0.278 | NR | 0.7577 | BF 0.24 |
| 109 | NR | -30.3579 | 0.8749 | 0.134 | NR | 0.8749 | BF 0.13 |
| 110 | NR | -26.4764 | 0.9943 | 0.006 | NR | 0.9943 | |
| 111 | NR | -33.2915 | 0.9469 | 0.055 | NR | 0.9469 | |
| 112 | NR | -35.3393 | 0.9537 | 0.047 | NR | 0.9537 | |
| 113 | NR | -14.9523 | 0.5807 | 0.543 | NR | 0.5807 | BF 0.42 |
| 114 | NR | -34.1460 | 0.9653 | 0.035 | NR | 0.9653 | |
| 115 | NR | -31.3962 | 0.9970 | 0.003 | NR | 0.9970 | |
| 116 | NR | -15.7784 | 0.9999 | 0.000 | NR | 0.9999 | |
| 117 | BF | -25.6082 | 0.3104 | 1.170 | NR | 0.6896 | |
| 118 | BF | -21.8648 | 0.6448 | 0.439 | BF | 0.6448 | NR 0.36 |
| 119 | BF | -29.9007 | 0.7532 | 0.283 | BF | 0.7532 | NR 0.25 |
| 120 | BF | -36.2649 | 0.7102 | 0.342 | BF | 0.7102 | NR 0.29 |
| 121 | BF | -29.9087 | 0.2520 | 1.378 | NR | 0.7470 | |
| 122 | BF | -12.1365 | 0.8528 | 0.159 | BF | 0.8528 | NR 0.15 |
| 123 | BF | -34.6586 | 0.4901 | 0.713 | NR | 0.5099 | |
| 124 | BF | -28.2108 | 0.3485 | 1.054 | NR | 0.6514 | |
| 125 | BF | -22.1327 | 0.9150 | 0.089 | BF | 0.9150 | |
| 126 | BF | -15.6838 | 0.5245 | 0.645 | BF | 0.5245 | NR 0.48 |
| 127 | BF | -22.5062 | 0.8972 | 0.108 | BF | 0.8972 | NR 0.10 |
| 128 | BF | -20.1201 | 0.9750 | 0.025 | BF | 0.9750 | |
| 129 | BF | -27.8989 | 0.1229 | 2.096 | NR | 0.8770 | |
| 130 | BF | -33.8064 | 0.6411 | 0.445 | BF | 0.6411 | NR 0.36 |
| 131 | BF | -33.3227 | 0.4022 | 0.911 | NR | 0.5300 | |
| 132 | BF | -35.1206 | 0.3990 | 0.919 | NR | 0.6010 | |
| 133 | BF | -29.0556 | 0.5083 | 0.677 | BF | 0.5083 | NR 0.49 |
| 134 | BF | -31.9108 | 0.8521 | 0.160 | BF | 0.8521 | NR 0.15 |
| 135 | BF | -18.3116 | 0.8388 | 0.176 | BF | 0.8388 | NR 0.16 |
| 136 | BF | -30.9807 | 0.5091 | 0.675 | BF | 0.5091 | NR 0.49 |
| 137 | BF | -16.9849 | 0.6398 | 0.447 | BF | 0.6398 | NR 0.36 |
| 138 | BF | -3.1806 | 1.0000 | 0.000 | BF | 1.0000 | |
| 139 | BF | -31.6270 | 0.7309 | 0.314 | BF | 0.7309 | NR 0.27 |
| 140 | NR | -22.0427 | 0.9936 | 0.006 | NR | 0.9936 | |
| 141 | NR | -24.7469 | 0.6310 | 0.460 | NR | 0.6310 | BF 0.37 |
| 142 | NR | -21.6403 | 0.4706 | 0.754 | BF | 0.5294 | |
| 143 | NR | -30.5360 | 0.4889 | 0.716 | BF | 0.5008 | |
| 144 | NR | -35.9805 | 0.5757 | 0.552 | NR | 0.5757 | BF 0.42 |
| 145 | NR | -32.3518 | 0.5030 | 0.687 | NR | 0.5030 | BF 0.50 |
| 146 | NR | -18.2195 | 0.2919 | 1.231 | BF | 0.7081 | |
| 147 | NR | -35.6383 | 0.9110 | 0.093 | NR | 0.9110 | |
| 148 | NR | -32.2305 | 0.9423 | 0.059 | NR | 0.9423 | |
| 149 | NR | -34.4448 | 0.0452 | 3.097 | FLAKE | 0.8475 | BF 0.11 |

| Row | Actual | SqDist (Actual) | Prob (Actual) | -Log (Prob) | Predicted | Prob (Pred) | Others |
|---|---|---|---|---|---|---|---|
| 150 | NR | -17.1836 | 0.9315 | 0.071 | NR | 0.9315 | |
| 151 | NR | -25.4541 | 0.9819 | 0.018 | NR | 0.9819 | |
| 152 | NR | -32.7159 | 0.8842 | 0.123 | NR | 0.8842 | BF 0.12 |
| 153 | NR | -31.7997 | 0.9483 | 0.053 | NR | 0.9483 | |
| 154 | NR | -29.7446 | 0.2720 | 1.302 | BF | 0.7280 | |
| 155 | NR | -26.8152 | 0.0885 | 2.425 | BF | 0.9115 | |
| 156 | NR | -28.3488 | 0.5411 | 0.614 | NR | 0.5411 | BF 0.46 |
| 157 | NR | -28.4616 | 0.3633 | 1.012 | BF | 0.6367 | |
| 158 | NR | -28.4390 | 0.9967 | 0.003 | NR | 0.9967 | |
| 159 | NR | -25.2872 | 0.9690 | 0.031 | NR | 0.9690 | |
| 160 | NR | -29.7830 | 0.9987 | 0.001 | NR | 0.9987 | |
| 161 | NR | -28.0959 | 0.8341 | 0.181 | NR | 0.8341 | BF 0.17 |
| 162 | NR | -30.1809 | 0.9760 | 0.024 | NR | 0.9760 | |
| 163 | NR | -29.7529 | 0.9235 | 0.080 | NR | 0.9235 | |
| 164 | NR | -28.9518 | 0.9863 | 0.014 | NR | 0.9863 | |
| 165 | NR | -33.5485 | 0.7196 | 0.329 | NR | 0.7196 | BF 0.28 |
| 166 | BF | -32.8319 | 0.4925 | 0.708 | NR | 0.5075 | |
| 167 | BF | -33.5969 | 0.3552 | 1.035 | NR | 0.6448 | |
| 168 | BF | -26.0957 | 0.5509 | 0.596 | BF | 0.5509 | NR 0.45 |
| 169 | BF | -33.3645 | 0.8523 | 0.160 | BF | 0.8523 | NR 0.12 |
| 170 | BF | -25.0216 | 0.3685 | 0.998 | NR | 0.6315 | |
| 171 | BF | -31.8817 | 0.3256 | 1.122 | NR | 0.6744 | |
| 172 | BF | -29.6930 | 0.4049 | 0.904 | NR | 0.5833 | |
| 173 | BF | -36.4816 | 0.6004 | 0.510 | BF | 0.6004 | FLAKE 0.26 NR 0.14 |
| 174 | BF | -33.1578 | 0.8857 | 0.121 | BF | 0.8857 | NR 0.11 |
| 175 | BF | -31.9649 | 0.4422 | 0.816 | BF | 0.4422 | FLAKE 0.30 NR 0.26 |
| 176 | BF | -27.8609 | 0.3578 | 1.028 | NR | 0.6422 | |
| 177 | BF | -34.9184 | 0.4770 | 0.740 | NR | 0.5229 | |
| 178 | BF | -31.8172 | 0.7667 | 0.266 | BF | 0.7667 | NR 0.23 |
| 179 | BF | -33.4903 | 0.3856 | 0.953 | NR | 0.6144 | |
| 180 | BF | -29.5808 | 0.8581 | 0.153 | BF | 0.8581 | NR 0.14 |
| 181 | BF | -32.4880 | 0.4037 | 0.907 | NR | 0.5963 | |
| 182 | BF | -20.8381 | 0.7409 | 0.300 | BF | 0.7409 | NR 0.26 |
| 183 | BF | -33.5140 | 0.8541 | 0.158 | BF | 0.8541 | NR 0.12 |
| 184 | BF | -33.0825 | 0.7419 | 0.298 | BF | 0.7419 | FLAKE 0.23 |
| 185 | BF | -26.3758 | 0.8322 | 0.184 | BF | 0.8322 | NR 0.17 |
| 186 | BF | -27.6851 | 0.9473 | 0.054 | BF | 0.9473 | |
| 187 | BF | -33.5230 | 0.4528 | 0.792 | NR | 0.5472 | |
| 188 | BF | -32.7322 | 0.9755 | 0.025 | BF | 0.9755 | |
| 189 | NR | -28.0191 | 0.9925 | 0.008 | NR | 0.9925 | |
| 190 | NR | -29.5253 | 0.7304 | 0.314 | NR | 0.7304 | BF 0.27 |
| 191 | NR | -32.8746 | 0.7450 | 0.294 | NR | 0.7450 | BF 0.26 |
| 192 | NR | -31.6720 | 0.6523 | 0.427 | NR | 0.6523 | BF 0.35 |
| 193 | NR | -29.5825 | 0.3087 | 1.175 | BF | 0.6913 | |
| 194 | NR | -31.5654 | 0.7494 | 0.288 | NR | 0.7494 | BF 0.25 |
| 195 | NR | -31.1712 | 0.9569 | 0.044 | NR | 0.9569 | |
| 196 | NR | -21.9996 | 0.8964 | 0.109 | NR | 0.8964 | BF 0.10 |
| 197 | NR | -26.5458 | 0.2530 | 1.374 | BF | 0.7451 | |
| 198 | NR | -27.9649 | 0.4481 | 0.803 | BF | 0.5519 | |
| 199 | NR | -22.2938 | 0.9973 | 0.003 | NR | 0.9973 | |
| 200 | NR | -29.8568 | 0.9547 | 0.046 | NR | 0.9547 | |
| 201 | NR | -30.3805 | 0.1854 | 1.685 | BF | 0.8146 | |

| Row | Actual | SqDist (Actual) | Prob (Actual) | -Log (Prob) | Predicted | Prob (Pred) | Others |
|---|---|---|---|---|---|---|---|
| 202 | NR | -30.8852 | 0.9314 | 0.071 | NR | 0.9314 | |
| 203 | NR | -31.1900 | 0.9868 | 0.013 | NR | 0.9868 | |
| 204 | NR | -32.5987 | 0.8807 | 0.127 | NR | 0.8807 | BF 0.12 |
| 205 | NR | -32.3512 | 0.8337 | 0.182 | NR | 0.8337 | BF 0.17 |
| 206 | NR | -28.3835 | 0.6747 | 0.394 | NR | 0.6747 | BF 0.33 |
| 207 | NR | -30.0274 | 0.7661 | 0.266 | NR | 0.7661 | BF 0.23 |
| 208 | NR | -35.5909 | 0.7469 | 0.292 | NR | 0.7469 | BF 0.25 |
| 209 | NR | -25.5543 | 0.6869 | 0.376 | NR | 0.6869 | BF 0.31 |
| 210 | NR | -21.1819 | 0.6982 | 0.359 | NR | 0.6982 | BF 0.29 |
| 211 | NR | -33.8789 | 0.5065 | 0.680 | NR | 0.5065 | BF 0.20 CORE 0.29 |
| 212 | NR | -24.3939 | 0.9089 | 0.095 | NR | 0.9089 | |
| 213 | BF | -14.9380 | 0.9175 | 0.086 | BF | 0.9175 | |
| 214 | BF | -29.9253 | 0.9992 | 0.001 | BF | 0.9992 | |
| 215 | BF | -25.7183 | 0.5959 | 0.518 | BF | 0.5959 | FLAKE 0.40 |
| 216 | BF | -27.5014 | 0.9730 | 0.027 | BF | 0.9730 | |
| 217 | BF | -31.2025 | 0.4871 | 0.719 | BF | 0.4871 | CORE 0.27 FLAKE 0.19 |
| 218 | BF | -33.3251 | 0.9391 | 0.063 | BF | 0.9391 | |
| 219 | BF | -19.6799 | 0.7320 | 0.312 | BF | 0.7320 | FLAKE 0.27 |
| 220 | BF | -26.5189 | 0.0943 | 2.361 | FLAKE | 0.8700 | |
| 221 | BF | -32.4979 | 0.6924 | 0.368 | BF | 0.6924 | FLAKE 0.31 |
| 222 | BF | -32.5746 | 0.9932 | 0.007 | BF | 0.9932 | |
| 223 | BF | -25.7014 | 0.9954 | 0.005 | BF | 0.9954 | |
| 224 | BF | -31.9144 | 0.8604 | 0.150 | BF | 0.8604 | FLAKE 0.14 |
| 225 | BF | -31.7825 | 0.9407 | 0.061 | BF | 0.9407 | |
| 226 | BF | -24.2823 | 0.4432 | 0.814 | NR | 0.5568 | |
| 227 | BF | -27.4324 | 0.2896 | 1.239 | NR | 0.7104 | |
| 228 | BF | -17.8358 | 0.9483 | 0.053 | BF | 0.9483 | |
| 229 | BF | -29.0485 | 0.9856 | 0.015 | BF | 0.9856 | |
| 230 | BF | -19.8017 | 0.4821 | 0.730 | NR | 0.5179 | |
| 231 | FLAKE | -32.1892 | 0.9993 | 0.001 | FLAKE | 0.9993 | |
| 232 | FLAKE | -38.3809 | 0.9989 | 0.001 | FLAKE | 0.9989 | |
| 233 | FLAKE | -29.4441 | 1.0000 | 0.000 | FLAKE | 1.0000 | |
| 234 | FLAKE | -34.5001 | 0.9683 | 0.032 | FLAKE | 0.9683 | |
| 235 | FLAKE | -41.6398 | 0.9977 | 0.002 | FLAKE | 0.9977 | |
| 236 | FLAKE | -35.5175 | 0.9924 | 0.008 | FLAKE | 0.9924 | |
| 237 | FLAKE | -40.7806 | 0.9973 | 0.003 | FLAKE | 0.9973 | |
| 238 | FLAKE | -40.6438 | 0.9043 | 0.101 | FLAKE | 0.9043 | |
| 239 | FLAKE | -33.7141 | 0.9069 | 0.098 | FLAKE | 0.9069 | |
| 240 | FLAKE | -34.7138 | 0.5657 | 0.570 | FLAKE | 0.5657 | BF 0.13 NR 0.31 |
| 241 | FLAKE | -29.7360 | 1.0000 | 0.000 | FLAKE | 1.0000 | |
| 242 | FLAKE | -35.3414 | 0.4391 | 0.823 | FLAKE | 0.4391 | BF 0.25 NR 0.31 |
| 243 | FLAKE | -29.8885 | 0.1210 | 2.112 | BF | 0.7245 | NR 0.15 |
| 244 | FLAKE | -37.4309 | 0.7379 | 0.304 | FLAKE | 0.7379 | BF 0.25 |
| 245 | FLAKE | -36.3756 | 0.9687 | 0.032 | FLAKE | 0.9687 | |
| 246 | FLAKE | -35.8501 | 0.4759 | 0.743 | FLAKE | 0.4759 | BF 0.36 NR 0.16 |
| 247 | FLAKE | -35.8073 | 0.5210 | 0.652 | FLAKE | 0.5210 | BF 0.43 |
| 248 | FLAKE | -32.9383 | 0.9437 | 0.058 | FLAKE | 0.9437 | |
| 249 | CORE | -38.4965 | 0.9740 | 0.026 | CORE | 0.9740 | |
| 250 | CORE | -31.6805 | 0.7499 | 0.288 | CORE | 0.7499 | BF 0.22 |
| 251 | CORE | -32.8253 | 0.9997 | 0.000 | CORE | 0.9997 | |
| 252 | CORE | -32.1466 | 0.9195 | 0.084 | CORE | 0.9195 | |
| 253 | CORE | -31.8310 | 0.9986 | 0.001 | CORE | 0.9986 | |

| Row | Actual | SqDist (Actual) | Prob (Actual) | -Log (Prob) | Predicted | Prob (Pred) | Others |
|---|---|---|---|---|---|---|---|
| 254 | CORE | -31.6388 | 0.9320 | 0.070 | CORE | 0.9320 | |
| 255 | CORE | -31.9670 | 0.3748 | 0.981 | BF | 0.5315 | |
| 256 | CORE | -31.8829 | 0.9931 | 0.007 | CORE | 0.9931 | |
| 257 | CORE | -32.5843 | 0.6734 | 0.395 | CORE | 0.6734 | BF 0.31 |
| 258 | CORE | -31.7643 | 0.1342 | 2.009 | BF | 0.5424 | NR 0.30 |
| 259 | CORE | -32.1405 | 0.9997 | 0.000 | CORE | 0.9997 | |
| 260 | BF | -12.2097 | 1.0000 | 0.000 | BF | 1.0000 | |
| 261 | BF | -25.5072 | 0.8640 | 0.146 | BF | 0.8640 | NR 0.14 |
| 262 | BF | -24.2212 | 0.5059 | 0.681 | BF | 0.5059 | NR 0.49 |
| 263 | CORE | -31.6457 | 1.0000 | 0.000 | CORE | 1.0000 | |
| 264 | NR | -11.3927 | 0.9923 | 0.008 | NR | 0.9923 | |
| 265 | BF | -7.7533 | 0.9781 | 0.022 | BF | 0.9781 | |
| 266 | NR | -8.8790 | 0.4103 | 0.891 | BF | 0.5897 | |
| 267 | BF | -12.8129 | 1.0000 | 0.000 | BF | 1.0000 | |
| 268 | BF | -9.2040 | 1.0000 | 0.000 | BF | 1.0000 | |
| 269 | NR | -21.6777 | 0.9993 | 0.001 | NR | 0.9993 | |
| 270 | NR | -16.1922 | 0.9994 | 0.001 | NR | 0.9994 | |
| 271 | BF | -12.6368 | 0.1852 | 1.686 | NR | 0.8148 | |
| 272 | BF | -18.5976 | 0.1279 | 2.056 | CORE | 0.8687 | |
| 273 | NR | -25.7948 | 0.9996 | 0.000 | NR | 0.9996 | |
| 274 | FLAKE | -32.2796 | 0.9988 | 0.001 | FLAKE | 0.9988 | |
| 275 | BF | -11.7618 | 0.9994 | 0.001 | BF | 0.9994 | |
| 276 | BF | 5.0768 | 0.9999 | 0.000 | BF | 0.9999 | |

'*' indicates misclassified
"~" indicates excluded row